UNIVERSITY OF HAWAII
LIBRARY
APR 2 '51

The PHILOSOPHICAL MAGAZINE

FIRST PUBLISHED IN 1798

42 SEVENTH SERIES No. 325 February, 1951

A Journal of Theoretical Experimental and Applied Physics

EDITOR
PROFESSOR N. F. MOTT, M.A., D.Sc., F.R.S.

EDITORIAL BOARD
SIR LAWRENCE BRAGG, O.B.E., M.C., M.A., D.Sc., F.R.S.
ALLAN FERGUSON, M.A., D.Sc.
SIR GEORGE THOMSON, M.A., D.Sc., F.R.S.
PROFESSOR A. M. TYNDALL, C.B.E., D.Sc., F.R.S.

PRICE 12s. 0d.
Annual Subscription £6 0s. 0d. payable in advance.

AND PUBLISHED BY TAYLOR & FRANCIS LTD., RED LION COURT, FLEET ST., LONDON, E.C.4.

Early Scientific Publications

ALERE FLAMMAM

DIARY OF ROBERT HOOKE, M.A., M.D., F.R.S.
1672-1680

25/-
net

Edited by **H. W. ROBINSON** and **W. ADAMS**
Recommended for publication by the Royal Society, London

"This vivid record of the scientific, artistic and social activities of a remarkable man during remarkable years has too long remained in obscurity."—Extract from foreword by Sir Frederick Gowland Hopkins, O.M., President of the Royal Society.

MATHEMATICAL WORK OF JOHN WALLIS, D.D., F.R.S.

12/6
net

By **J. F. SCOTT, Ph.D., B.A.**

"His work will be indispensable to those interested in the early history of The Royal Society. I commend to all students of the Seventeenth Century, whether scientific or humane, this learned and lucid book."—Extract from foreword by Prof. E. N. da C. Andrade, D.Sc., Ph.D., F.R.S.

Recommended for publication by University of London

CORRESPONDENCE AND PAPERS OF EDMOND HALLEY

21/-
net

Arranged and Edited by **EUGENE FAIRFIELD MACPIKE**

First published on behalf of The History of Science Society by Oxford University Press. Now re-issued by Taylor & Francis, Ltd.

MEMOIRS OF SIR ISAAC NEWTON'S LIFE

5/-
net

By **WILLIAM STUKELEY, M.D., F.R.S., 1752**
From an Original Manuscript
Now in the possession of the Royal Society, London

HEVELIUS, FLAMSTEED AND HALLEY

12/6
net

Three Contemporary Astronomers and their Mutual Relations
By **EUGENE FAIRFIELD MACPIKE**
Published by arrangement with The History of Science Society

Established
over 150 years

TAYLOR & FRANCIS, LTD.
RED LION COURT, FLEET ST., LONDON E.C.
PRINTERS & PUBLISHERS OF SCIENTIFIC BOOKS

XII. *The Waveforms of Atmospherics and the Propagation of very Low Frequency Radio Waves.*

By P. W. A. Bowe,
Cavendish Laboratory, Cambridge*.

[Received November 28, 1950.]

[Plate VI.]

Summary.

The responses of narrow-band receivers to individual radio atmospherics have been observed in order to describe the propagation of radio waves of frequency 2 kc./s. to 10 kc./s. over the surface of the earth. It has been found that the atmospherics from a fixed distance are sufficiently uniform to enable the relative attenuations of different frequencies to be deduced. The study reveals that waves of frequency below about 8 kc./s. are heavily attenuated during the daytime but are propagated freely at night. The attenuation is greater during a sudden ionospheric disturbance.

These results confirm and extend those obtained recently by Gardner. They can be explained in outline on a theory recently proposed by Budden.

§1. Introduction.

Several workers have shown that the waveforms of some atmospherics can be interpreted in terms of irregularly shaped radio impulses reflected one, two and more times from the ionosphere (Laby, McNeill, Nicholls, Nickson, 1940 ; Schonland, Elder, Hodges, Philips and van Wyk, 1940). Under good conditions it is often possible to deduce the height of reflection of these impulses, and heights of about 85 km. have been deduced.

Other workers (Bracewell, Budden, Ratcliffe, Straker and Weekes 1951) have investigated the propagation of very long radio waves emitted by commercial senders, and a considerable body of knowledge now exists concerning the height from which these waves are reflected by the ionosphere, and their intensity.

It is clearly of interest to compare the results of the two types of experiment. Unfortunately, when this comparison is attempted, a serious difficulty arises because in the atmospherics observed the shape of the impulse which is successively reflected from the ionosphere is usually irregular, and varies from sample to sample, so that it is impossible to specify with any accuracy the radio frequency to which it corresponds.

---

* Communicated by Mr. J. A. Ratcliffe.

In the work to be described in this paper radio atmospherics are used in a different way to investigate the propagation of very long radio waves. A single atmospheric is applied simultaneously to four narrow-band receivers tuned to different very low frequencies between 2 kc./s. and 10 kc./s., and the responses are compared. The relative responses on the different frequencies (which might be called the spectrum at the receiver) will depend on (*a*) the relative intensities excited in the different frequencies by the particular lightning flash being measured (which might be called the spectrum at the source), and (*b*) the characteristics of the transmission path between the flash and the receiver. In order to separate these two factors, the atmospherics received from flashes at different distances have been compared.

The assumption is made that, statistically, all flashes excite the same spectrum at the source, at least in the region of very low frequencies here considered, and a search is made for some significant change produced in the received spectrum as the distance of the flash changes. For one of the two classes of atmospherics received, described in more detail below, it has been found possible to establish a change of this kind accompanying a change of distance. This provides confirmation of the original assumption that there is some statistical constancy in the spectrum produced at the source by different lightning flashes. That change in the spectrum which accompanies increase of distance is attributed to the propagation conditions. It is also found that the propagation conditions, deduced in this way, change from day to night and during a sudden ionospheric disturbance. The results are summarized and discussed in § 5.

The recorded atmospherics fell into two easily distinguishable classes as follows.

Class I. had a fairly smooth "waveform" with marked low frequency periodicity of a more or less regular nature. The narrow-band amplifiers tuned to frequencies below 10 kc./s. gave a large response with atmospherics of this class. An example is shown in Pl. VI. (i.).

Class II. had a highly irregular "waveform" which showed an erratic variation with many short period fluctuations. When the overall amplitude of this type of atmospheric, as recorded on the wide-band receiver, was of the same order as that of an atmospheric of Class I., the response of the narrow-band amplifiers was much smaller for frequencies below 10 kc./s. An example of Class II. is shown in Pl. VI. (ii.) and can be compared with the atmospheric of Class I. shown in Pl. VI. (i.).

It appears that these two classes of atmospheric are different at the source, and in this paper only those of Class I., which gave an appreciable response on the narrow-band receivers, are considered. They formed about 75 per cent of the atmospherics recorded. The two different classes have been noticed by most workers in the subject, and Appleton and Chapman (1937) have ascribed them to the leader (Class II.) and return (Class I.) strokes of the lightning flash. For the purposes of the present paper, it is sufficient to distinguish between them by the nature of the recorded waveforms.

It will be shown in §4 that, when atmospherics of Class I. are selected in this way, their spectrum at the source is, within limits, the same for all atmospherics, so that changes in the spectrum due to propagation conditions can be shown up. Since atmospherics of Class II. produce only small radiation at the frequencies here considered, we assume that they do not radiate appreciably at these frequencies and therefore have a different spectrum at the source. Both classes of atmospheric have been received from distances up to 1700 kilometres.

The sources of atmospherics which were received and analysed in the way here described were simultaneously located by radio direction finding methods by the "Sferic" section of the Meteorological Office. This provided the measure of distance to the source of the atmospheric.

In the work described here each atmospheric was received on four narrow-band receivers tuned to four different very low frequencies, and for the sake of comparison, the waveform of the atmospheric as received on an aperiodic amplifier was simultaneously recorded. The responses at the four spot frequencies represent four points on the spectrum of the received atmospheric and could be deduced if that spectrum were known. In several cases the spectrum of the received atmospheric has therefore been deduced from the waveform by numerical Fourier analysis and it has been shown that the responses on the four tuned receivers correctly represented the four points on the spectrum. It was at one time thought that the method of numerical Fourier analysis of the waveform would be simpler than the method of reception on four narrow-band receivers, but it has proved that the latter method is in fact simpler and quicker. Since a large number of results are required for making a statistical analysis, the method of observation with the four receivers has therefore been used.

The results described in this paper confirm and extend those recently obtained by Gardner (1950). He recorded the integrated "level" of atmospherics received on four narrow-band receivers tuned to four different very low frequencies and observed how these levels altered with time of day and with the distance of a storm centre. He deduced information about the propagation conditions on the different frequencies.

While he was working in Cambridge, Gardner also constructed the equipment, described in outline in this paper, for recording the response of narrow-band receivers to individual atmospherics, and obtained some preliminary results with it before the present author took over the work from him. It is hoped that the equipment will be described in detail in a paper by Gardner.

The results given in this paper, and the corresponding results of Gardner, have been explained, at least in outline, by Budden (1951). A preliminary comparison of his theory with the present results is made in §5.

§ 2. EXPERIMENTAL METHOD.

The atmospherics were received on a vertical aerial and passed through a cathode follower to an aperiodic receiver and four tuned receivers all in parallel, as shown in fig. 1. The output of each receiver was applied to a separate cathode ray tube and when an atmospheric arrived all five tubes were photographed. Thus the waveform of the transient was recorded together with the response of four tuned receivers to it.

Fig. 1.

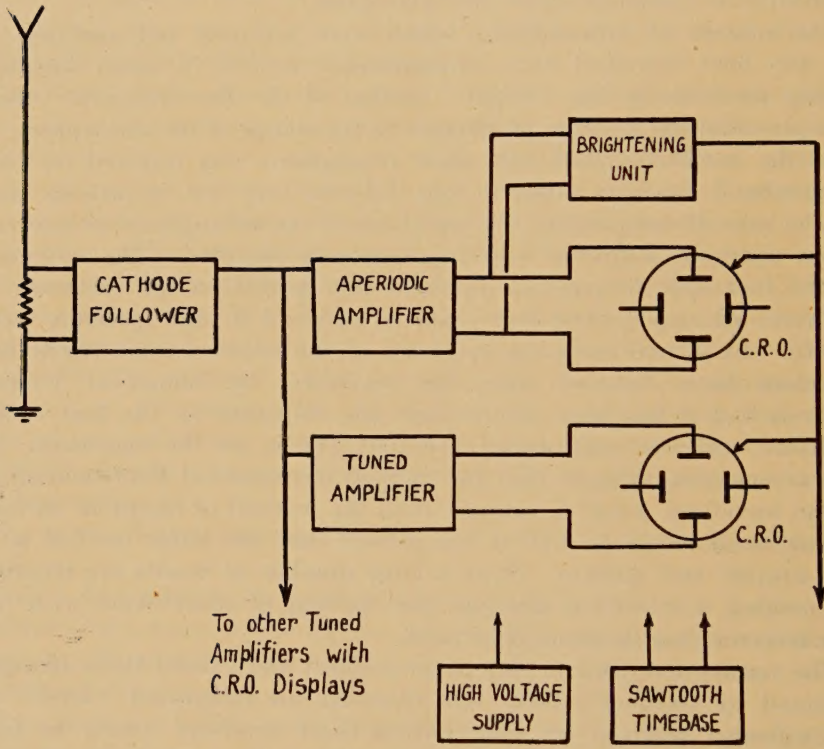

Diagram showing the experimental arrangement for recording atmospherics on an aperiodic and several narrow-band receivers.

2.1. *Receiving Unit.*

The vertical aerial, which was erected on a site near Cambridge relatively free from noise, had a length of 9 metres and a capacity to ground of 120 $\mu\mu$F. The voltage in the aerial was applied to the grid of a cathode follower across a grid resistor of 10^6 ohms, situated at the bottom of the aerial. A long cable connected the low impedance output of the cathode follower to a pre-amplifier with a step attenuator, the output of which was applied to the five receivers in parallel.

The aperiodic receiver had a gain which was constant to within 1 db. for frequencies between 800 c./s. and 50 kc./s. and gave an output which was proportional to the electric field at the aerial. It had two stages of amplification followed by cathode and anode followers to give a push–pull output to the cathode ray tube.

Each tuned receiver had a bandwidth of about 180 c./s. between half-power points, and each was tuned to a different frequency somewhere between 2 kc./s. and 10 kc./s. Each receiver consisted of an amplifier with a tuned-grid stage followed by a second amplifier, from which positive and negative feedback were applied to the first amplifier in order to narrow the bandwidth. Each receiver was followed by anode and cathode followers to give push–pull output for the cathode ray tube.

2.2. *Display Unit.*

The output from each of the four receivers was applied to the Y deflection plates of four 3-in. cathode ray tubes. The same sawtooth time-base voltage was applied to the X plates of each tube ; the time of sweep was about 2 milliseconds and the time of fly-back was less than 5 microseconds. This time-base was freely running so that the atmospheric appeared at a random place on the trace.

The grids of the cathode ray tubes were normally maintained at a negative potential so that no trace appeared. The output of the aperiodic receiver was connected to a brightening unit which, when an atmospheric above a certain small amplitude arrived, applied a positive pulse to the grids so as to brighten the tubes for the duration of one time-base sweep, and this trace was automatically photographed. The film was moved on manually and, to avoid double exposure, a delay was provided in the brightening unit so that, after brightening once, the circuit was inoperative for about half a second.

A typical record obtained in this way is shown in Pt. VI. (i.). The waveform as received by the aperiodic amplifier is shown on the centre trace and the responses of the four narrow-band receivers on the other traces. Each trace brightened at a point (*a*) and continued bright to (*b*), whence the fly-back returned the spot to (*c*) and the rest of the time-base was completed.

2.3. *Measurement of Distance.*

The distance to the source of the atmospherics was determined by taking advantage of the " Sferic " direction finding organization of the Air Ministry Meteorological Office (Ockenden 1947), and the grateful thanks of the author are due to the Director and staff for helpful co-operation.

Use was made of the routine service by which the sources of individual atmospherics are located by the intersections of radio bearings taken simultaneously at four widely-spaced observing stations. The use of telephone connection during an experiment enabled individual atmospherics recorded at Cambridge to be identified with sources located by the " Sferic " organization.

The distance to the source was then measured directly. There was a small chance of mis-identification, but this was not serious enough to affect the results. The sources could generally be located to an accuracy of about 10 per cent up to 1000 km. and less accurately beyond, but this was quite sufficient for the present purpose.

§ 3. THE SPECTRUM OF THE RECEIVED ATMOSPHERICS.

We shall here discuss the spectrum of the received atmospheric as deduced from Fourier analysis of the recorded waveform and relate it to the observed responses from the narrow-band receivers.

3.1. *The Output from the Tuned Receivers.*

It is interesting to notice the way in which the narrow-band receivers respond to the input transient depicted at (2), Pl. VI. (i.). If we look, for example, at the recorded response of the receiver tuned to 7·5 kc./s. we see that, while the original transient is arriving, the amplitude is building up so that, when the transient is over, the circuit is left performing a decaying oscillation with a decay time determined by the band-width of the amplifier. The amplitude of this oscillation represents the amplitude of the appropriate Fourier component in the analysis of the transient. The amplitude of the final decaying oscillation cannot, of course, be decided until the transient is over, so that the response during the building-up period need not bear any relation to the final amplitude when the transient is over. The record of the response on 3·5 kc./s. shows this well: during the "build-up" period there is quite a large response, but when the transient is over, the circuit has settled down to give a negligibly small decaying oscillation, corresponding to the fact that the Fourier component of frequency 3·5 kc./s. is too small to record.

The four narrow-band receivers were calibrated by observing their responses to a test signal which consisted of a rectangular pulse of voltage of known amplitude and of duration 14 μsec. This pulse was repeated fifty times per second but, of course, only occasional ones were recorded. Each of these pulses had an effectively uniform spectrum over the relevant range of frequencies 2 kc./s. to 10 kc./s. Although it is considered that the absolute response of the different receivers could be made equal by this method of calibration, it will become apparent, in what follows, that the conclusions to be reached in this paper do not depend on this adjustment for equality. All the measurements were made in terms of the ratio of the responses at two frequencies, and the way in which that ratio changes from time to time. It is only necessary, then, that the ratio of the responses should be determined, and this was done by the method of calibration described.

A similar argument helps us to avoid a difficulty in the measurement of the responses on the narrow-band receivers. There might be some doubt as to whether the amplitude of the decaying oscillation should be measured at the time when the transient is finished, or whether the decay should be allowed for, and the amplitude be estimated at the time when the transient started. Since, however, we are only concerned with the ratio of amplitudes on the different frequencies, it does not matter which measurement is taken, provided it is kept the same for all frequencies.

Records of the type illustrated in Pl. VI. were made on photographic film and were measured by projecting and comparing with a scale.

3.2. *Direct Fourier Analysis of the Transient.*

The method described in the previous section could be thought of as giving four points on the frequency spectrum of the received atmospheric. It was at one time thought that this information could be more easily obtained by performing a Fourier analysis of the transient recorded on the wide-band amplifier, and, moreover, it appeared that if the analysis were performed in this way, attention need not be restricted to four frequencies. Some of the records of transient responses were therefore analysed by ordinary methods of Fourier analysis, as described below. It soon became apparent, however, that the labour of performing a full Fourier analysis was considerable, and, since the aim of the work was to record numerous atmospherics from which statistical deductions could be made, this method was not continued. It proved to be much simpler and quicker to use the apparently more complicated method of the four tuned receivers to obtain the Fourier components at the four chosen frequencies.

It is, however, of interest to see how far the Fourier analysis of the recorded wave-form agreed with the magnitudes of the Fourier components deduced from the responses of the four narrow-band amplifiers. For this purpose the transient waveform was redrawn on as large a scale as possible and three standard methods of Fourier analysis were used. These were :—

(1) An electro-mechanical analyser developed by the Admiralty Research Laboratory (Barber, Ursell, Darbyshire and Tucker 1946).

(2) Beevers Lipson Strips (Ross 1943).

(3) Hollerith Computing Machine (Hodgson, Clews and Cochran 1949).

Fig. 2 (*a*) gives the results of applying methods (1) and (2) to the waveform shown and fig. 2 (*b*) shows the results of applying methods (2) and (3) to another waveform. It will be seen that in each case the deductions made by the two different methods agree quite well. The points marked by crosses show the relative magnitudes of the Fourier components as determined by measurement of the responses on the narrow band receiver. These magnitudes have been adjusted so that the point for 7·5 kc./s. falls on the computed curve. It will be seen that they agree well with the results calculated by direct Fourier analysis of the transients, and we are satisfied that the method of using the four tuned receivers gives reliable results for the ratio of Fourier components at the relevant frequencies.

Fig. 2 (*a*).

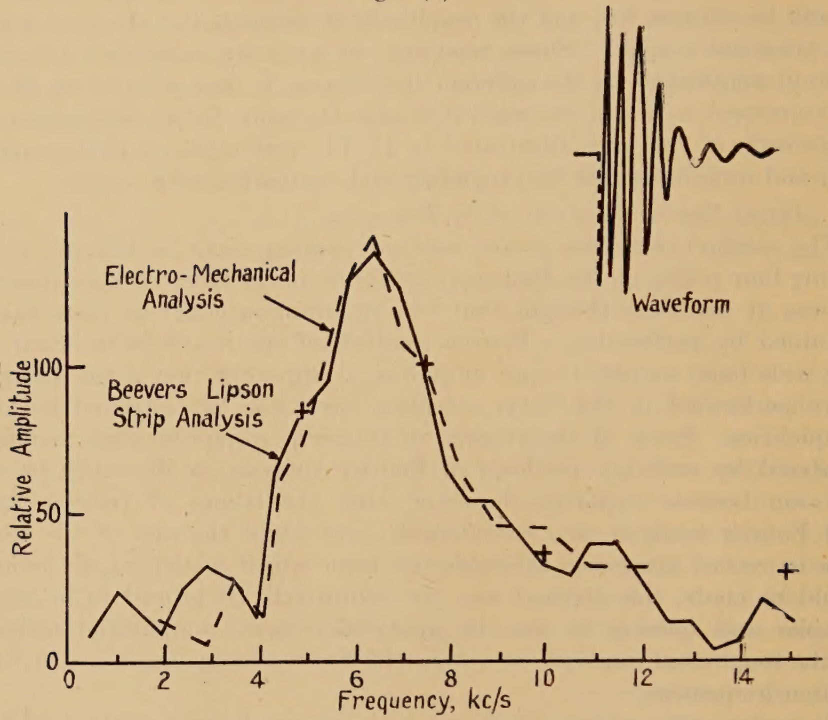

Fig· 2 (*b*).

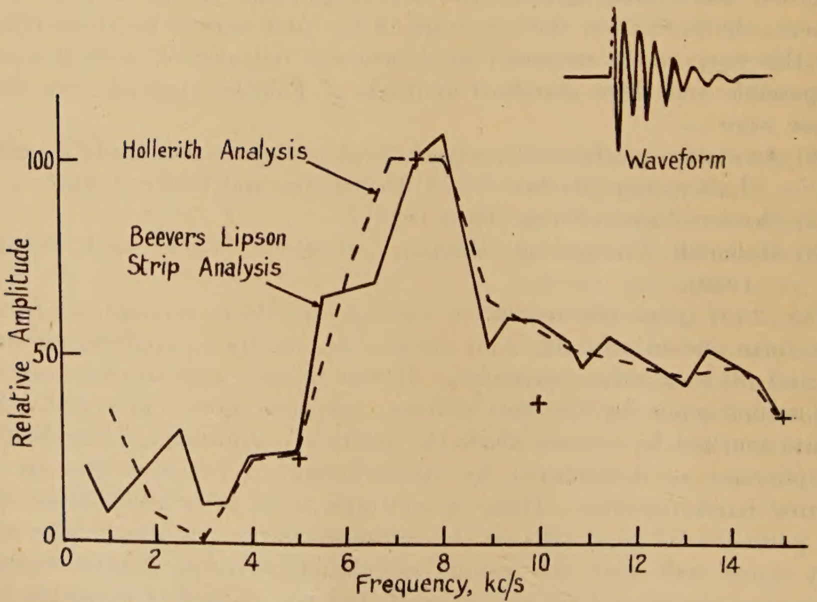

The received spectra of two atmospherics as deduced by the methods indicated. The four points deduced from the responses of the tuned receivers are indicated by crosses. The waveform analysed is also shown.

It might be thought that an important part of the atmospheric waveform might fail to be recorded on the wide-band receiver because of the time lost before the cathode-ray trace was brightened by the atmospheric. The good agreement between the spectra computed from the recorded waveform and the responses of the four narrow-band receivers shows that there is no difficulty of this kind in the range of frequencies here considered.

§ 4. ANALYSIS OF RESULTS.

4.1. *Method of Analysis.*

In order to clarify the method of analysis, it is convenient to define some attenuation factors. Consider a lightning flash which has a radiation field $A\phi(f)$ at the source, where A depends on the strength of the source and $\phi(f)$ represents the way in which the field varies with the frequency f. Then in free space the field received at a distance r would be given by $A\phi(f)/r$. Suppose now that this atmospheric were transmitted a distance r over the surface of the earth and that as a result each component frequency f suffered an attenuation $\rho(f, r)$; so that the received field would be given by

$$E(f, r)=\frac{A}{r}\phi(f)\,\rho(f, r).$$

Now let the field produced by a source at a distance r be measured at a series of different frequencies $f_0, f_1, f_2 \ldots f_n$, and let the result be expressed as a ratio between the field at the frequency f_n and the field at a reference frequency f_0 so that we obtain the quantity

$$E(f_n, r)/E(f_0, r)=\{\phi(f_n)/\phi(f_0)\}\{\rho(f_n, r)/\rho(f_0, r)\}.$$

Next, suppose that these measurements are made for several atmospherics at a series of different distances, and that the ratio $E(f_n, r)/E(f_0, r)$ is plotted as a function of r. The resulting curve will show how the ratio $\rho(f_n, r)/\rho(f_0, r)$ of the attenuation factors at the two frequencies f_n and f_0 varies with distance. Since the attenuation factor $\rho(f, r)$ is unity for all frequencies when the distance is small, the intercept on the axis at $r=0$ will give the magnitude of $\phi(f_n)/\phi(f_0)$, which depends on the spectrum of the atmospheric at the source.

It is of course most unlikely that the spectrum $\phi(f)$ of the atmospheric at the source is the same for all atmospherics. If, however, they do not differ too much among themselves then, by taking enough observations on atmospherics originating at all distances, it may be possible to draw a smooth curve through the set of observed points so as to show, with some real significance, how the ratio $\rho(f_n, r)/\rho(f_0, r)$ of the attenuation factors varies with distance. We shall show that, in fact, the spectra $\phi(f)$ are sufficiently nearly the same for frequencies between 2 and 10 kc./s. for this procedure to be of use.

4.2. *Measurements under Normal Conditions.*

In order to examine seasonal changes the observations are grouped in four sets as summarized in Table I. which lists the frequencies used, the number of experimental runs, the number of atmospherics recorded, and the distances between which the sources were located.

Table I.

Set	Occasion	Frequencies kc./s.	No. of runs	No. of atmospherics	Distance of sources, km.
A	Winter day	(3·5), 5, 7·5, 10	11	70	600–3600
B	Night	3·5, 5, 7·5, 10	10	55	1000–3000
C	Summer day	3·5, 5, 7·5, 10	11	195	300–2000
D	Summer day	2·25, 4·25, 6·25, 7·5	21	255	0–3000

In order to analyse the results the frequency 7·5 kc./s. was taken as the standard frequency f_0, and for each atmospheric observed the ratio $E(f_n, r)/E(f_0, r)$ was deduced and plotted against the measured distance r of the source. A series of plots of this kind was made for each of the frequencies observed. Fig. 3 (a) shows the results obtained on summer days for $f_1 = 4{\cdot}25$ kc./s. and $f_0 = 7{\cdot}5$ kc./s.

Fig. 3 (a).

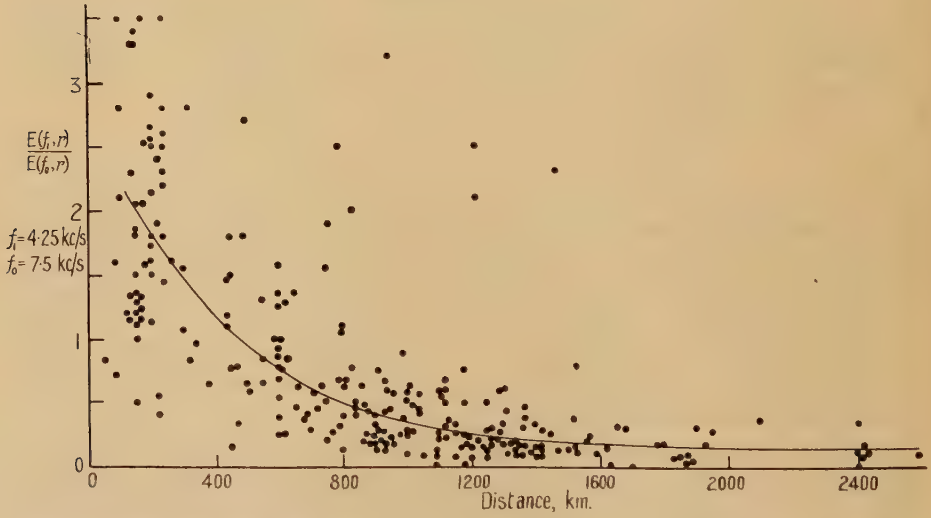

To show how the ratio $E(f_1, r)/E(f_0, r)$ of field strengths at 4·25 kc./s. ($=f_1$) and 7·5 kc./s. ($=f_0$) for atmospherics at different distances, varies with distance. All observations were made in daytime.

It will be seen that although there is a considerable spread in the observed points, of the order of about 10 : 1 at all distances, it is nevertheless possible to draw a smooth curve through them which clearly has some significance and which shows that the ratio decreases as the distance increases. We deduce from this curve that the intensity of waves of frequency 4·25 kc./s. decreases more rapidly with distance than that of waves of frequency 7·5 kc./s.

There is, of course, a very considerable spread amongst the observed points plotted in the figure. This is caused largely by the differences in the ratio $\phi(f_1)/\phi(f_0)$ from one atmospheric to another, but some of it is also probably due to inaccuracies in the measurements of the distance of the source, and to wrong identifications between some of the atmospherics whose distance was measured and those whose spectral response was determined. Examination of the results on all frequencies and at all times has led us to think that the ratio $\phi(f_1)\phi(f_0)$ varies by a factor of about 10 : 1 from atmospheric to atmospheric.

Fig. 3 (*b*).

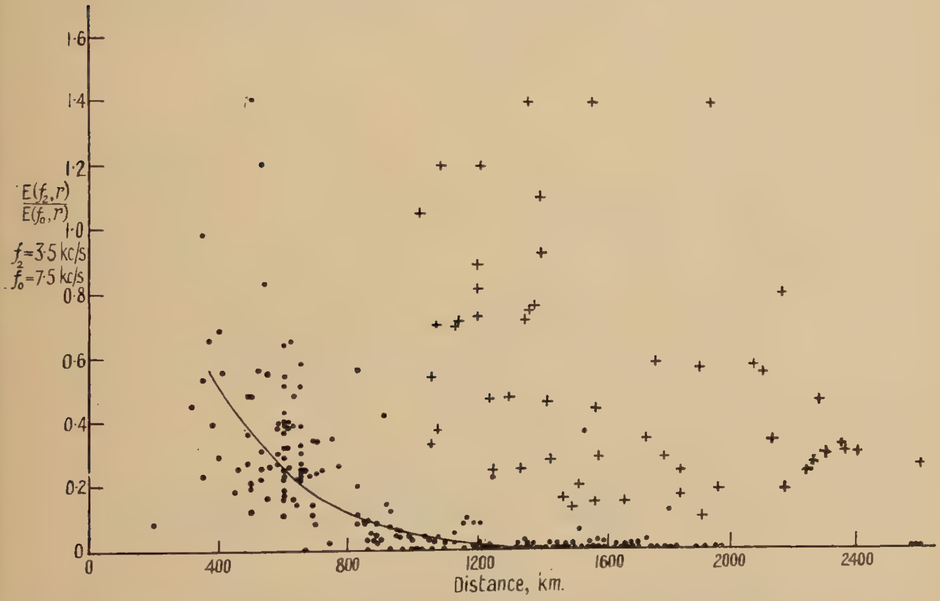

To show how the ratio $E(f_2, r)/E(f_0, r)$ of field strengths at 3·5 kc./s. ($=f_2$) and 7·5 kc./s. ($=f_0$) for atmospherics at different distances, varies with distance.

+ Observations at night.
● Observations during the day.

Fig. 3 (*b*) in which the ratio $E(f_2, r)/E(f_0/r)$ is plotted against r for $f_2=3\cdot5$ kc./s. and $f_0=7\cdot5$ kc./s., shows similar results. Observations obtained by day are shown as dots, and a smooth curve has been drawn to lie evenly amongst them. Observations taken by night are shown by crosses. It will be seen that, during the day, for distances greater than about 1200 km. the response on 3·5 kc./s. is in nearly all cases so small as to be negligible and is less than 1/100th of the response on a frequency of 7·5 kc./s.* It is clear that, whereas waves of frequency 7·5 kc./s. can be transmitted over these distances during the day with comparative ease, those of frequency 3·5 kc./s. are heavily attenuated. This result, shown clearly by these observations alone, is the most striking feature of the transmission characteristic which we shall summarize in the next section.

The other important point which arises from fig. 3 (*b*) is concerned with the marked difference between the results for day and night. It is clear that although waves of frequency 3·5 kc./s. cannot be transmitted over distances greater than 1200 km. by day they are transmitted almost as easily as those on 7·5 kc./s. by night.

Fig. 4.

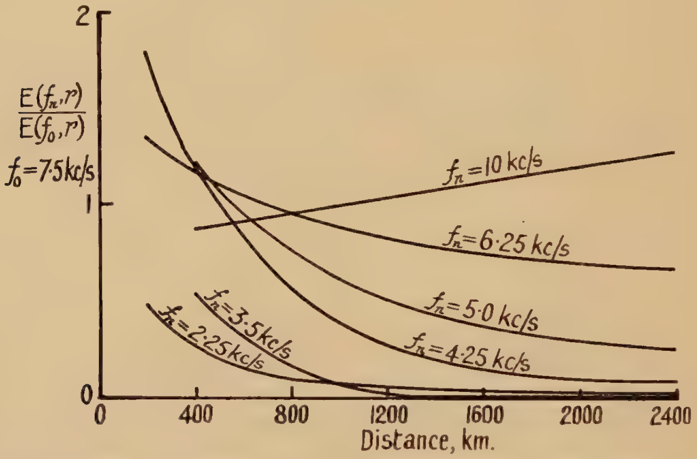

Curves showing how the average ratio of field strength $E(f_n, r)/E(f_0, r)$ varies with distance for $f_0=7{\cdot}5$ kc./s. and f_n as indicated.

Results obtained with the other frequencies have been plotted in the same way and smooth curves have been drawn through the points. The complete plots are not reproduced, but the smooth curves are shown in fig. 4 for the summer day observations. These observations were nearly all made within two hours of local noon, and most of the atmospherics came from directions between 030° and 135° E. of N. The analysis was based on those recorded atmospherics for which a definite location was obtained by the Sferics organization.

The night and winter-day observations did not include a sufficient number of atmospherics to enable similar curves to be drawn, and they are not presented here in detail. However, the observations on 3·5 kc./s. already mentioned do establish the important fact that the received amplitude $E(f_2, r)/E(f_0, r)$ for $f_2=3{\cdot}5$ kc./s., $f_0=7{\cdot}5$ kc./s., $r=1000$ km. is at night about ten times what it is during the day. This means that the attenuation factor $\rho(f_2, r)/\rho(f_0, r)$ is at night ten times what it is during the day.

---

* The different response on the two frequencies of 7·5 and 3·5 kc./s. for a distant atmospheric in the daytime is well illustrated by the example shown in Pl. VI. (i.).

4.3. *Deduction of Attenuation Curves.*

The curves of figs. 3 and 4 show how the quantities

$$\{\phi(f_n)/\phi(f_0)\}\{\rho(f_n, r)/\rho(f_0, r)\}$$

vary with distance when f_0 is taken as 7·5 kc./s. It is now desirable to normalize these curves so that they pass through the value unity for small distances ; they then give information about the attenuation coefficients alone, but not about the ratios $\phi(f_n)/\phi(f_0)$. The normalizing factor was obtained by extrapolating the curves to zero distance. It is also convenient to take a new frequency, 10 kc./s., for f_0*, and we then obtain, for summer daytime, the series of curves shown in fig. 5 in which $\rho(f_n, r)/\rho(f_0, r)$ is plotted against distance with $f_0=10$ kc./s.

Fig. 5.

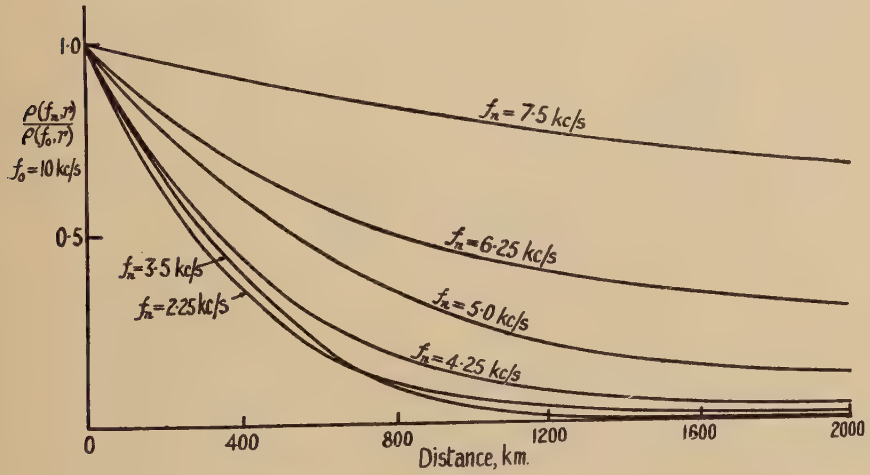

Curves showing how the ratio of attenuation coefficients $\rho(f_n, r)/\rho(f_0, r)$ varies with distance for $f_0=7{\cdot}5$ kc./s. and f_n as indicated.

It is convenient to present the same results in still another way, as shown in fig. 6, in which the ratios $\rho(f, r)/\rho(f_0, r)$ are plotted against frequency f for three different distances $r=500$, 1000 and 2000 km. In these curves f_0 was taken as 10 kc./s. and if there were no attenuation at this frequency, the curves would represent attenuation as a function of frequency at the three distances; if there be some attenuation on 10 kc./s., the curves showing total attenuation as a function of frequency would have their scales altered by different amounts so that they would no longer all pass through the same point at 10 kc./s.

---

* In the preliminary calculations it was more convenient to take $f_0=7{\cdot}5$ kc./s. because one of the receivers was working on this frequency in every experiment, but there was not always a receiver tuned to 10 kc./s.

By a different experimental method Gardner (1950) has plotted similar curves, and the cross at 5 kc./s. (fig. 6) represents his results for atmospherics originating from a distance of about 1500 km. It agrees well with the present results.

Neither the winter nor the night observations are sufficient to enable similar attenuation curves to be drawn. The night observations on 3·5 kc./s. shown in fig. 3 (*b*) do, however, indicate, as has been mentioned before, that the attenuation factor $\rho(f_2, r)/\rho(f_0, r)$ for $f_2=3{\cdot}5$ kc./s., $f_0=7{\cdot}5$ kc./s., $r=1000$ km. during the night is about ten times what it is during the day. Since the day attenuation is about 0·05, this gives a value of 0·5 for the attenuation at 3·5 kc./s. This value is shown by the open circle on fig. 6.

Fig. 6.

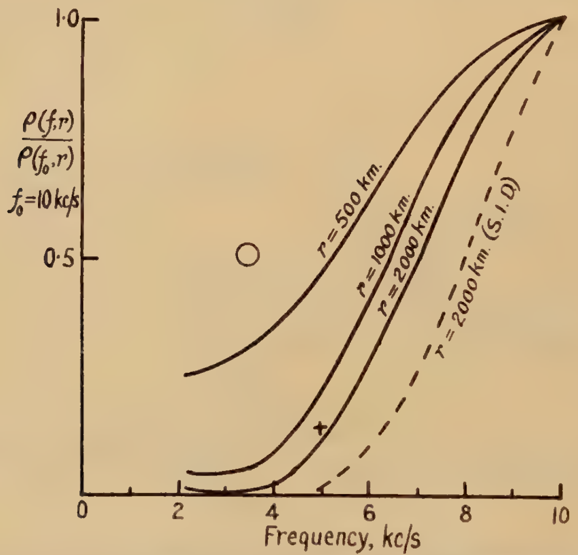

Summary of attenuation coefficients for different conditions.

——— Variation of ratio of attenuation coefficients $\rho(f, r)/\rho(f_0, r)$ with frequency f for $f_0=10$ kc./s. and r as indicated. Normal day conditions.

– – – Similar curve for $r=2000$ km. during an S.I.D.

+ Value obtained by Gardner for atmospherics from about 1500 km.

○ Night attenuation on 3·5 kc./s. for atmospherics from 1000 km.

4.4. *Measurements during a Sudden Ionospheric Disturbance.*

It has been noted by Gardner (1950) that, during a Sudden Ionospheric Disturbance (S.I.D.), the integrated level of atmospherics decreases on frequencies below 7 kc./s., so that the spectrum of an individual atmospheric might be expected to show a similar change. Fortunately it was possible to make observations during a large S.I.D. on 20th February 1950. Atmospherics were recorded at five separate times before, during and after the S.I.D., as indicated in fig. 7. The set of observations at 1550 G.M.T. was made while the " Sferic " organization was operating,

Fig. 7.

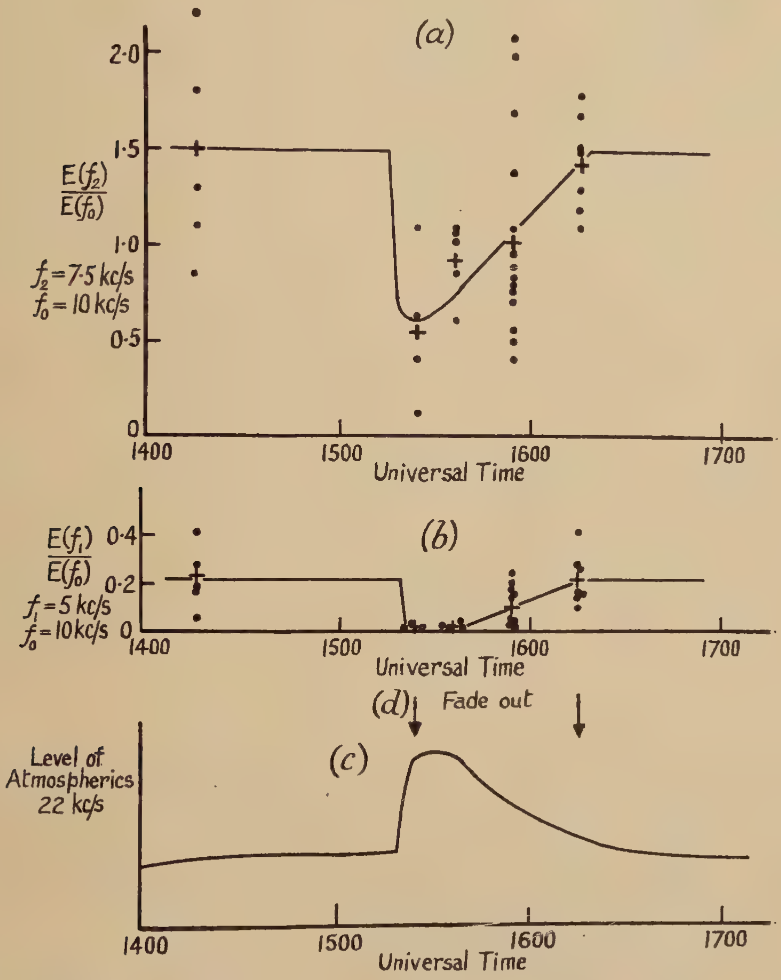

Effect of S.I.D. on 20th February 1950, on atmospherics from 2400 km.

(*a*) Change in ratio of received field strength of atmospherics, $E(f_2, r)/E(f_0, r)$ when S.I.D. occurs.

(*b*) Change in ratio of received field strength of atmospherics $E(f_1, r)/E(f_0, r)$ when S.I.D. occurs.

(*c*) Sudden enhancement of integrated level of atmospherics on 22 kc./s.

(*d*) Beginning and end of fadeout reported by B.B.C.

Crossss indicate mean values for sets of points.

so that definite distances were available for the atmospherics recorded. In addition the routine " Sferic " charts of the Meteorological Office indicated that there was a strong source of atmospherics at a distance of 2400 km. throughout the whole day and very little activity elsewhere. From this it can be stated, with some certainty, that the recorded atmospherics originated in this distant storm.

The results are shown in fig. 7. In (*b*) the quantity $E(f_1)/E(f_0)$ is plotted for $f_1=5$ kc./s. and $f_0=10$ kc./s., in (*a*) the same ratio is plotted for $f_1=7{\cdot}5$ kc./s. and $f_0=10$ kc./s., in (*c*) the integrated " level " of atmospherics as recorded on 22 kc./s. is shown, and (*d*) shows the extent of the " fade out " as reported by the B.B.C. In (*a*) and (*b*) each recorded atmospheric is indicated by a dot, and the mean values for the set of dots in each series is shown by a cross. The curves are drawn through the crosses. The most striking effect is seen in curve (*b*) which shows that, near the peak of the S.I.D., the component of frequency 5 kc./s. decreased about ten times compared with the component of frequency 10 kc./s. This is in good agreement with Gardner's observation that the integrated " level " of atmospherics as received at 5 kc./s. may often become too low to observe during an S.I.D. Although the corresponding decrease on 7·5kc./s., shown in curve (*a*), is also noticeable, it is not so marked.

It is possible to apply the results shown in fig. 7 to the daytime attenuation curve of fig. 6 so as to derive an attenuation curve which would represent the conditions during an intense S.I.D. Since fig. 7 applies to a distance of about 2400 km., we use it to modify the attenuation curve of fig. 6 drawn for the approximate distance of 2000 km., and we arrive at the dashed curve in fig. 6 to represent the conditions during the S.I.D.

§ 5. CONCLUSIONS.

The final conclusions of this work are represented by the attenuation curves of fig. 6. These curves show how the attenuation factor $\rho(f, r)$ at different distances varies with frequency relative to the attenuation $\rho(f_0, r)$ at a standard frequency f_0. The three full curves are for normal daytime conditions, the dotted curve for abnormal daytime conditions during a sudden ionospheric disturbance and the open circle indicates the result for 3·5 kc./s. during the night.

From the nature of the results it cannot be claimed that the curves are accurate to more than about 50 per cent. It can be seen, however, that an accuracy of this order is adequate to establish the general nature of the propagation characteristics of the space between the earth and the ionosphere in the frequency range 2 kc./s. to 10 kc./s.

A first attempt at a theoretical explanation of these results has been made by Budden (1951). From consideration of the waveguide formed by the earth and ionosphere, he has deduced theoretical curves similar to those of fig. 6. Budden proceeds on the assumption that the ionosphere has a sharp lower boundary at high h, with appropriate values of electron density and collision frequency. From an extension of his theory, attenuation curves for 1000 km. path for heights of 62·5 km. and 50 km. have been obtained. These are shown in fig. 8, together with the experimental curve for the attenuation 1000 km. from the source. It can be seen that there is semi-quantitative agreement between the theory and the experimental results. According to Budden's theory, the curve will be moved to the right for decrease in reflection height and to the left for increase. It is probable that movements of this kind explain the different experimental curves obtained during an S.I.D. and during the night.

Fig. 8.

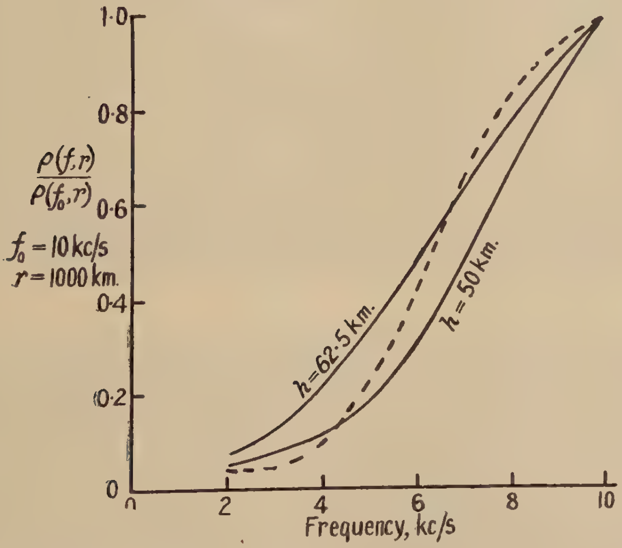

Comparison of experimental attenuation curve with curves deduced from theory of Budden.

– – – – – Experimental curve for r=1000 km.

———— Theoretical curves for 1000 km. path and height of reflecting layer h as indicated.

ACKNOWLEDGMENTS.

This work was done as part of a programme of radio research supported by the Department of Scientific and Industrial Research at the Cavendish Laboratory, Cambridge. The author wishes to acknowledge the debt due to F. F. Gardner for his part in the construction of the equipment. The author is a Scientific Trainee of the Australian Department of Supply and wishes to thank the Department for enabling him to work at the Cavendish Laboratory.

REFERENCES.

APPLETON, E. V., and CHAPMAN, F. W., 1937, *Proc. Roy. Soc.*, **158**, 1.

BARBER, N. F., URSELL, F., DARBYSHIRE, J., and TUCKER, M. J., 1946, *Nature, Lond.*, **158**, 329.

BRACEWELL, R. N., BUDDEN, K. G., RATCLIFFE, J. A., STRAKER, T. W., and WEEKES, K., 1951. Submitted for publication to Institution of Electr. Engs.

BUDDEN, K. G., 1951, *Phil. Mag.*, **42**, 1.

GARDNER, F. F., 1950, *Phil. Mag.*, **41**, 1259.

HODGSON, M. L., CLEWS, C. J. B., and COCHRAN, W., 1949, *Acta Crystallographica*, **2**, 113.

LABY, T. H., MCNEILL, J. J., NICHOLLS, F. G., NICKSON, A. S. B., 1940, *Proc. Roy. Soc.*, **174**, 145.

OCKENDEN, C. V., 1947, *Meterological Magazine*, **76**, 1.

ROSS, M. A. S., 1943, *Nature, Lond.*, **152**, 302.

SCHONLAND, B. F. J., ELDER, J. S., HODGES, D. B., PHILLIPS, W. E., and VAN WYK, J. W., 1940, *Proc. Roy. Soc.*, **176**, 180.

CAPTION FOR PLATE VI.

Two examples of the record made on individual atmospherics. For both examples (i.) and (ii.) the traces are the responses of different amplifiers as follows :—

1. Tuned to 10 kc./s.
2. Wide-band.
3. Tuned to 3·5 kc./s.
4. Tuned to 7·5 kc./s.
5. Tuned to 5 kc./s.

In example (i.), trace 2, (*a*) indicates the beginning of the atmospheric when the trace is brightened, and (*b*) is when the time-base starts the fast return to (*c*). The trace is bright for the duration of one timebase stroke so that the trace finishes just before (*a*). All traces in both (i.) and (ii.) are obtained in the same way.

Example (i.) is typical of Class I. mentioned in the text and example (ii.) of Class II.

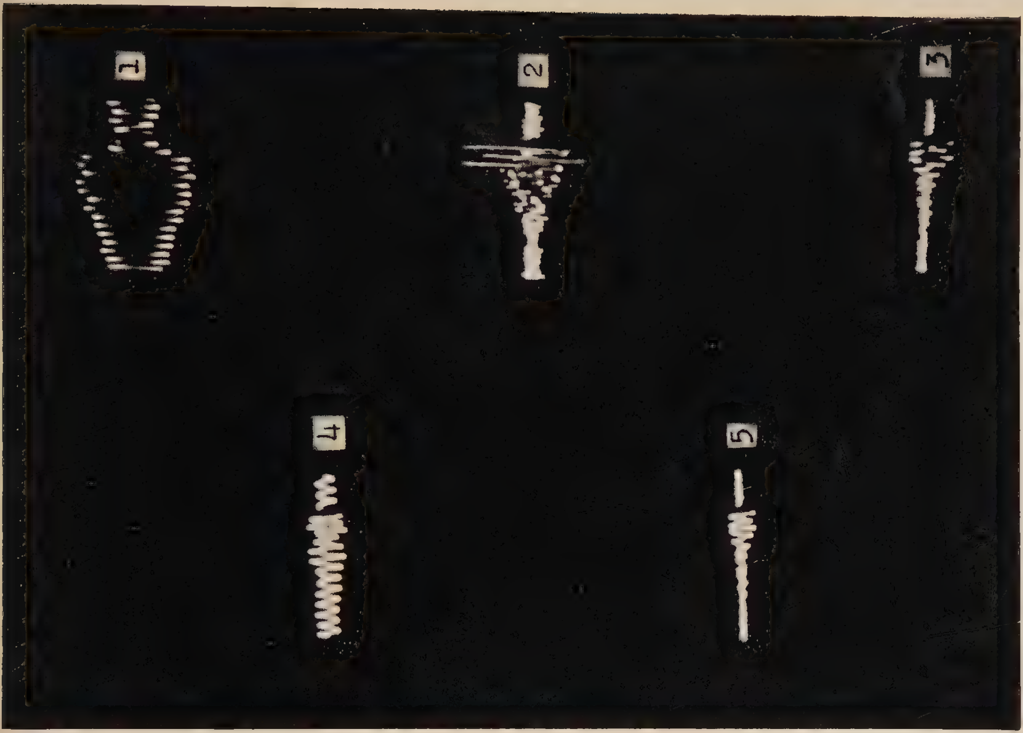

(ii)

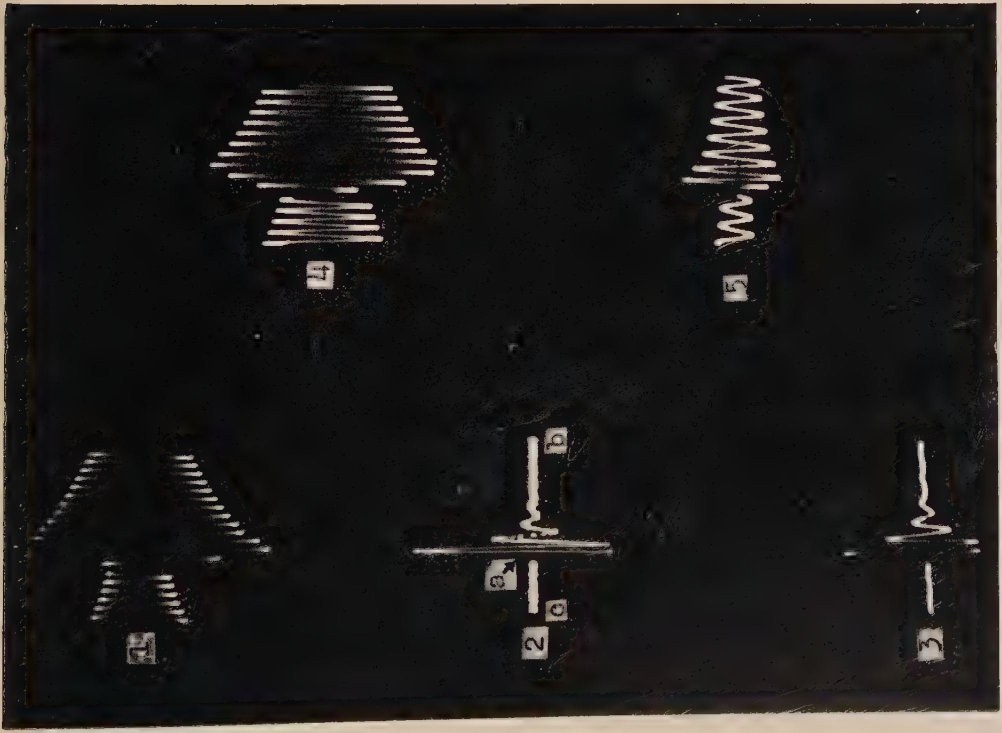

(i.)

To face page 138

XIII. *A Calculation of the Elastic Constants of Aluminium.*

By R. S. Leigh,
Mathematics Department, Imperial College, London*.

[Received November 21, 1950]

Summary.

A calculation is made of the elastic constants of aluminium which correspond to pure shears without change of volume, and an explanation is given for the fact that aluminium crystals are almost elastically isotropic. Conclusions are drawn about the nature of the density of states near the Fermi surface, and it is shown how the elastic constants may be expected to depend on electron concentration in aluminium solid solutions.

§1. Introduction.

It is well known that the total energy of a metal may be expressed approximately as a sum of separate terms. If we can calculate how these terms change as the metal is sheared, we can obtain the elastic constants of the metal as a corresponding sum of separate contributions.

Calculations of the shear constants (*i. e.* the elastic constants which relate to homogeneous strains without change of volume) of single crystals of metals have hitherto only been carried out for monovalent metals, namely the alkali metals and copper (Fuchs 1936). In these metals two important contributions appear, which arise respectively from (i.) the purely electrostatic correction term which has to be added to the potential energy obtained by using the sphere approximation of Wigner and Seitz, and (ii.) the term in the energy which is due to the non-Coulomb forces between the ion-cores. The first of these contributions is very anisotropic, the anisotropy ratio $\{C_{44}/\frac{1}{2}(C_{11}-C_{12})\}_{\text{el. st.}}$ being 8·9 for a face-centred cubic, and 7·4 for a body-centred cubic structure. For these monovalent metals the Fermi surface is approximately a sphere lying wholly inside the first Brillouin zone. The effect on the Fermi energy of movements of the bounding planes of the zone as the metal is sheared is therefore small, and the corresponding contribution to the elastic constants is negligible. In the case of metals of higher valency, however, this is no longer the case. In this paper we make an estimate of the contribution to the elastic constants from the Fermi energy in the case of aluminium, this metal being chosen for the following reason. Jones (1949) has pointed out that in the case of aluminium the contribution to the elastic constants from the non-Coulomb interaction between the ions must be negligible because of the large clearance between the ion-cores. The experimental values of the constants for aluminium, however, which are almost isotropic, are not consistent with their arising solely from the very anisotropic electrostatic contribution.

---

* Communicated by Professor H. Jones.

We are therefore led to look for another important contribution. The room temperature values for aluminium, as given by Lazarus (1949), are

$\frac{1}{2}(C_{11}-C_{12})=2{\cdot}085\,.\,10^{11}$ dynes cm.$^{-2}$ and $C_{44}=2{\cdot}853\,.\,10^{11}$ dynes cm.$^{-2}$.

It is shown in this paper that it is in fact possible to account for each of these observed values as a sum of contributions from the Fermi energy and from purely electrostatic energy terms. The large positive contribution to C_{44} from the electrostatic terms is balanced, apparently accidentally, by a correspondingly large negative contribution from the Fermi energy. In order to obtain agreement with the observed values of both C_{44} and $\frac{1}{2}(C_{11}-C_{12})$, it is necessary to assume that there are some overlapping electrons over the square faces of the Brillouin zone as well as over the hexagonal faces.

Following on these calculations it is also possible to see how the elastic constants would be expected to change with electron concentration as metals of higher or lower valency are dissolved in aluminium. There does not appear to be any experimental data relating to this.

§ 2. THE TOTAL ENERGY IN THE HARTREE APPROXIMATION.

In metals with more than one valence electron per atom, the approximate form for the wave functions of the higher states used by Wigner and Seitz for monovalent metals, viz., $\psi_0(\mathbf{r})\exp(i\mathbf{k}.\mathbf{r})$, where $\psi_0(\mathbf{r})$ is the wave function of the lowest state, can no longer be used. It follows that the Fermi energy now contains a potential as well as a kinetic part, and the valence electron density is no longer given by $-e|\psi_0|^2$. In view of this, it is necessary to reconsider the theory of the division of the total energy into separate terms.

In what follows we shall, as a first approximation, neglect valence electron exchange and correlation effects, and use the simple Hartree approximation. We do this because of the extreme difficulty of making any estimate of the contribution to the elastic constants from the correlation energy, which in metals of valency higher than one must depend on the zone structure. It would in principle be possible to make an estimate of the contribution from the exchange energy, which must also depend on the zone structure, but as these two terms are so closely related to each other it would be difficult to interpret the significance of the results.

In the Hartree approximation, the total energy W per atom, referred to a system of separated ion-cores and valence electrons, is given by the equation

$$\mathrm{NW}=2\Sigma_{\mathbf{k}}\epsilon_{\mathbf{k}}-\frac{e^2}{2}\int\!\!\int\frac{\rho(\mathbf{r})\rho(\mathbf{s})}{|\mathbf{r}-\mathbf{s}|}\,d\mathbf{r}\,d\mathbf{s}+\tfrac{1}{2}\Sigma_{\mathbf{l}}\Sigma_{\mathbf{l}'}\mathrm{U}_i(|\mathbf{R}_{\mathbf{l}}-\mathbf{R}_{\mathbf{l}'}|),\quad(\mathbf{l}\neq\mathbf{l}'),\qquad(1)$$

where the summation over **k** extends over all occupied states, the integrations, and summations over **l** and **l**′, are taken over the space occupied by N atoms, and the $\epsilon_{\mathbf{k}}$ are the one-electron energy parameters in the Hartree equations

$$\left[-\frac{h^2}{8\pi^2 m}\nabla^2+\mathrm{V}(\mathbf{r})\right]\psi_{\mathbf{k}}=\epsilon_{\mathbf{k}}\psi_{\mathbf{k}}.\qquad.\ .\ .\ .\ .\ \ (2)$$

Here $V(\mathbf{r})$ is the self-consistent field given by the equation

$$V(\mathbf{r})=\phi(\mathbf{r})+e^2\int\frac{\rho(\mathbf{s})}{|\mathbf{r}-\mathbf{s}|}\,d\mathbf{s},$$

where $\phi(\mathbf{r})$ is the potential energy of an electron in the field of all the ions in a given volume, $\rho(\mathbf{r})$ is the number density of valence electrons given by the relation $\rho(\mathbf{r})=2\Sigma_{\mathbf{k}}|\psi_{\mathbf{k}}(\mathbf{r})|^2$, and the integration is taken over the same volume. The $\psi_{\mathbf{k}}$ are supposed normalised over the volume occupied by the N atoms. $\mathbf{R}_1$ denotes the position vector of an ion, and $U_i(R)$ is the energy of interaction between two ions at a distance R apart.

Let us now define an energy $E(\mathbf{k})$ for every state by the relation $\epsilon_{\mathbf{k}}=\epsilon_0+E(\mathbf{k})$, and let us introduce the wave function of the lowest state normalized over a single atomic cell, viz., $u_0(\mathbf{r})$, where $u_0(\mathbf{r})=\sqrt{N}\psi_0(\mathbf{r})$. If we then use equation (2) for $\mathbf{k}=0$, and let Z denote the number of valence electrons per atom, we find that NW is equal to the sum of the following four terms :

(i.)
$$-NZ\frac{h^2}{8\pi^2m}\int_{\text{cell}}u_0\nabla^2u_0\,d\mathbf{r},$$

the kinetic energy of the lowest state multiplied by the number of electrons ;

(ii.)
$$2\Sigma_{\mathbf{k}}E(\mathbf{k}),$$

the Fermi energy ;

(iii.)
$$\tfrac{1}{2}\Sigma_1\Sigma_{1'}U_i(|\mathbf{R}_1-\mathbf{R}_{1'}|)+Z\int\phi(\mathbf{r})u_0^2(\mathbf{r})d\mathbf{r}+\frac{Z^2e^2}{2}\iint\frac{u_0^2(\mathbf{r})u_0^2(\mathbf{s})}{|\mathbf{r}-\mathbf{s}|}\,d\mathbf{r}\,d\mathbf{s},\quad(\mathbf{1}\neq\mathbf{1}'),$$

which is the potential energy of a system consisting of the ion-cores and a charge distribution of density $-Zeu_0^2(\mathbf{r})$; and

(iv.)
$$-\frac{e^2}{2}\iint\frac{[Zu_0^2(\mathbf{r})-\rho(\mathbf{r})][Zu_0^2(\mathbf{s})-\rho(\mathbf{s})]}{|\mathbf{r}-\mathbf{s}|}\,d\mathbf{r}\,d\mathbf{s},$$

which is the negative of the self potential energy of the charge distribution $-e[Zu_0^2(\mathbf{r})-\rho(\mathbf{r})]$ which vanishes identically in the case when the approximation $\psi_{\mathbf{k}}=\psi_0\exp(i\mathbf{k}.\mathbf{r})$ is valid.

We have now to consider the contributions made by these terms to the elastic constants.

Calculations by Raimes (1950) of u_0 in magnesium, using the sphere approximation of Wigner and Seitz, indicate that in divalent as well as monovalent metals the wave function of the lowest state is very flat near to the boundary of the atomic cell. The first stages of a similar calculation for aluminium indicate that the same is true in this case. It follows, as has been shown in the case of monovalent metals, that there is no appreciable contribution to the elastic constants from the kinetic energy of the lowest state.

The term in (iii.) which represents the ion–ion interaction may be separated into a Coulomb term, and non-Coulomb terms arising from polarization effects and exchange repulsion between closed shells. An estimate of the clearance between ion-cores, as given by Jones (1949), shows that in the case of aluminium contributions to the elastic constants from these non-Coulomb terms are negligible.

§ 3. THE COULOMB TERMS.

Let us now consider the contributions to the elastic constants from the term (iv.) above and the Coulomb part of (iii.). With regard to the latter, there is nothing different from the case of a monovalent metal. We assume that the distribution $u_0^2(\mathbf{r})$ around each lattice point moves, effectively unchanged, with that lattice point as the metal is sheared. Then the contributions to the elastic constants are approximately the same as those from a set of positive charges $Ze\Omega u_0^2(r_s)$ in a uniform sea of negative charge of density $-Zeu_0^2(r_s)$, where Ω is the atomic volume in the metal and $u_0^2(r_s)$ is the value of $u_0^2(\mathbf{r})$ at the boundary of an atomic cell.

We now consider whether it is possible to estimate the contributions from the term (iv.) in a similar way. As the boundary conditions of those wave functions which correspond to states on the bounding planes of the Brillouin zone require that they vanish over certain planes of the atomic polyhedron, we should expect that the value of $\rho(\mathbf{r})$ at a point on the boundary of the atomic polyhedron would be less than $Zu_0^2(r_s)$. The distribution $-e[Zu_0^2(\mathbf{r})-\rho(\mathbf{r})]$, which is electrostatically neutral as a whole, has thus a resultant positive charge in a region about a lattice point, and is negative outside this region. Let us now consider what happens as the metal is sheared. Since both the self-consistent field and the shape of the atomic polyhedron change, it follows that the wave functions, and so $\rho(\mathbf{r})$, will change in a very complex way. $\rho(\mathbf{r})$ has, however, two general properties, apart from its periodicity, which depend only on the symmetry of the metal lattice; its normal gradient over the boundary of an atomic polyhedron is zero, and it has in the equilibrium position, in common with $V(\mathbf{r})$ and $\psi_0(\mathbf{r})$, the full cubic symmetry of the lattice. It is thus, like $u_0^2(\mathbf{r})$, very nearly spherically symmetrical near the centre of an atomic cell. It is reasonable to assume that this nearly spherically symmetrical part moves almost unchanged with the lattice point. It also seems reasonable, as a first approximation, to average over the surface of the atomic cell and neglect actual details of what happens near to and over the different parts of the boundary. The contributions to the elastic constants are then approximately the same as those from a set of point charges $e\Omega[Zu_0^2(r_s)-\rho(r_s)]$ in a uniform sea of negative charge of density $-e[Zu_0^2(r_s)-\rho(r_s)]$, where $\rho(r_s)$ is the mean value of $\rho(\mathbf{r})$ over the boundary of an atomic cell.

The contributions to the elastic constants from a face-centred cubic lattice of point charges $+e$ set in a uniform sea of negative charge of density $-e\Omega$ have been evaluated by Fuchs (1936), and are

$$\tfrac{1}{2}(C_{11}-C_{12})=0{\cdot}1058(e^2/2a) \quad \text{and} \quad C_{44}=0{\cdot}9479(e^2/2a) \text{ per atom,}$$

where a is the lattice constant in A.U. From our discussion above it follows that we have to multiply these values by a factor $Z^2_{\rm eff}$ given by the relation

$$Z^2_{\rm eff} = \Omega^2\{[Zu_0^2(r_s)]^2 - [Zu_0^2(r_s) - \rho(r_s)]^2\}.$$

In aluminium, $u_0^2(r_s)$ is almost equal to the average value of $u_0^2(\mathbf{r})$, so that putting $Z=3$ we have

$$Z^2_{\rm eff} = 9 - [3 - \Omega\rho(r_s)]^2. \qquad \ldots\ldots\ldots \quad (3)$$

Finally, inserting the value of the lattice constant for aluminium ($a=4{\cdot}041$ A.U. at room temperature), we have for an estimate of the contributions to the shear constants from Coulomb terms :

$$\tfrac{1}{2}(C_{11} - C_{12}) = Z^2_{\rm eff}\,.\,0{\cdot}183\,.\,10^{11} \text{ dynes cm.}^{-2},$$

and $C_{44} = Z^2_{\rm eff}\,.\,1{\cdot}639\,.\,10^{11}$ dynes cm.$^{-2}$, where $Z^2_{\rm eff}$ is given by (3).

We see at once that this contribution to C_{44} is already by itself much greater than the observed value. It is difficult to see how the value of $\Omega\rho(r_s)$ could be less than say 1·5, and this gives a minimum value for $Z^2_{\rm eff}$ of 6·75, and corresponding contributions to the elastic constants of $\frac{1}{2}(C_{11}-C_{12}) = 1{\cdot}2\,.\,10^{11}$ dynes cm.$^{-2}$ and $C_{44} = 11{\cdot}1\,.\,10^{11}$ dynes cm.$^{-2}$, to be compared with the observed values of 2·1 and 2·9 . 10^{11} dynes cm.$^{-2}$ respectively.

§ 4. THE FERMI ENERGY.

Since we have no exact knowledge of the energy surfaces in momentum space, and moreover no idea of how they change as the metal is sheared, we can only proceed by making simple assumptions consistent with known general properties of these surfaces.

Aluminium has a face-centred cubic structure and therefore a body-centred reciprocal lattice, and the Brillouin zone is the well known truncated octahedron. The energy surfaces cut the bounding planes of the zone normally; they are also generally considered to be approximately spherical near to the origin, and spheroidal in the second zone near to the centres of the faces. There are three valency electrons per atom, the first zone containing sufficient states for exactly two of these with each state doubly occupied. The remaining electrons occupy states overlapping the hexagonal faces, which are the nearest to the origin, with possibly a few overlapping the square faces. There is also the possibility that the first zone may be not quite full.

Let us consider how the reciprocal lattice, and so the Brillouin zone, changes as the metal undergoes a shear. The strain energy W of a cubic lattice is given in terms of the three independent elastic constants, C_{11}, C_{12} and C_{44}, by the equation

$$W = W_0 + \tfrac{1}{2}C_{11}(e_x^2 + e_y^2 + e_z^2) + C_{12}(e_y e_z + e_z e_x + e_x e_y) + \tfrac{1}{2}C_{44}(\gamma_{yz}^2 + \gamma_{zx}^2 + \gamma_{xy}^2), \qquad \ldots \quad (4)$$

where e_x, e_y and e_z are the diagonal components of the strain tensor $\mathbf{e}$, and $\frac{1}{2}\gamma_{yz}$, $\frac{1}{2}\gamma_{zx}$ and $\frac{1}{2}\gamma_{xy}$ are the shear components. We shall choose two pure shears which correspond respectively to $\frac{1}{2}(C_{11}-C_{12})$ and C_{44}.

A shear corresponding to $\frac{1}{2}(C_{11}-C_{12})$. Consider a strain consisting of compression or extension in the (001) direction accompanied by that uniform expansion or contraction in the perpendicular plane necessary to keep the volume constant. We can express the sheared face-centred cubic lattice as follows :

$$\mathbf{a}_1=\frac{a}{2}\frac{1}{A}\left(0,\ 1,\ \frac{1}{\xi}\right),\qquad \mathbf{a}_2=\frac{a}{2}\frac{1}{A}\left(1,\ 0,\ \frac{1}{\xi}\right),\qquad \mathbf{a}_3=\frac{a}{2}\frac{1}{A}\ (1,\ 1,\ 0),$$

where in the equilibrium position $A=\xi=1$, and to keep the volume constant during a finite strain we must take $A^3=1/\xi$. Remembering that the displacement $\boldsymbol{\tau}$ at $\mathbf{r}$ is given by $\boldsymbol{\tau}=\mathbf{r}.\mathbf{e}$, it follows that the components of e in this case are as follows :

$$e_x=e_y=1/A-1,\quad e_z=1/\xi A-1,\quad \text{and}\quad \gamma_{yz}=\gamma_{zx}=\gamma_{xy}=0.$$

Inserting these values into (4) we find that

$$\tfrac{1}{2}(C_{11}-C_{12})=\frac{3}{4}\left(\frac{d^2W}{d\xi^2}\right)_0, \qquad \text{. . . . . . .} \quad (5)$$

where the suffix zero implies the value at the equilibrium position. The sheared reciprocal lattice, defined by the relations $\mathbf{a}_i.\mathbf{b}_j=2\pi\delta_{ij}$, where δ_{ij} is the Kronecker delta, is given by the vectors $\mathbf{b}_j$ as follows :

$$\mathbf{b}_1=\frac{2\pi}{a}A(-1,\ 1,\ \xi),\qquad \mathbf{b}_2=\frac{2\pi}{a}A(1,\ -1,\ \xi),\qquad \mathbf{b}_3=\frac{2\pi}{a}A(1,\ 1,\ -\xi).$$

A shear corresponding to C_{44}. Consider a strain which is the same as the previous one except that the (001) is replaced by the (111) direction. The metal lattice in this case may be expressed in the form :

$$\mathbf{a}_1=\frac{a}{2}\frac{\delta}{B}(\eta-1,\ 1,\ 1),\qquad \mathbf{a}_2=\frac{a}{2}\frac{\delta}{B}(1,\ \eta-1,\ 1),\qquad \mathbf{a}_3=\frac{a}{2}\frac{\delta}{B}(1,\ 1,\ \eta-1),$$

where $\delta=2[(1+\eta)(2-\eta)]^{-1}$, and in the equilibrium position $B=\delta=\eta=1$. For constant volume we must take $B^3=4[(1+\eta)^2(2-\eta)]^{-1}$. In this case we have $\epsilon_x=\epsilon_y=\epsilon_z=\frac{1}{2}(\delta/B)(3-\eta)-1$, $\gamma_{yz}=\gamma_{zx}=\gamma_{xy}=(\delta/B)(\eta-1)$, and

$$C_{44}=\frac{1}{3}\left(\frac{d^2W}{d\eta^2}\right)_0. \qquad \text{. . . . .} \quad (6)$$

The reciprocal lattice is given by the vectors

$$\mathbf{b}_1=\frac{2\pi}{a}\ B\ (-\eta,\ 1,\ 1),\qquad \mathbf{b}_2=\frac{2\pi}{a}\ B\ (1,\ -\eta,\ 1),\qquad \mathbf{b}_3=\frac{2\pi}{a}\ B\ (1,\ 1,\ -\eta).$$

In each case of course the first derivatives of the energy vanish at the equilibrium position.

The faces of the Brillouin zone are formed by the planes which bisect perpendicularly the lines joining the origin of the reciprocal lattice to its nearest and next nearest neighbours. We can thus determine in each of the two strains the altered positions of these planes and of the corner points where they meet.

We shall consider separately the contributions to the elastic constants from a completely filled first zone and from overlapping electrons. We shall also consider what the effect of holes in the first zone would be if they were present.

Contributions from a completely filled first zone. The following treatment is suggested by regarding the actual energy surfaces as the spherical surfaces given by the relation

$$E(\mathbf{k})=\alpha_0\frac{h^2k^2}{8\pi^2m} \qquad . \; . \; . \; . \; . \; . \; . \; . \; . \; . \qquad (7)$$

so modified as to cut the faces of the zone normally. We find that when we approximate to these modifications in a simple empirical way the resulting contributions to the elastic constants differ only slightly from the values we would obtain by considering simply the change in the energy of a zone in which the surfaces are given by (7). We conclude that this is true whatever the exact nature of the surfaces near to the faces.

Fig. 1.

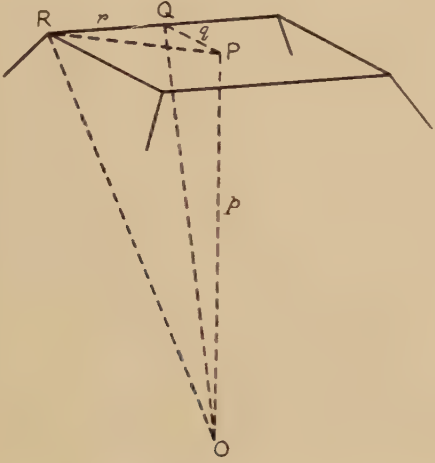

A typical tetrahedron, in this case at a square face.

Let us suppose that the first zone energies at the centres of all the faces and at the corner points are the same fraction $(1-\lambda)$ of the energies at these points given by (7). Let us also suppose that α_0 and λ remain constant during a shear, so that the energies at these points vary as the squares of the distances from the origin. Let us then divide the zone into tetrahedra (fig. 1) whose vertices are the origin O, the symmetrical centre P of a face (which even in the strained zone is the point at which it is met by the perpendicular from the origin), a corner point R of that face, and the foot Q of the perpendicular from P to an edge of the face adjacent to R. There are 144 of these tetrahedra, 12 to each hexagonal face and 8 to each square face.

We have now to find an empirical relation which expresses E(**k**) as a function of **k** within a single tetrahedron and satisfies the following conditions. If taken in all the tetrahedra with the appropriate dimensions in each one, it must fill the whole zone with energy surfaces which are continuous and continuously differentiable. We require it to satisfy the assumptions we have made, and it must possess the general features we have already described. Such a relation is

$$\mathrm{E}(\mathbf{k})=\alpha_0\frac{h^2}{8\pi^2 m}\left\{k^2-\lambda\left[p^2\left(\frac{k_z'}{p}\right)^{2/\lambda}+q^2\left(\frac{k_y'}{q}\right)^{2/\lambda}+r^2\left(\frac{k_x'}{r}\right)^{2/\lambda}\right]\right\}, \quad . \quad (8)$$

where k_z', k_y' and k_x' are measured in each tetrahedron in the directions of OP, PQ and QR respectively, and p, q and r are the appropriate lengths of these edges. Fig. 2 shows how the parameter λ modifies the surfaces so that they cut the faces normally. $\mathrm{E}(\mathbf{k})/(\alpha_0 h^2 p^2/8\pi^2 m)$ is shown as a function of k_z'/p along OP for different values of λ.

Fig. 2.

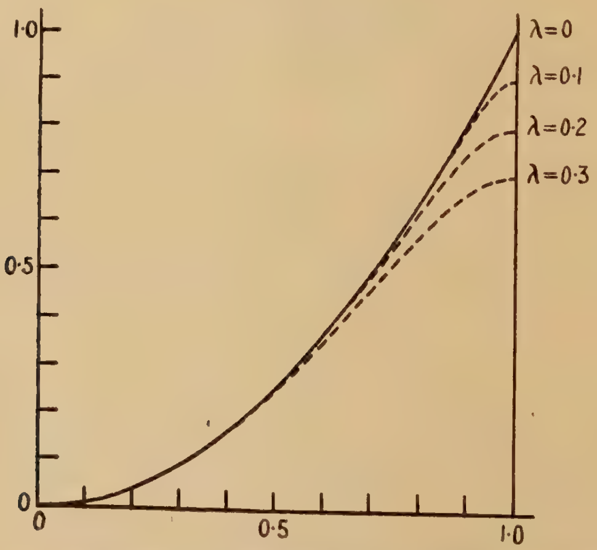

The effect of the parameter λ in expression (8). $\mathrm{E}(\mathbf{k})/(\alpha_0 h^2 p^2/8\pi^2 m)$ is shown as a function of k_z'/p along OP.

We have now to use these surfaces to calculate the first zone part $\mathrm{W}_{\mathrm{F}}^{\mathrm{I}}$ of the Fermi energy. The contribution from a single tetrahedron is

$$\frac{2}{8\pi^3}\alpha_0\frac{h^2}{8\pi^2 m}pqr[\mathrm{F}p^2+\mathrm{G}q^2+\mathrm{H}r^2],$$

where

$$\mathrm{F}=\frac{1}{10}-\frac{\lambda^2}{2(2+3\lambda)}, \qquad \mathrm{G}=\frac{1}{20}-\frac{\lambda^3}{2(2+3\lambda)(1+\lambda)},$$

$$\mathrm{H}=\frac{1}{60}-\frac{\lambda^4}{2(2+3\lambda)(1+\lambda)(2+\lambda)}.$$

For each tetrahedron p, q, and r are functions of the strain parameter, ξ or η. We find that because of the high symmetry of the distortions we have chosen there are only six different tetrahedra in the first shear, and five in the second. Summing over all the tetrahedra we obtain W_F^I as a function of the strain parameter in each case. For the shear corresponding to $\frac{1}{2}(C_{11}-C_{12})$ we find for the contribution to the energy per unit volume

$$W_F^I=\frac{\alpha_0 h^2}{2ma^5}\xi^{-5/3}[F(16\xi+36\xi^3-16\xi^5+3\xi^7)+G(16\xi-12\xi^3+16\xi^5-5\xi^7)$$
$$+H(16\xi-20\xi^3+8\xi^5+2\xi^7)],$$

and for the shear corresponding to C_{44}

$$W_F^I=\frac{3\alpha_0 h^2}{2ma^5}\left[\frac{4}{(1+\eta)^2(2-\eta)}\right]^{5/3}\frac{1}{(1+\eta)^2}[F(16-128\eta+406\eta^2-341\eta^3$$
$$+96\eta^4+10\eta^5-6\eta^6-\eta^7)$$
$$-G(40-300\eta+578\eta^2-499\eta^3+184\eta^4-22\eta^5-2\eta^6+\eta^7)$$
$$+H(64-152\eta+158\eta^2-121\eta^3+96\eta^4-46\eta^5+10\eta^6-\eta^7)].$$

From these expressions we find that

$$\left(\frac{dW_F^I}{d\xi}\right)_0=\left(\frac{dW_F^I}{d\eta}\right)_0=0,$$

and, using relations (5) and (6), that the contributions to the elastic constants from a completely filled first zone are

$$\tfrac{1}{2}(C_{11}-C_{12})=\frac{\alpha_0 h^2}{3ma^5}\left[1+\frac{6\lambda^2(4+2\lambda-11\lambda^2)}{(2+3\lambda)(1+\lambda)(2+\lambda)}\right],$$

and

$$C_{44}=\frac{\alpha_0 h^2}{ma^5}\left[1-\frac{2\lambda^3(8+7\lambda)}{(2+3\lambda)(1+\lambda)(2+\lambda)}\right].$$

We see that the effect of taking a value of λ different from zero is very small. Even with a value of λ as large as 0·3 the variation in the elastic constants is only of the order of $0{\cdot}3\times10^{11}$ dynes cm.$^{-2}$. We shall therefore take as our estimates of the contributions to the elastic constants from a filled first zone the values corresponding to $\lambda=0$. These are

$$\tfrac{1}{2}(C_{11}-C_{12})=1{\cdot}5\alpha_0\,.\,10^{11}\text{ dynes cm.}^{-2}\quad\text{and}\quad C_{44}=4{\cdot}5\alpha_0\,.\,10^{11}\text{ dynes cm.}^{-2}$$

at room temperature. We do not know the value of α_0 in aluminium, but we are unlikely to be involved in serious error by taking it to be unity.

Contributions from overlapping electrons. We shall make here the simple assumption that during shear the energy surfaces over a face in the second zone move with that face without change relative to it. We shall also neglect the small effect of finite temperature on the Fermi distribution, and suppose that the states are completely filled with two electrons each up to an energy ζ.

It is easy to see what happens as the metal is sheared, if we remember that the number of electrons per atom remains exactly three, and the energy ζ, while changing its value, is the same for different parts of the Fermi surface. As the distances of the faces from the origin vary, electrons will transfer from those faces receding from the origin to those approaching it. The change in the Fermi energy has thus two causes : the shift of the energy surfaces as a whole with the faces, and the relaxation effect of the electron transfer. Let us examine this in detail.

It follows from the symmetry of the reciprocal lattice that the perpendicular distances from the origin of opposite faces of the zone are always equal, so that we may take these faces together in pairs. Since faces of one kind, hexagonal or square, do not in general remain at equal distances from the origin during shear, we shall refer to the pairs of faces by two suffices, i denoting the kind of face, and j the different pairs of that kind. Let us define the density of states N(E) as the number of electrons per atom per unit energy range, allowing for two electrons being in each state, and denote by $\mathrm{N}_i(\mathrm{E}-\mathrm{E}_{ij})$ the contribution to N(E) from the pair of faces with energy E_{ij} at the centre of a face. Then the total number of electrons per atom, n_{ij}, occupying states over this pair of faces in the sheared state is given by

$$n_{ij}=\int_0^{\zeta-\mathrm{E}_{ij}}\mathrm{N}_i(\epsilon)\,d\epsilon. \quad . \quad . \quad . \quad . \quad . \quad . \quad . \quad . \quad (9)$$

If we denote by $\mathrm{W}_{\mathrm{F}}^{\mathrm{II}}$ the total contribution to the Fermi energy from overlapping electrons, we have that

$$\mathrm{W}_{\mathrm{F}}^{\mathrm{II}}=\Sigma_{i,j}\,\mathrm{W}_{ij},$$

where

$$\mathrm{W}_{ij}=\int_{\mathrm{E}_{ij}}^{\zeta}\mathrm{N}_i(\mathrm{E}-\mathrm{E}_{ij})\mathrm{E}\,d\mathrm{E}$$

$$=n_{ij}\mathrm{E}_{ij}+\int_0^{\zeta-\mathrm{E}_{ij}}\mathrm{N}_i(\epsilon)\epsilon\,d\epsilon. \quad . \quad . \quad . \quad . \quad . \quad . \quad . \quad (10)$$

If we let x stand for either strain parameter, ξ or η, and differentiate equation (9) with respect to x, we have

$$\frac{dn_{ij}}{dx}=\mathrm{N}_i(\zeta-\mathrm{E}_{ij})\left(\frac{d\zeta}{dx}-\frac{d\mathrm{E}_{ij}}{dx}\right). \quad . \quad . \quad . \quad . \quad . \quad . \quad (11)$$

Since the number of electrons per atom does not depend on x, we have

$$\Sigma_{i,j}\frac{dn_{ij}}{dx}=0. \quad . \quad . \quad . \quad . \quad . \quad . \quad . \quad . \quad . \quad . \quad (12)$$

If we assume that during shear the energies at the centres of all faces of one kind, hexagonal or square, are the same function of the perpendicular distance of the face from the origin, it follows that $d\mathrm{E}_{ij}/dx$ is proportional to dp_{ij}/dx, where the constant of proportionality depends only on i, and so $\Sigma_j d\mathrm{E}_{ij}/dx$ is proportional to $\Sigma_j dp_{ij}/dx$. We find below that the vanishing of $\Sigma_j(dp_{ij}/dx)_0$ for all i follows as a geometrical consequence of the volume remaining constant. We have then

$$\Sigma_j\left(\frac{d\mathrm{E}_{ij}}{dx}\right)_0=0. \quad . \quad . \quad . \quad . \quad . \quad . \quad . \quad . \quad . \quad (13)$$

Taking together equations (11) and (12) in the equilibrium position, and using equation (13), we find that

$$\left(\frac{d\zeta}{dx}\right)_0=0. \quad . \quad . \quad . \quad . \quad . \quad . \quad . \quad . \quad . \quad (14)$$

If we now differentiate equation (10) twice with respect to x, use equations (11), (12), (13) and (14), and sum over i and j, we find that $(d\mathrm{W}_{\mathrm{F}}^{\mathrm{II}}/dx)_0=0$, and

$$\left(\frac{d^2\mathrm{W}_{\mathrm{F}}^{\mathrm{II}}}{dx^2}\right)_0=\Sigma_i\left[n_i\Sigma_j\left(\frac{d^2\mathrm{E}_{ij}}{dx^2}\right)_0-\mathrm{N}_i(\zeta_0-\mathrm{E}_i)\Sigma_j\left(\frac{d\mathrm{E}_{ij}}{dx}\right)_0^2\right], \quad . \quad (15)$$

where n_i, ζ_0 and E_i are the equilibrium position values of n_{ij}, ζ and E_{ij} respectively.

We can obtain estimates of the values of the summations over j in equation (15) by assuming that the energies E_{ij} vary as the squares of the distances from the origin of the points they refer to. Equation (15) then has the form

$$\left(\frac{d^2\mathrm{W}_{\mathrm{F}}^{\mathrm{II}}}{dx^2}\right)_0=\Sigma_i[\lambda_i n_i\mathrm{E}_i-\mu_i\mathrm{N}_i(\zeta_0-\mathrm{E}_i)\mathrm{E}_i^2], \quad . \quad . \quad . \quad . \quad (16)$$

where the λ_i and μ_i are numerical coefficients.

The squared distances of the faces from the origin in each shear are as follows. In the shear corresponding to $\frac{1}{2}(\mathrm{C}_{11}-\mathrm{C}_{12})$, the four pairs of hexagonal faces are at the same distance $(\pi/a)\mathrm{A}(2+\xi^2)^{\frac{1}{2}}$ from the origin, the pair of square faces in the (001) direction are at a distance $(2\pi/a)\mathrm{A}\xi$, and the other two pairs are at a distance $(2\pi/a)\mathrm{A}$. In the shear corresponding to C_{44}, the pair of hexagonal faces in the (111) direction are at a distance $(\pi/a)\sqrt{3}\mathrm{B}(2-\eta)$ from the origin, the other three pairs are at a distance $(\pi/a)\mathrm{B}(2+\eta^2)^{\frac{1}{2}}$, and the three pairs of square faces are at a distance $(\pi/a)\sqrt{2}\mathrm{B}(3-2\eta+\eta^2)^{\frac{1}{2}}$. From a knowledge of these distances it is easy to evaluate the coefficients λ_i and μ_i for each shear, and to verify the result $\Sigma_j(dp_{ij}/dx)_0=0$ in each case. The following table shows the contributions to the elastic constants per atom from overlapping electrons over hexagonal and square faces, obtained from equation (16) using relations (5) and (6).

	Hexagonal faces	Square faces
$\frac{1}{2}(\mathrm{C}_{11}-\mathrm{C}_{12})$	$\frac{8}{3}n_a\mathrm{E}_a$	$2n_b\mathrm{E}_b-2\mathrm{N}_b\mathrm{E}_b^2$
C_{44}	$\frac{8}{3}n_a\mathrm{E}_a-\frac{16}{9}\mathrm{N}_a\mathrm{E}_a^2$	$2n_b\mathrm{E}_b$

n_a and n_b are the numbers of electrons per atom in the equilibrium position over one pair of hexagonal and square faces respectively, N_a and N_b the corresponding contributions to the density of states per atom at the Fermi surface, and E_a and E_b the equilibrium position energies at the centres of the faces. In each case the positive term involving the λ coefficient may be regarded as arising directly from the shift of the energy surfaces as a whole with the faces, and the negative term involving the μ coefficient as arising from electron transfer between the faces. This electron transfer term only arises of course when some of the faces in question approach the origin and others recede from it. Thus it does not appear in the contributions from hexagonal faces to $\frac{1}{2}(C_{11}-C_{12})$ or from square faces to C_{44}, as in these cases the faces remain at an equal distance from the origin.

We can further reduce the number of parameters involved by approximating to the energy surfaces with spheroids. For the surfaces over the face given by the sufficies i and j, we have

$$E=E_{ij}+\frac{h^2}{8\pi^2 m}[k_x'^2+k_y'^2+\alpha_i(k_z'-p_{ij})^2],$$

where k_z' is measured perpendicular to the face, and α_i remains constant during shear. We then have

$$n_i=\frac{\Omega}{4\pi^3}\,\frac{4\pi}{3}\,\frac{1}{\sqrt{\alpha_i}}\left[\frac{8\pi^2 m}{h^2}(\zeta_0-E_i)\right]^{3/2}.$$

and
$$N_i=\frac{3}{2}\,\frac{n_i}{\zeta_0-E_i}. \qquad (17)$$

The effect of the presence of holes in the first zone. We can proceed exactly as with overlapping electrons, the only differences being changes of sign. The following table shows contributions to the elastic constants corresponding to two ways in which holes could occur, viz. (i.) at the corner points, and (ii.) in approximately plane regions over the square faces, as suggested by Matyas (1948).

	Holes at the corner points	Holes over the square faces
$\frac{1}{2}(C_{11}-C_{12})$	$-\frac{44}{5}n_c E_c-\frac{4}{25}N_c E_c^2$	$-2n_d E_d \;\; -2N_d E_d^2$
C_{44}	$-\frac{28}{5}n_c E_c$	$-2n_d E_d$

n_c is the number of holes per atom in one closed region, formed by the holes at four corner points (there are six closed regions in all), and n_d is the number over one pair of square faces; N_c and N_d are the corresponding contributions to the density of states per atom at the Fermi surface; and E_c and E_d are the first zone energies at the corner points and the centres of the square faces respectively. It will be noticed that the terms arising from the shift of the energy surfaces are negative for holes.

§ 5. DISCUSSION.

As we do not know the values of any of the parameters which appear in our results, viz. $\rho(r_s)$, α_a and α_b, E_a and E_b etc., we cannot make a direct calculation of the elastic constants. We can however see whether it is possible, by assuming reasonable values for these parameters, to account for the observed values of the constants as the sum of the three contributions which enter into the present theory. In doing this we can make use of two observed quantities which depend on the band structure. These are: (i.) the width of the soft X-ray emission spectrum, given by Skinner (1940) as 11·8 eV., which corresponds to ζ_0; and (ii.) the electronic specific heat, given by Kok and Keesom (1937) as $3{\cdot}484\times10^{-4}$T cal. deg.$^{-1}$mol.$^{-1}$, which is given in terms of the density of states per atom at the Fermi surface by the expression $(\pi^2/3)k\mathrm{N}(\zeta_0)\mathrm{RT}$, giving $\mathrm{N}(\zeta_0)=0{\cdot}614$ per eV. per atom.

Let us leave aside for the moment the possibility of holes in the first zone. If there is only overlap over the hexagonal faces, then we have $4n_a=1$ and $4\mathrm{N}_a=\mathrm{N}(\zeta_0)$, and the contributions from overlapping electrons to $\frac{1}{2}(\mathrm{C}_{11}-\mathrm{C}_{12})$ and C_{44} are $\frac{2}{3}\mathrm{E}_a$ and $\frac{2}{3}\mathrm{E}_a-\frac{4}{9}\mathrm{N}(\zeta_0)\mathrm{E}_a^2$ respectively. Using relation (17) we find $\zeta_0-\mathrm{E}_a=2{\cdot}4$ eV., and therefore $\mathrm{E}_a=9{\cdot}4$ eV. These contributions to the elastic constants are then $\frac{1}{2}(\mathrm{C}_{11}-\mathrm{C}_{12})=6{\cdot}3$ eV. per atom$=6{\cdot}1\times10^{11}$ dynes cm.$^{-2}$, and $\mathrm{C}_{44}=-17{\cdot}8$ eV. per atom$=-17{\cdot}3\times10^{11}$ dynes cm.$^{-2}$. The very large negative contribution to C_{44}, due to electron transfer between the hexagonal faces, is just what we are looking for to balance the large positive Coulomb and first zone contributions. The contribution to $\frac{1}{2}(\mathrm{C}_{11}-\mathrm{C}_{12})$ however is even by itself much greater than the observed value of this constant, viz., $2{\cdot}1\times10^{11}$ dynes cm.$^{-2}$. This value can only be reduced by supposing that there is some overlap over the square faces as well as the hexagonal faces. We then have a negative contribution to $\frac{1}{2}(\mathrm{C}_{11}-\mathrm{C}_{12})$ from electron transfer between them. We now have five parameters, viz. $\rho(r_s)$, E_a, E_b, α_a and α_b, to relate to four observed quantities, viz. ζ_0, $\mathrm{N}(\zeta_0)$, and the two elastic constants. Since the number of overlapping electrons over the square faces is small, it is reasonable to use the approximate expression for α_b derived from the theory of nearly free electrons, viz. $\alpha_b=1+2\mathrm{E}_b^{(0)}/(\mathrm{E}_b-\mathrm{E}_b^{(0)})$, where $\mathrm{E}_b^{(0)}$ is the free electron energy at the centre of a square face, *i. e.* $(h^2/8\pi^2m)(2\pi/a)^2=9{\cdot}2$ eV. We then find that the values we have to assign to the parameters, in order to reproduce the observed values of the elastic constants, are as follows: $\mathrm{Z}^2_{\mathrm{eff}}=6{\cdot}9_7$, and therefore $\Omega\rho(r_s)=1{\cdot}5_8$; $\mathrm{E}_a=9{\cdot}0_8$ eV. and $\alpha_a=1{\cdot}9_4$; $\mathrm{E}_b=11{\cdot}2_1$ eV. and $\alpha_a=10{\cdot}2_1$. The corresponding values of n_a and n_b are $0{\cdot}24_2$ and $0{\cdot}01_1$ per atom respectively, and those of N_a and N_b are $0{\cdot}133_4$ per eV. per atom and $0{\cdot}027_0$ per eV. per atom respectively. The following table shows the constitution of the observed elastic constants as explained by this model. The units are 10^{11} dynes cm.$^{-2}$.

Contributions	$\frac{1}{2}(\mathrm{C}_{11}-\mathrm{C}_{12})$	C_{44}
Coulomb	1·3	11·4
First zone	1·5	4·5
Overlapping electrons	−0·7	$-13{\cdot}0_5$
Total (observed)	2·1	$2{\cdot}8_5$

It will be noticed that the value we have to assume for α_a is much lower than would be given by an expression corresponding to the one we have used for α_b. This is not a serious objection, however, as the region of occupied states over the hexagonal faces goes well beyond the range of validity of such an expression. On the other hand it still seems reasonable to approximate, as we have done, to the general shape of the energy surfaces with spheroids, while leaving α_a unspecified.

It is of interest to enquire whether the observed constants could be explained by assuming the existence of holes in the first zone instead of overlap over the square faces. We see however that in the case of holes at the corner points the coefficient of the term in $\frac{1}{2}(C_{11}-C_{12})$ arising from electron transfer is very small. In fact, if we assume spherical energy surfaces about the corner points, we find that in order to account for the observed values of both elastic constants consistently with known values of ζ_0 and $N(\zeta_0)$, and with a value of $\Omega\rho(r_s)$ not less than 1·5, it is necessary to assume that there are at least 0·3 holes per atom (*i. e.* 0·05 in a single closed region), and that the corner point energy E_c is at least as high as 16·5 eV. This is 5 eV. above the free-electron energy of $(h^2/8\pi^2m)\ 5(\pi/a)^2=11{\cdot}5$ eV. In the case of holes over the square faces, the coefficients of the terms are of course the same as for overlapping electrons there, the only difference being the sign of the term arising directly from the shift of the energy surfaces, and this is very small as long as the number of electrons or holes is small. It is thus possible to explain the elastic constants in the same way. We should however have to assume a value of E_d a little greater than ζ_0, *i. e.* about 3 eV. above the free-electron energy of 9·2 eV. These high first zone energies would imply energy surfaces which are very different from those of the simple model we have been using, and the present theory is not really adequate for their discussion. It is clear, however, that the elastic constants cannot be explained by assuming a small number of holes at the corner points in the same way as they can be by assuming a small number of overlapping electrons over the square faces. This is because in the shear corresponding to $\frac{1}{2}(C_{11}-C_{12})$ the corner points do not move as much as the centres of the square faces, so that the resulting amount of electron transfer is smaller, and the corresponding negative contribution to the elastic constant is not large enough to balance the large positive contribution from the hexagonal faces. There still remains the possibility that there are a small number of holes at the corner points, as well as overlapping electrons over the square faces, but this would have only a very small effect on the elastic constants.

§ 6. VARIATION OF THE ELASTIC CONSTANTS WITH ELECTRON CONCENTRATION.

When metals of valency higher or lower than three are dissolved substitutionally in aluminium, and the valency electrons of the soluble atoms are shared with the whole metal, there is a change in the number of occupied states in the band scheme. The consequent change in the height of the filled region leads to a change in the contributions to the elastic constants from overlapping electrons. The full curves in fig. 3 show the effect on the total elastic constants of the variation of these contributions with the electron concentration per atom. The large rise in $\frac{1}{2}(C_{11}-C_{12})$ with falling electron concentration is due to the decrease in magnitude of the negative term arising from electron transfer between the square faces in the corresponding shear. This term is proportional to the contribution from these faces to the density of states at the Fermi surface, and so is proportional to the cube root of the number of overlapping electrons there. There is thus a very sharp change in $\frac{1}{2}(C_{11}-C_{12})$ at an electron concentration of approximately 2·67 per atom, which is the point at which there is just no overlap over the square faces. Similarly, as the electron concentration falls still further, and the number of overlapping electrons over the hexagonal faces becomes small, C_{44} begins to rise rapidly. There are also changes in the details of the energy surfaces in momentum space, and so in the density of states curve, but we should expect the effect of these changes on the elastic constants to be relatively small.

Fig. 3.

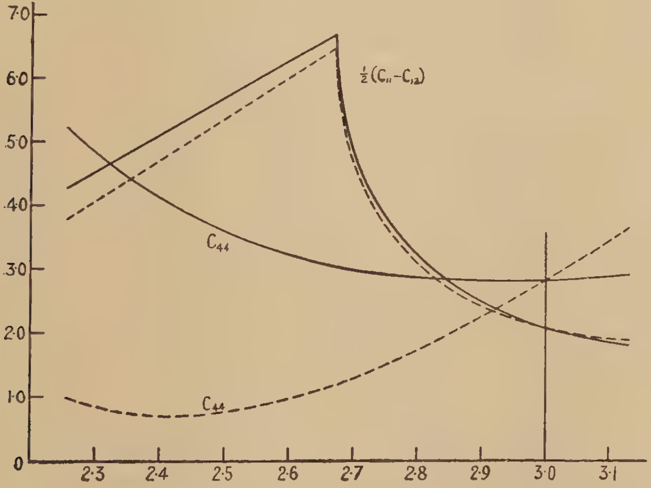

Variation of the elastic constants with electron concentration (units 10^{11} dynes cm.$^{-2}$). The full curves show the effect of the variation of the contributions from overlapping electrons alone. In the broken curves an allowance has been made for the change in the Coulomb contribution.

At some point as the electron concentration decreases, holes will appear in the first zone. From the results we have obtained in §4 for the contributions to the elastic constants from holes, we should expect that this would have little effect on C_{44} but would lead to a sharp fall in the value of $\frac{1}{2}(C_{11}-C_{12})$. The magnitude of this would depend on the curvature of the energy surfaces near the point of highest energy in the first zone. If there were no overlap over the square faces in pure aluminium, but instead holes in the first zone, then the variation of the elastic constants with electron concentration would be different from that shown in fig. 3, and would depend on the position of the point of highest energy in the first zone. If the holes were at the corner points there would be a rather large decrease in both $\frac{1}{2}(C_{11}-C_{12})$ and C_{44} with decreasing electron concentration. If they were over the square faces the effect for small changes of electron concentration would be similar to that shown in fig. 3; it is not possible to say what would happen at lower electron concentrations, except that we should not expect a sharp change in $\frac{1}{2}(C_{11}-C_{12})$ of the kind that arises from the disappearance of overlap over the square faces.

Fig. 4.

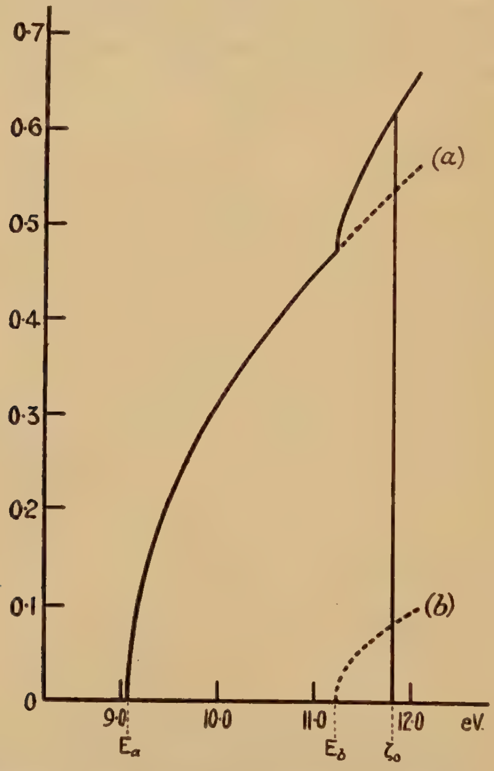

The contributions to the density of states, N(E) per eV. per atom from overlapping electrons over (*a*) hexagonal faces, and (*b*) square faces. The full curve is the sum of curves (*a*) and (*b*).

As well as changes in the Fermi energy contributions to the elastic constants, there are also changes in the Coulomb contributions arising from the changes in electron density in the metal. This effect is probably small in the case of $\frac{1}{2}(C_{11}-C_{12})$ because of the small Coulomb contribution, but it is important in the case of C_{44}. In order to obtain an estimate of the size of this effect in the case, for example, of a divalent solute, let us consider a crystal of the pure solute in a hypothetical face-centred cubic phase with the same lattice constant as aluminium. We should expect the value of $\Omega\rho(r_s)$ in this crystal to lie between say 1·0 and 2·0, and so Z^2_{eff} between 3·0 and 4·0. As the concentration of this solute in aluminium varies from zero to unity, the Coulomb contributions to the elastic constants change from the values for pure aluminium to those for this hypothetical crystal. The values between these two limits will depend on the exact nature of the changes in the electron density. The broken curves in fig. 3 have been obtained by supposing that Z^2_{eff} varies linearly with solute concentration between the values of $6{\cdot}9_7$ for pure aluminium and 3·5 for an electron concentration of 2·0 per atom. It is difficult to see how the net effect on the elastic constants can be such as to give rise to values which are very different from these.

There does not appear to be any experimental data available relating to the change in the single crystal elastic constants with electron concentration. One difficulty is that only very small quantities of other metals are soluble in aluminium at room temperature without a phase change occurring. The most soluble are magnesium and zinc, which dissolve to the extent of about 2 atomic per cent, corresponding to a fall in electron concentration of 0·02 per atom. This should give, according to the broken curves in fig. 3, an increase in $\frac{1}{2}(C_{11}-C_{12})$ of approximately $0{\cdot}05 . 10^{11}$ dynes cm.$^{-2}$ and a decrease in C_{44} of approximately $0{\cdot}12 . 10^{11}$ dynes cm.$^{-2}$. This corresponds to a change in the ratio $C_{44}/\frac{1}{2}(C_{11}-C_{12})$ from 1·37 to 1·28, a decrease of 6·4 per cent. The only way to measure the effect of larger changes of electron concentration would be to make observations either at higher temperatures or on quenched solutions. The most favourable case for this is that of zinc, which has a maximum solubility of 66·5 atomic per cent at 382° C. This corresponds to an electron concentration of 2·335 per atom. Other possibilities are magnesium, with a maximum solubility of 16 atomic per cent at 450° C., and silver, with a maximum solubility of 18 atomic per cent at 538° C. These correspond to electron concentrations of 2·84 and 2·64 per atom respectively. Copper has a maximum solubility of 2·5 atomic per cent at 548° C, corresponding to an electron concentration of 2·95 per atom. Silicon appears to be the only element with more than three valency electrons per atom which is appreciably soluble even at high temperatures, the maximum solubility in this case being approximately 2 atomic per cent at 577° C. This corresponds to an electron concentration of 3·02 per atom.

ACKNOWLEDGMENTS.

The author is indebted to Professor H. Jones, who suggested the problem, for his continual help and advice, and to the Senate of the University of London for the award of a Postgraduate Studentship.

REFERENCES.

FUCHS, K., 1936, *Proc. Roy. Soc.* A, **153**, 622 and **157**, 444.
JONES, H., 1949, *Physica*, **15**, 13.
KOK, J. A., and KEESOM, W. H., 1937, *Physica*, **4**, 835.
LAZARUS, D., 1949, *Phys. Rev.* [2], **76**, 544.
MATYAS, Z., 1948, *Phil. Mag.* [7], **39**, 429.
RAIMES, S., 1950, *Phil. Mag.* [7], **41**, 568.
SKINNER, H. W. B., 1940, *Phil. Trans. Roy. Soc.* A, **239**, 95.

XIV. *The Condensation of a Perfect Bose–Einstein Gas.—I.*

By A. R. Fraser,
Royal Society Mond Laboratory, Cambridge*.

[Received October 24, 1950.]

Abstract.

Schubert (1946) and others have drawn attention to the fact that the standard derivations of the formulæ for the behaviour of a perfect Bose–Einstein gas are invalid in the region where condensation should occur. In this paper a new and rigorous derivation is given of formulæ for the macroscopic behaviour of such a gas.

§1. Introduction.

Schubert (1946) and Dingle (1949) have pointed out that discussions of the phenomenon of condensation in a perfect Bose–Einstein gas by London (1938) and Fowler and Jones (1938) are invalid because of the divergence of some of the series used. Temperley (1949) has considered the behaviour of a model with equally spaced energy levels and has concluded that the usually accepted formulæ are incorrect in this case.

In this paper formulæ for the macroscopic behaviour of a perfect Bose–Einstein gas will be found by a method similar to one used by Kahn and Uhlenbeck (1938) in considering the condensation of an imperfect gas. We shall have in mind the particular case of a perfect gas in a cubic box, but the results will be expressed in a more general form so that they may be applied to a perturbed system such as a perfect gas in an external field.

In a second paper (Fraser 1951) formulæ for the occupation numbers of the energy levels will be obtained.

All the thermodynamic functions for a perfect gas of N particles can be found from the partition function†

$$Z_N = \Sigma' \exp\{-\mu \sum_i n_i \epsilon_i\}, \quad . \; . \; . \; . \; . \; . \; . \; . \; . \quad (1)$$

where $\mu = 1/kT$, Σ' means the sum over all values of the set of positive integers $n_0, n_1, n_2 \ldots$ such that $\sum_i n_i = N$, and $\epsilon_0, \epsilon_1, \epsilon_2, \ldots$ are the energy levels for the individual particles. In particular, the free energy of the gas is given by the relation

$$F = -kT \log Z_N, \quad . \; . \; . \; . \; . \; . \; . \quad (2)$$

---

* Communicated by the Author.

† See, for instance, Schroedinger, E. *Statistical Thermodynamics* (Cambridge, 1945).

and all other thermodynamic functions can be derived from this by well known relations.

For a Bose–Einstein gas it is easily seen that Z_N is the coefficient of ζ^N in

$$\prod_i[1+\zeta \exp(-\mu\epsilon_i)+\zeta^2 \exp(-2\mu\epsilon_i)+\ldots]^{\omega_i}=\prod_i[1-\zeta \exp(-\mu\epsilon_i)]^{-\omega_i}, \quad . \; . \; . \; (3)$$

where ω_i is the weight of the level with energy ϵ_i. We can therefore write

$$Z_N=\frac{1}{2\pi i}\oint\zeta^{-(N+1)}\prod_i[1-\zeta \exp(-\mu\epsilon_i)]^{-\omega_i}d\zeta, \quad . \; . \; . \; . \; . \; (4)$$

where the contour includes the origin, but excludes the poles $\zeta=\exp(\mu\epsilon_i)$ on the real axis. In the method used by Fowler (1936) this integral is evaluated by the method of steepest descents, but this has been shown by Schubert to be invalid in the neighbourhood of the condensation point.

In this paper we shall find an expression for the free energy per particle as the volume and the number of particles tend to infinity in such a way that the number per unit volume remains constant.

§2. THE ASYMPTOTIC FORM OF THE PARTITION FUNCTION.

The energy levels ϵ_i will depend on the volume of the gas and we must first impose some restrictions on this dependence. We write

$$\frac{1}{s}\sum_i\omega_i\exp(-s\mu\epsilon_i)=a_s(V), \quad . \; . \; . \; . \; . \; . \; . \; (5)$$

where $a_s(V)$ is a function of the volume only, and require that there exists a set of functions $b_s(\rho)$, depending only on the density $\rho=N/V$, such that, for $N>M$, where M is any integer,

$$\left.\begin{array}{ll}\text{(i) } a_s(V)<(1+\delta_M)Nb_s(\rho) & \text{for all } s,\\ \text{(ii) } a_s(V)>(1-\delta_M)Nb_s(\rho) & \text{for all } s<s_M,\\ \multicolumn{2}{l}{\text{(iii) the radius of convergence of } \sum_{s=1}^{\infty} b_s(\rho)x^s \text{ is unity,}}\\ \multicolumn{2}{l}{\text{and (iv) } \sum_{s=1}^{\infty} sb_s(\rho) \text{ is finite,}}\end{array}\right\} \quad . \; . \; (6)$$

where δ_M tends to zero and s_M tends to infinity as M tends to infinity. We will in future write merely b_s for $b_s(\rho)$. A discussion of these restrictions will be relegated to the appendix where it will be shown that they are satisfied by the energy levels for a perfect gas in a cubic box. We see from the definitions that the b_s's are always positive.

Rewriting (3), we find that Z_N is the coefficient of ζ^N in $\exp\sum_r a_r\zeta^r$, and hence that Z_N may be considered as a monotonically increasing function of the a_r's. It follows that if we define functions $Z'_{N,M}$ and $Z''_{N,M}$ such that

$$\left.\begin{aligned} Z'_{N,M} &= \frac{1}{2\pi i}\oint \zeta^{-(N+1)} \exp\left\{N(1+\delta_M)\sum_{s=1}^{\infty} b_s\zeta^s\right\}d\zeta, \\ Z''_{N,M} &= \frac{1}{2\pi i}\oint \zeta^{-(N+1)} \exp\left\{N(1-\delta_M)\sum_{s=1}^{s_M} b_s\zeta^s\right\}d\zeta, \end{aligned}\right\} \quad . \quad (7)$$

then $Z'_{N,M} > Z_N > Z''_{N,M}$ for all $N > M$.

The contours are to be taken round the origin but inside the radius of convergence of $\sum\limits_s b_s\zeta^s$. $Z'_{N,M}$ and $Z''_{N,M}$ are always positive since the b_s's are.

We can now find

$$\log R' = -\underset{N\to\infty}{\mathrm{Lt}}\left(\frac{1}{N}\log Z'_{N,M}\right) \quad \text{and} \quad \log R'' = -\underset{N\to\infty}{\mathrm{Lt}}\left(\frac{1}{N}\log Z''_{N,M}\right)$$

by observing, following Kahn and Uhlenbeck (1938), that R′ and R″ are the radii of convergence of the series $\sum\limits_N Z'_{N,M}x^N$ and $\sum\limits_N Z''_{N,M}x^N$. In these two series, $Z'_{N,M}$ and $Z''_{N,M}$ refer to the same density for all N, while in generating series of the type (3) the Z_N refer to a fixed set of energy levels and therefore to a fixed volume

We can now transform the functions $\sum Z'_{N,M}x^N$ and $\sum Z''_{N,M}x^N$ in a manner which is precisely the same as that of Kahn and Uhlenbeck (1938) and which we shall consequently only outline here.

Using (7) we may write

$$\begin{aligned} \sum_N Z'_{N,M}x^N &= \frac{1}{2\pi i}\sum x^N \oint \zeta^{-(N+1)} \exp\left\{N(1+\delta_M)\sum_{s=1}^{\infty} b_s\zeta^s\right\}d\zeta \\ &= \frac{1}{2\pi i}\oint \frac{d\zeta}{\zeta - x\exp\left\{(1+\delta_M)\sum\limits_{s=1}^{\infty} b_s\zeta^s\right\}}, \quad . \quad . \quad (8) \end{aligned}$$

so long as we choose the contour so that

$$\left| x\frac{\exp\left\{(1+\delta_M)\sum\limits_{s=1}^{\infty} b_s\zeta^s\right\}}{\zeta}\right| < 1-\epsilon, \qquad \epsilon > 0,$$

everywhere on the contour. This condition is sufficient for the validity of the interchange of the sum and integral operations, and can always be satisfied for small enough x.

For sufficiently small x it may be shown that

$$\zeta - x\exp\left\{(1+\delta_M)\sum_{s=1}^{\infty} b_s\zeta^s\right\}$$

has only one root, ζ'_{M}, say, inside the contour. This is the only pole which contributes to the integral (8). We can therefore write

$$\Sigma Z'_{\mathrm{N,\,M}}x^{\mathrm{N}}=\frac{1}{1-xf_{1,\,\mathrm{M}}(\zeta'_{\mathrm{M}})}=\frac{1}{1-g_{1,\,\mathrm{M}}(\zeta'_{\mathrm{M}})}, \qquad (9)$$

where

$$f_{1,\,\mathrm{M}}(\zeta)=\frac{d}{d\zeta}\exp\left\{(1+\delta_{\mathrm{M}})\sum_{s=1}^{\infty}b_s\zeta^s\right\}, \qquad (10)$$

$$g_{1,\,\mathrm{M}}(\zeta)=(1+\delta_{\mathrm{M}})\sum_{s=1}^{\infty}sb_s\zeta^s, \qquad (11)$$

$$\frac{1}{x}=\frac{\exp\left\{(1+\delta_{\mathrm{M}})\sum_{s=1}^{\infty}b_s\zeta'^s_{\mathrm{M}}\right\}}{\zeta'_{\mathrm{M}}}, \qquad (12)$$

and

$$\frac{dx}{x}=\frac{d\zeta'_{\mathrm{M}}}{\zeta'_{\mathrm{M}}}\{1-g_{1,\,\mathrm{M}}(\zeta'_{\mathrm{M}})\}. \qquad (13)$$

Since we have shown that (9) is true for small x, it follows that, if the series in (10), (11) and (12) are replaced by their analytical continuations, (9) will be the analytical continuation of $\Sigma Z'_{\mathrm{N,\,M}}x^{\mathrm{N}}$.

Since all the $Z'_{\mathrm{N,\,M}}$ are positive, the radius of convergence R′ is such that $x=\mathrm{R}'$ is the first singularity of $\Sigma Z'_{\mathrm{N,\,M}}x^{\mathrm{N}}$ as x increases along the positive real axis.

$\Sigma Z'_{\mathrm{N,\,M}}x^{\mathrm{N}}$ and its analytical continuation will be regular in that region of the x-plane which is mapped by the region of the ζ'_{M}-plane in which

$$\left.\begin{array}{ll} & (a)\ g_{1,\,\mathrm{M}}(\zeta'_{\mathrm{M}})\neq 1 \\ \text{and} & (b)\ g_{1,\,\mathrm{M}}(\zeta'_{\mathrm{M}})\text{ is regular.}\end{array}\right\} \qquad (14)$$

Conversely, at points corresponding to those at which (a) or (b) is violated, $\Sigma Z'_{\mathrm{N,\,M}}x^{\mathrm{N}}$ and its analytical continuation will have a singularity.

We see from (13) that ζ'_{M} is a monotonically increasing function of x as x moves along the positive real axis until (a) is violated. Hence $x=\mathrm{R}'$ corresponds to the smallest real positive value of ζ'_{M} for which (a) or (b) is violated. Because of postulate (6, iii), the first singularity of $g_{1,\,\mathrm{M}}(\zeta)$ is at $\zeta=1$, and it follows that (a) will be violated before (b) if and only if $g_{1,\,\mathrm{M}}(\zeta)=1$ has a real positive root less than 1.

Hence, if $(1+\delta_{\mathrm{M}})\sum_{s}sb_s\zeta^s=1$ has a real positive root $\zeta'_{0,\,\mathrm{M}}<1$,

$$\frac{1}{\mathrm{R}'}=\frac{\exp\left\{(1+\delta_{\mathrm{M}})\sum_{s=1}^{\infty}b_s\zeta'^s_{0,\,\mathrm{M}}\right\}}{\zeta'_{0,\,\mathrm{M}}},$$

while, if no such root exists,

$$\frac{1}{\mathrm{R}'}=\exp\left\{(1+\delta_{\mathrm{M}})\sum_{s=1}^{\infty}b_s\right\}.$$

Since $\underset{N\to\infty}{\mathrm{Lt}}\,(Z'_{N,M})^{1/N}=1/R'$ and $Z_N<Z'_{N,M}$ for all M, we can write

$$\underset{N\to\infty}{\mathrm{Lt}}\left(\frac{1}{N}\log Z_N\right)\leqslant \underset{M\to\infty}{\mathrm{Lt}}\ \underset{N\to\infty}{\mathrm{Lt}}\left(\frac{1}{N}\log Z'_{N,M}\right)=\sum_{s=1}^{\infty} b_s\zeta_0'^{s}-\log\zeta_0', \quad . \quad (15\,a)$$

when $\sum_s sb_s\zeta^s=1$ has a real positive root $\zeta_0'<1$, and

$$\underset{N\to\infty}{\mathrm{Lt}}\left(\frac{1}{N}\log Z_N\right)\leqslant \underset{M\to\infty}{\mathrm{Lt}}\ \underset{N\to\infty}{\mathrm{Lt}}\left(\frac{1}{N}\log Z'_{N,M}\right)=\sum_{s=1}^{\infty} b_s \quad . \quad . \quad . \quad (15\,b)$$

if no such root exists.

In a precisely similar manner we find that

$$\Sigma Z''_{N,M}=\frac{1}{1-g_{2,M}(\zeta''_M)},$$

where

$$g_{2,M}(\zeta)=(1-\delta_M)\sum_{s=1}^{s_M} sb_s\zeta^s$$

and

$$\frac{1}{x}=\frac{\exp\left\{(1-\delta_M)\sum_{s=1}^{s_M} b_s\zeta''^{s}_M\right\}}{\zeta''_M}.$$

In this case, since $g_{2,M}(\zeta)$ is a finite series, $\Sigma Z''_{N,M}x^N$ can only become singular if $g_{2,M}(\zeta_M)=1$. Hence

$$\left.\begin{aligned}&\underset{N\to\infty}{\mathrm{Lt}}\left(\frac{1}{N}\log Z''_{N,M}\right)=(1-\delta_M)\sum_{s=1}^{s_M} b_s\zeta''^{s}_{0,M}-\log\zeta''_{0,M},\\ &\text{where}\quad (1-\delta_M)\sum_{s=1}^{s_M} sb_s\zeta''^{s}_{0,M}=1.\end{aligned}\right\} \quad . \quad (16)$$

Since $Z_N>Z''_{N,M}$ for all M,

$$\underset{N\to\infty}{\mathrm{Lt}}\left(\frac{1}{N}\log Z_N\right)\geqslant \underset{M\to\infty}{\mathrm{Lt}}\ \underset{N\to\infty}{\mathrm{Lt}}\left(\frac{1}{N}\log Z''_{N,M}\right),$$

and therefore we can deduce from equation (16) that, if $\sum_{s=1}^{\infty} sb_s\zeta^s=1$ has a real positive root $\zeta''_0<1$,

$$\underset{N\to\infty}{\mathrm{Lt}}\left(\frac{1}{N}\log Z_N\right)\geqslant \sum_{s=1}^{\infty} b_s\zeta''^{s}_0-\log\zeta''_0. \quad . \quad . \quad . \quad . \quad . \quad (17)$$

If, however, $\sum_{s=1}^{\infty} sb_s\zeta^s=1$ has no solution less than one, the solution of $(1-\delta_M)\sum_{s=1}^{s_M} sb_s\zeta^s=1$ will tend to one from above as M tends to infinity, since $\sum_{s=1}^{\infty} sb_s\zeta^s$ diverges for $\zeta>1$. In order to find the value of the limit of the right-hand side of (16) as M tends to infinity, we must evaluate

$$\underset{M\to\infty}{\mathrm{Lt}}\left\{(1-\delta_M)\sum_{s=1}^{s_M} b_s\zeta''^{s}_{0,M}\right\},$$

where

$$(1-\delta_M)\sum_{s=1}^{s_M} sb_s\zeta''^{s}_{0,M}=1.$$

We write $\zeta''_{0,\mathrm{M}}=1+\epsilon_{\mathrm{M}}$. Since $\sum\limits_{s=1}^{\infty} sb_s\zeta^s$ diverges for $\zeta>1$, ϵ_{M} tends to zero through positive values as M tends to infinity. Now

$$\begin{aligned}(1-\delta_{\mathrm{M}})\sum_{s=1}^{s_{\mathrm{M}}} b_s\zeta''^s_{0,\mathrm{M}}&=(1-\delta_{\mathrm{M}})\sum_{s=1}^{s_{\mathrm{M}}} b_s(1+\epsilon_{\mathrm{M}})^s\\ &=(1-\delta_{\mathrm{M}})\left\{\sum_{s=1}^{s_{\mathrm{M}}} b_s+\epsilon_{\mathrm{M}}\sum_{s=1}^{s_{\mathrm{M}}} sb_s(1+\theta\epsilon_{\mathrm{M}})^{s-1}\right\},\quad(0<\theta<1)\\ &<(1-\delta_{\mathrm{M}})\sum_{s=1}^{s_{\mathrm{M}}} b_s+\epsilon_{\mathrm{M}}.\end{aligned}$$

We also have the inequality

$$(1-\delta_{\mathrm{M}})\sum_{s=1}^{s_{\mathrm{M}}} b_s\zeta''^s_{0,\mathrm{M}}>(1-\delta_{\mathrm{M}})\sum_{s=1}^{s_{\mathrm{M}}} b_s.$$

Therefore $\underset{\mathrm{M}\to\infty}{\mathrm{Lt}}\left\{(1-\delta_{\mathrm{M}})\sum\limits_{s=1}^{s_{\mathrm{M}}} b_s\zeta''^s_{0,\mathrm{M}}\right\}=\underset{\mathrm{M}\to\infty}{\mathrm{Lt}}\left\{(1-\delta_{\mathrm{M}})\sum\limits_{s=1}^{s_{\mathrm{M}}} b_s\right\}=\sum\limits_{s=1}^{\infty} b_s.$

Hence, if $\sum\limits_{s=1}^{\infty} sb_s\zeta^s=1$ has no solution less than one, equation (16) yields, in the limit of M tending to infinity,

$$\underset{\mathrm{N}\to\infty}{\mathrm{Lt}}\left(\frac{1}{\mathrm{N}}\log \mathrm{Z}_{\mathrm{N}}\right)\geqslant\sum_{s=1}^{\infty} b_s. \qquad . \quad . \quad . \quad . \quad . \quad . \quad . \quad (18)$$

§ 3. ASYMPTOTIC FORM OF THE FREE ENERGY.

By combining the inequalities (15), (17) and (18) we obtain an equality which, combined with equation (2), may be written

$$f=\underset{\mathrm{N}\to\infty}{\mathrm{Lt}}\frac{\mathrm{F}}{\mathrm{N}}=-k\mathrm{T}\underset{\mathrm{N}\to\infty}{\mathrm{Lt}}\left(\frac{1}{\mathrm{N}}\log \mathrm{Z}_{\mathrm{N}}\right)=-k\mathrm{T}\left\{\sum_{s=1}^{\infty} b_s\zeta_0^s-\log\zeta_0\right\}, \qquad (19\,a)$$

if $\sum\limits_{s=1}^{\infty} sb_s\zeta^s=1$ has a real positive solution $\zeta_0<1$; if, on the other hand, there is no such solution,

$$f=-k\mathrm{T}\underset{\mathrm{N}\to\infty}{\mathrm{Lt}}\left(\frac{1}{\mathrm{N}}\log \mathrm{Z}_{\mathrm{N}}\right)=-k\mathrm{T}\sum_{s=1}^{\infty} b_s, \qquad . \quad . \quad (19\,b)$$

where f is the free energy per particle.

The change in the form of the free energy which occurs when $\zeta_0=1$ corresponds to " condensation ". We shall show, in the appendix, that for a perfect gas in a cubic box

$$b_s=\frac{(2\pi mk\mathrm{T})^{3/2}}{\rho h^3 s^{5/2}}.$$

Therefore, for such a gas, the free energy per particle is

$$f=-\frac{(2\pi m)^{3/2}}{\rho h^3}(kT)^{5/2}\sum_{s=1}^{\infty}\frac{\zeta_0^s}{s^{5/2}}+kT\log\zeta_0, \qquad (T>T_0)$$

$$f=-\frac{(2\pi m)^{3/2}}{\rho h^3}(kT)^{5/2}\sum_{s=1}^{\infty}\frac{1}{s^{5/2}}, \qquad (T<T_0)$$

where
$$\frac{(2\pi mkT)^{3/2}}{\rho h^3}\sum_{s=1}^{\infty}\frac{\zeta_0^s}{s^{3/2}}=1,$$

and T_0 is defined by the equation

$$\frac{(2\pi mkT_0)^{3/2}}{\rho h^3}\sum_{s=1}^{\infty}\frac{1}{s^{3/2}}=1.$$

These expressions are equivalent to those derived by London (1938) and Fowler and Jones (1938). and all the macroscopic characteristics of the condensation phenomenon can be derived from them.

The expressions (19 *a*) and (19 *b*) can be written in a more familiar way by observing that

$$sb_s=\underset{N\to\infty}{\mathrm{Lt}}\left\{\frac{1}{N}\sum_i\omega_i\exp(-s\mu\epsilon_i)\right\},$$

the limit to be taken with the density kept constant. If all the series are uniformly convergent, we can write

$$\sum_{s=1}^{\infty}b_s\zeta_0^s=\underset{N\to\infty}{\mathrm{Lt}}\left\{\frac{1}{N}\sum_i\omega_i\sum_{s=1}^{\infty}\frac{\{\zeta_0\exp(-\mu\epsilon_i)^s\}}{s}\right\}$$

$$=\underset{N\to\infty}{\mathrm{Lt}}\left\{\frac{1}{N}\sum_i\omega_i\log\left[1-\zeta_0\exp(-\mu\epsilon_i)\right]\right\}.$$

Similarly
$$\sum_{s=1}^{\infty}sb_s\zeta_0^s=\underset{N\to\infty}{\mathrm{Lt}}\left\{\frac{1}{N}\sum_i\frac{\omega_i}{\zeta_0^{-1}\exp(\mu\epsilon_i)-1}\right\}.$$

Thus, we can write the free energy per particle, in the limit as N tends to infinity, in the form

$$f=-\underset{N\to\infty}{\mathrm{Lt}}\left[\frac{kT}{N}\left\{\sum_i w_i\log\left[1-\zeta_0\exp(-\mu\epsilon_i)\right]-N\log\zeta_0\right\}\right],$$

where
$$\underset{N\to\infty}{\mathrm{Lt}}\frac{1}{N}\sum_i\frac{\omega_i}{\zeta_0^{-1}\exp(\mu\epsilon_i)-1}=1,$$

or, if there is no solution ζ_0 to this equation, $\zeta_0=1$. This expression for the free energy is identical with that which is obtained by the method of steepest descents.

APPENDIX.

It remains to discuss the validity of the postulates (6).

In order that postulates (i.) and (ii.) should be justified, were quire that the number of energy levels for each particle between E and E+dE should be of the form $V\{g(E)+h(E, V)\}\,dE$ where $h(E, V)$ tends to zero as V tends to infinity. An assumption of this nature is necessary if the free energy per particle is to tend to a definite value as V tends to infinity. If the density of energy levels has the form assumed, then

$$\begin{aligned}\sum_i \omega_i \exp(-s\mu\epsilon_i) &= V\int_0^\infty \{g(E)+h(E, V)\}\exp(-s\mu E)\,dE\\ &= \frac{V}{s\mu}\left\{\int_0^\infty g\left(\frac{x}{s\mu}\right)e^{-x}\,dx+\int_0^\infty h\left(\frac{x}{s\mu}, V\right)e^{-x}\,dx\right\}\\ &\sim \frac{N}{\rho s\mu}\int_0^\infty g\left(\frac{x}{s\mu}\right)e^{-x}\,dx=\frac{N}{s}\,b_s \quad \text{as} \quad V\to\infty.\end{aligned}$$

The validity of the inequalities (i.) and (ii.) depends on the form of the functions $g(E)$ and $h(E, V)$, and a general discussion is impracticable. Husimi (1939) has given expressions for $g(E)$ and $h(E, V)$ for a perfect gas in a cubic box, but it is more convenient, in this case, to evaluate the b_s by the following method. If the gas is in a cubic box of side a, the energy levels are

$$\epsilon_{l,m,n}=\alpha kT(l^2+m^2+n^2),$$

where $\alpha=h^2/8mkTa^2$ and l, m, n are positive integers. Therefore

$$\sum_i \omega_i \exp(-s\mu\epsilon_i)=\left[\sum_{l=1}^{\infty}\exp(-s\alpha l^2)\right]^3.$$

Now $$\sum_{l=1}^{\infty}\exp(-s\alpha l^2)<\int_0^\infty \exp(-s\alpha x^2)\,dx<\sum_{l=0}^{\infty}\exp(-s\alpha l^2),$$

and therefore $$\frac{1}{2}\left(\frac{\pi}{s\alpha}\right)^{1/2}-1<\sum_{l=1}^{\infty}\exp(-s\alpha l^2)<\frac{1}{2}\left(\frac{\pi}{s\alpha}\right)^{1/2}.$$

Hence $$\Sigma\,\omega_i \exp(-s\mu\epsilon_i)<\frac{N}{\rho h^3}\left(\frac{2\pi mkT}{s}\right)^{3/2} \quad \text{for all } s,$$

and

$$\sum_i \omega_i \exp(-s\mu\epsilon_i)>\frac{N}{\rho h^3}\left(\frac{2\pi mkT}{s}\right)^{3/2}(1-\delta_M) \quad \text{for} \quad N>M \text{ and } s<s_M,$$

where $$s_M=\frac{2\pi mkT}{9h^2}\left(\frac{M}{\rho}\right)^{2/3}\delta_M^2.$$

Thus, we see that postulates (i) and (ii) are justified in this case with

$$b_s=\left(\frac{2\pi mkT}{s}\right)^{3/2}\frac{1}{\rho s h^3}.$$

Postulate (iii.), that $\sum_s b_s x^s$ has radius of convergence unity, is not essential and has been made for simplicity only. If we assume, more generally, that the radius of convergence is r, the condition for (19a) to hold becomes $\zeta_0 < r$ and (19 b) becomes

$$f = -k\mathrm{T}\sum_{s=1}^{\infty} b_s r^s.$$

Since $\exp(-s\mu\epsilon_i)$ is a decreasing function of s, we see from (5) and (6, i. and ii.) that r cannot be less than one. r will be greater than one only if b_s contains a factor $\exp(-s\beta)$, and this can only happen if $g(\mathrm{E})$ is zero for $0 < \mathrm{E} < \beta/\mu$. This case, however, can be reduced to the case of $r = 1$ by a change of the zero of energy.

Postulate (iv.) has also been made for simplicity only. If $\sum_s sb_s$ is divergent, condition (a) of (14) will always be violated before condition (b). This means that the gas will not condense, since equation (19b) will never apply. An example of this behaviour is to be found in the two-dimensional Bose–Einstein gas, for which $b_s = 2\pi mk\mathrm{T}/\rho s^2 h^2$.

REFERENCES.

DINGLE, R. B., 1949, *Proc. Cam. Phil. Soc.*, **45**, 275.
FOWLER, R. H., 1936, *Statistical Mechanics* (Cambridge : University Press).
FOWLER, R. H., and JONES, H., 1938, *Proc. Cam. Phil. Soc.*, **34**, 573.
FRASER, A. R., 1951, *Phil. Mag.*, **42,** 165.
HUSIMI, K., 1939, *Proc. Phys.-Math. Soc. Japan* (3rd series), **21**, 759.
KAHN, B., and UHLENBECK, G. E., 1938, *Physica*, **5**, 399.
LONDON, F., 1938, *Phys. Rev.*, **54**, 947.
SCHUBERT, G., 1946 and 1947, *Z. Naturforsch*, **1**, 113 and **2** *a*, 250.
TEMPERLEY, H. N. V., 1949, *Proc. Roy. Soc.*, A, **199**, 361.

XV. *The Condensation of a Perfect Bose–Einstein Gas.—II*

By A. R. Fraser,
Royal Society Mond Laboratory, Cambridge*.

[Received October 24, 1950.]

Abstract.

In an earlier paper formulæ were given for the macroscopic behaviour of a perfect Bose–Einstein gas. In this paper formulæ are given for the mean occupation numbers of the energy levels and for the fluctuations in these numbers. These formulæ are in agreement with those obtained by earlier (invalid) methods.

§ 1. Itroduction.

As in the earlier paper (Fraser 1951), we shall consider a perfect Bose–Einstein gas of N particles in which the energy levels of the individual particles are ϵ_0, ϵ_1, ϵ_2, ... with weights ω_0, ω_1, ω_2, ... We shall find asymptotic expressions for $\overline{n}_i$, the mean occupation number of the ith level, in the limit as N tends to infinity.

Schubert (1946) and Dingle (1949) have pointed out that the derivation of the mean occupation numbers by the method of steepest descents is invalid at low temperatures. Expressions for the occupation numbers in the *most probable* configuration of the system may be obtained by other methods, but these are also open to criticism (see, for example, Dingle 1949.) It is well known that expressions for the occupation numbers which are obtained by the "mean value" and "maximum probability" methods are, in general, identical, and it is of particular interest to verify this equivalence of a Bose–Einstein gas, since the fluctuations in the occupation numbers are unusually large. The formula usually given for the fluctuation is

$$\overline{(\overline{n}_i-n_i)^2}=\overline{n}_i+(\overline{n}_i)^2, \qquad (1)$$

which may be compared with

$$\overline{(\overline{n}_i-n_i)^2}=\overline{n}_i$$

and

$$\overline{(\overline{n}_i-n_i)^2}=\overline{n}_i-(\overline{n}_i)^2,$$

for a Boltzmann and a Fermi–Dirac gas respectively. The validity of equation (1) will be discussed in § 6.

---

* Communicated by the Author.

§2. EXACT EXPRESSIONS FOR THE MEAN OCCUPATION NUMBERS.

We start from the partition function Z_N, defined by the equation

$$Z_N=\Sigma' \exp\left(-\mu \sum_{i=0}^{\infty} n_i\epsilon_i\right),$$

in which $\mu=1/kT$, and Σ' means the sum over all values of the set of positive integers n_0, n_1, n_2, ... such that $\sum_i n_i=N$. Z_N may be considered as the coefficient of ζ^N in

$$\sum_N Z_N\zeta^N=\prod_{j=0}^{\infty}[1-\zeta\exp(-\mu\epsilon_j)]^{-\omega_j}. \quad . \quad . \quad . \quad . \quad . \quad . \quad (2)$$

Expressons for the mean values of the occupation numbers and their products can then be expressed as functions of Z_N (Schroedinger 1945).

$$\overline{n}_i=-\frac{1}{\mu Z_N}\frac{\partial Z_N}{\partial\epsilon_i}, \quad . \quad . \quad . \quad . \quad . \quad . \quad . \quad . \quad (3)$$

$$\overline{n_i n_j}=\frac{1}{\mu^2 Z_N}\frac{\partial^2 Z_N}{\partial\epsilon_i\partial\epsilon_j}. \quad . \quad . \quad . \quad . \quad . \quad . \quad . \quad . \quad . \quad (4)$$

If we differentiate equation (2) with respect to ϵ_i and pick out the coefficient of ζ^N, we see that (3) takes the form

$$\overline{n}_i(N)=\omega_i\sum_{r=1}^{N}\frac{Z_{N-r}}{Z_N}\exp(-r\mu\epsilon_i). \quad . \quad . \quad . \quad . \quad . \quad . \quad (5)$$

Here $\overline{n}_i(N)$ has been written instead of $\overline{n}_i$, since we will consider the behaviour of $\overline{n}_i$ as a function of the total number of particles N.

Since $\sum_i \overline{n}_i(N)=N$, equation (5) leads to

$$NZ_N=\sum_{r=1}^{N}Z_{N-r}\sum_i\omega_i\exp(-r\mu\epsilon_i). \quad . \quad . \quad . \quad . \quad . \quad . \quad (6)$$

Setting $N=1, 2, 3, \ldots$ in turn in equation (6), we have, in principle, a method of finding Z_N. Thus equations (5) and (6) are sufficient to determine $\overline{n}_i(N)$.

From (5) we can also obtain the important relation

$$\overline{n}_i(N+1)=\frac{Z_N}{Z_{N+1}}(\omega_i+\overline{n}_i(N))\exp(-\mu\epsilon_i). \quad . \quad . \quad . \quad . \quad (7)$$

This relation has been obtained by Ansbacher and Ehrenberg (1949) who point out that, if we assume that $\overline{n}_i(N+1)=(1+\delta)\overline{n}_i(N)$ and nelgect δ, we immediately obtain

$$\overline{n}_i(N)=\frac{\omega_i}{(Z_{N+1}/Z_N)\exp(\mu\epsilon_i)-1}. \quad . \quad . \quad . \quad . \quad . \quad . \quad (8)$$

However, this procedure is only justified if δ is small compared with $1-\exp(-\mu\epsilon_i)Z_N/Z_{N+1}$. In fact, if $i=0$ and the gas is condensed, both these quantities are of order $1/N$ and δ cannot be neglected. For $i\neq 0$ it seems that the neglect of δ is usually justified, but we shall make no assumption of this nature.

§3. PROPERTIES OF THE PARTITION FUNCTION.

We shall define a quantity $\lambda_i(N)$ by the relation

$$\overline{n}_i(N)=\frac{\omega_i}{\lambda_i^{-1}(N)\exp(\mu\epsilon_i)-1}, \qquad (9)$$

$\lambda_i(N)$ will, in general, be a function of the temperature as well as of i and N, but we shall only be concerned with its variation with N at constant temperature.

Substituting (9) into equation (7), we find

$$\overline{n}_i(N+1)=\frac{Z_N}{Z_{N+1}}\lambda_i^{-1}(N)\overline{n}_i(N) \qquad (10)$$

and

$$\lambda_i^{-1}(N+1)=\frac{Z_{N+1}}{Z_N}+\exp(-\mu\epsilon_i)\left(1-\lambda_i(N)\frac{Z_{N+1}}{Z_N}\right). \qquad (11)$$

Summing equation (10) over all i, we obtain

$$N+1=\frac{Z_N}{Z_{N+1}}\Sigma\,\lambda_i^{-1}(N)\overline{n}_i(N). \qquad (12)$$

We can now prove that

$$\frac{Z_N}{Z_{N+1}}<\exp(\mu\epsilon_0) \quad \text{for all N.} \qquad (13)$$

Let M be the lowest value of N for which (13) is untrue, so that

$$\frac{Z_M}{Z_{M+1}}\geqslant\exp(\mu\epsilon_0) \qquad (14)$$

(equation (6) shows that M is greater than zero). The inequality (13) is true for all $N<M$ and hence, by (5) and (9), $\lambda_i(N)<\exp(\mu\epsilon_0)$ for $N\leqslant M$. Therefore, from (10) and (14), $\overline{n}_i(M+1)>\overline{n}_i(M)$ for all i and, from (7) and (14), $\overline{n}_0(M+1)>1+\overline{n}_0(M)$. Thus $\Sigma_i\overline{n}_i(M+1)>1+\Sigma_i\overline{n}_i(M)$, which is impossible. Therefore there is no value M for which (14) is true and hence (13) is true for all N.

If we use the inequality (13) in the equation (5), we find

$$n_i(N)<\omega_i\sum_{r=1}^{N}\exp[-r\mu(\epsilon_i-\epsilon_0)],$$

$$<\frac{\omega_i}{\exp[\mu(\epsilon_i-\epsilon_0)]-1}. \qquad (15)$$

Therefore, if

$$N_c=\sum_{i\neq 0}\frac{\omega_1}{\exp[\mu(\epsilon_i-\epsilon_0)]-1}, \qquad (16)$$

is finite, we must have $\overline{n}_0(N)>N-N_c$ whenever $N>N_c$. Thus condensation must occur whenever the energy levels are such that the series defining N_c converges, since, when the total number of particles exceeds N_c, a finite proportion of the particles must be in the lowest state.

Since (16) can be considered as defining a characteristic temperature T_c, associated with a given number of particles, we can say that a gas containing a fixed number of particles must be condensed at temperatures less than T_c. It should be emphasized that this result, in common with all those obtained in this section, is true for a general set of energy levels (provided only that the series in (16) converges) and for a finite number of particles. In order to show that the gas is not condensed at temperatures above T_c and to find the exact distribution of particles among the energy levels, we must consider the limiting case of large numbers of particles, but finite densities.

We shall first prove some other useful inequalities which are always true. From equations (10) and (11) we obtain the relation

$$n_i(N+2) = \frac{Z_{N+1}}{Z_{N+2}}\left\{\frac{Z_{N+1}}{Z_N} + \exp(-\mu\epsilon_i)\left(1-\lambda_i(N)\frac{Z_{N+1}}{Z_N}\right)\right\}\bar{n}_i(N+1) \quad . \quad (17a)$$

$$= \frac{Z_{N+1}}{Z_{N+2}}\left\{\lambda_i^{-1}(N) + \frac{Z_N}{Z_{N+1}}\exp(-\mu\epsilon_i)\left(\lambda_i^{-1}(N) - \frac{Z_{N+1}}{Z_N}\right)\right\}\bar{n}_i(N). \quad . \quad . \quad . \quad (17b)$$

We can now prove, by induction, that

$$\frac{Z_N}{Z_{N+1}}\lambda_i^{-1}(N) > 1 \quad \text{for all N and } i. \quad . \quad . \quad . \quad . \quad . \quad (18)$$

We assume (18) to be true for all i when $N=M$. Therefore the inner bracket expressions on the right-hand sides of (17*a*) and (17*b*) are positive for $N=M$. If we also use the inequality (13) we can write

$$\frac{Z_{M+1}}{Z_{M+2}}\cdot\frac{Z_{M+1}}{Z_M}\bar{n}_i(M+1) < \bar{n}_i(M+2) < \frac{Z_{M+1}}{Z_{M+2}}\left\{2\lambda_i^{-1}(M) - \frac{Z_{M+1}}{Z_M}\right\}\bar{n}_i(M).$$

Hence, summing over all i and using (12), we find

$$\frac{Z_{M+1}}{Z_{M+2}}\cdot\frac{Z_{M+1}}{Z_M}(M+1) < M+2 < \frac{Z_{M+1}}{Z_{M+2}}\cdot\frac{Z_{M+1}}{Z_M}(M+2). \quad . \quad . \quad (19)$$

From equation (11) and the right-hand side of the inequality (19) we obtain

$$\frac{Z_{M+1}}{Z_{M+2}}\lambda_i^{-1}(M+1) > \frac{Z_{M+1}}{Z_{M+2}}\cdot\frac{Z_{M+1}}{Z_M} > 1.$$

Therefore (18) is true for $N=M+1$. It is true for $N=0$ and hence is always true. Consequently (19) is true for all M and can be rewritten in the form

$$\frac{Z_{N+1}}{Z_{N+2}}\,\frac{N+1}{N+2} < \frac{Z_N}{Z_{N+1}} < \frac{Z_{N+1}}{Z_{N+2}}. \quad . \quad . \quad . \quad . \quad . \quad (20)$$

This relation, expressing the fact that Z_N/Z_{N+1} is a slowly increasing function of N, is of great importance in evaluating the asymptotic values of the mean occupation numbers.

§ 4. THE MEAN OCCUPATION NUMBERS ABOVE THE CONDENSATION TEMPERATURE.

In this and the following sections we shall be concerned with the asymptotic behaviour of quantities such as $\overline{n}_i(\mathrm{N})$ when the number of particles N and the volume V tend to infinity in such a way that the density $\rho=\mathrm{N}/\mathrm{V}$ remains finite and constant. The volume enters into the expressions implicitly, since the distribution of the energy levels depends on it.

Since
$$\frac{Z_{N-r}}{Z_N}=\frac{Z_{N-r}}{Z_{N-r+1}}\cdot\frac{Z_{N-r+1}}{Z_{N-r+2}}\cdot\cdot\cdot\cdot\frac{Z_{N-1}}{Z_N},$$
the inequality (20) shows that
$$\left.\begin{aligned}&\left(\frac{Z_{N-1}}{Z_N}\right)^r>\frac{Z_{N-r}}{Z_N}>a_r\left(\frac{Z_{N-1}}{Z_N}\right)^r,\\ \text{where}\qquad &a_r=\frac{N(N-1)\,.\,.\,.\,.\,(N-r+1)}{Nr-1}.\end{aligned}\right\}\quad .\quad .\quad .\quad .\quad .\quad (21)$$

By the use of Stirling's expansion for log (N !), we find that
$$a_r=1-\frac{r^2}{2N}+\frac{r}{2N}+0\left(\frac{r^4}{N^2}\right).$$

From equation (5), we see that if M is any integer less than N,
$$\overline{n}_i(N)=\omega_i\sum_{r=1}^{M}\frac{Z_{N-r}}{Z_N}\exp\left(-r\mu\epsilon_i\right)+\omega_i\sum_{r=M+1}^{N}\frac{Z_{N-r}}{Z_N}\exp\left(-r\mu\epsilon_i\right),$$
and, by (21),
$$\sum_{r=1}^{M}\left(\frac{Z_{N-1}}{Z_N}\right)^r\exp\left(-r\mu\epsilon_i\right)>\sum_{r=1}^{M}\frac{Z_{N-r}}{Z_N}\exp\left(-r\mu\epsilon_i\right)>\sum_{r=1}^{M}a_r\left(\frac{Z_{N-1}}{Z_N}\right)^r\exp\left(-r\mu\epsilon_i\right).$$

Let $M=N^{\alpha}$, where α is less than $\frac{1}{2}$; then $a_r\sim 1$ as N tends to infinity, as long as r is not greater than M. Hence
$$\sum_{r=1}^{N^{\alpha}}\frac{Z_{N-r}}{Z_N}\exp\left(-r\mu\epsilon_i\right)\sim\sum_{r=1}^{N^{\alpha}}\left(\frac{Z_{N-1}}{Z_N}\right)^r\exp\left(-r\mu\epsilon_i\right).$$

Therefore
$$\begin{aligned}\overline{n}_i(N)&\sim\omega_i\sum_{r=1}^{N^{\alpha}}\left(\frac{Z_{N-1}}{Z_N}\right)^r\exp\left(-r\mu\epsilon_i\right)+\omega_i\sum_{r=N^{\alpha}+1}^{N}\frac{Z_{N-r}}{Z_N}\exp\left(-r\mu\epsilon_i\right)\\ &=\omega_i\sum_{r=1}^{\infty}\left(\frac{Z_{N-1}}{Z_N}\right)^r\exp\left(-r\mu\epsilon_i\right)\\ &\qquad-\omega_i\left\{\sum_{r=N^{\alpha}+1}^{\infty}\left(\frac{Z_{N-1}}{Z_N}\right)^r\exp\left(-r\mu\epsilon_i\right)-\sum_{r=N^{\alpha}+1}^{N}\frac{Z_{N-r}}{Z_N}\exp\left(-r\mu\epsilon_i\right)\right\}.\end{aligned}$$

Hence
$$\overline{n}_i(N)\sim\frac{\omega_i}{(Z_N/Z_{N-1})\exp\left(\mu\epsilon_i\right)-1}-\omega_i R(N,\alpha),$$

where, by (21),

$$0<\mathrm{R}(\mathrm{N},\alpha)<\sum_{r=\mathrm{N}^\alpha+1}^{\infty}\left(\frac{\mathrm{Z}_{\mathrm{N}-1}}{\mathrm{Z}_\mathrm{N}}\right)^r \exp\left(-r\mu\epsilon_i\right).$$

Thus

$$\bar{n}_i(\mathrm{N})\sim\frac{\omega_i}{(\mathrm{Z}_\mathrm{N}/\mathrm{Z}_{\mathrm{N}-1})\exp(\mu\epsilon_i)-1}\left\{1-\theta\left[\frac{\mathrm{Z}_{\mathrm{N}-1}}{\mathrm{Z}_\mathrm{N}}\exp(-\mu\epsilon_i)\right]^{\mathrm{N}^\alpha}\right\}, \quad . \quad (22)$$

where $0<\theta<1$, and α is any positive number less than $\frac{1}{2}$. Since, by (13), $\mathrm{Z}_{\mathrm{N}-1}/\mathrm{Z}_\mathrm{N}<\exp(\mu\epsilon_0)$, $1-(\mathrm{Z}_{\mathrm{N}-1}/\mathrm{Z}_\mathrm{N})\exp(-\mu\epsilon_0)$ is positive and less than 1. Thus if we write $x=1-(\mathrm{Z}_{\mathrm{N}-1}/\mathrm{Z}_\mathrm{N})\exp(-\mu\epsilon_0)$,

$$\begin{aligned}\lim_{\mathrm{N}\to\infty}\left(\frac{\mathrm{Z}_{\mathrm{N}-1}}{\mathrm{Z}_\mathrm{N}}\exp(-\mu\epsilon_i)\right)^{\mathrm{N}^\alpha} &= \lim_{\mathrm{N}\to\infty}\left\{\exp\left[-\mu\mathrm{N}^\alpha(\epsilon_i-\epsilon_0)\right](1-x)^{\mathrm{N}^\alpha x/x}\right\}\\ &< \lim_{\mathrm{N}\to\infty}\left\{\exp\left[-\mu\mathrm{N}^\alpha(\epsilon_i-\epsilon_0)\right]\exp\left[-\mathrm{N}^\alpha x\right]\right\}.\end{aligned}$$

Hence, if either $(\epsilon_i-\epsilon_0)$ or x is of order greater than $\mathrm{N}^{-\alpha}$, the coefficient of θ in (22) tends to zero as N tends to infinity.

Thus

$$\bar{n}_i(\mathrm{N})\sim\frac{\omega_1}{(\mathrm{Z}_\mathrm{N}/\mathrm{Z}_{\mathrm{N}-1})\exp(\mu\epsilon_i)-1}, \quad . \quad . \quad . \quad . \quad . \quad (23)$$

(*a*) at all temperatures if $(\epsilon_i-\epsilon_0)^{-1}=o(\mathrm{N}^\alpha)$,

or (*b*) for all i if $[1-(\mathrm{Z}_{\mathrm{N}-1}/\mathrm{Z}_\mathrm{N})\exp(-\mu\epsilon_0)]^{-1}=o(\mathrm{N}^\alpha)$, . (24)

where α is any number less than $\frac{1}{2}$.

(23) is, of course, the well- known formula for the occupation numbers, and (24*a*) shows that it is always true except for some levels with energy very close to that of the lowest level.

We will show, however, that the condition (*b*) under which (23) is valid is satisfied for all temperatures except those in the immediate neighbourhood of or below the condensation temperature. This conclusion is to be expected from the fact that (*b*) demands only that the number of particles in the lowest state should be of order less than $\mathrm{N}^{\frac{1}{2}}$.

For convenience we write $\lambda=\mathrm{Z}_{\mathrm{N}-1}/\mathrm{Z}_\mathrm{N}$, so that (23) takes the form

$$\bar{n}_i(\mathrm{N})=\frac{\omega_i}{\lambda^{-1}\exp(\mu\epsilon_i)-1}.$$

So long as the condition (24*b*) is obeyed, the identity $\sum_i \bar{n}_i(\mathrm{N})=\mathrm{N}$ takes the limiting form $\mathrm{F}(\lambda,\mathrm{T})=\rho$, where

$$\mathrm{F}(\lambda,\mathrm{T})=\operatorname*{Lt}_{\mathrm{V}\to\infty}\left\{\frac{1}{\mathrm{V}}\sum_{i\neq0}\frac{\omega_i}{\lambda^{-1}\exp(\mu\epsilon_i)-1}\right\}.$$

The omission of the term corresponding to $i=0$ makes no difference for large N, since $\bar{n}_0(\mathrm{N})$ is of order less than $\mathrm{N}^{\frac{1}{2}}$. The equation $\mathrm{F}(\lambda,\mathrm{T})=\rho$ may be used to define λ as a function of T (for given ρ) and the condensation temperature may be defined as the value of T, T_c say, for which $\lambda=\exp(\mu\epsilon_0)$.

This value of λ is clearly outside the range of validity of (24*b*) and this definition may be considered at present as purely conventional, although it should be observed that it corresponds to the definition of the condensation point given, for finite N, in equation (16). Any temperature $T' > T_c$, such that $(T' - T_c)$ is some finite temperature difference, however small, will correspond to a value of λ, λ' say, which differs from the limiting value $\exp(\mu\epsilon_0)$ by some finite amount. It is clear that, for large enough N, (24*b*) will be satisfied if Z_{N-1}/Z_N is equal to λ' and hence (23) will be true at the temperature T′. It follows that (23) is true, in the limit of large N, for all temperatures greater than T_c.

§5. THE MEAN OCCUPATION NUMBERS BELOW THE CONDENSATION TEMPERATURE.

In the last section we defined a temperature T_c by the equation

$$\underset{V\to\infty}{\mathrm{Lt}}\ \frac{1}{V}\sum_{i\neq 0}\frac{\omega_i}{\exp[\mu_c(\epsilon_i-\epsilon_0)]-1}=\rho=\underset{N,V\to\infty}{\mathrm{Lt}}(N/V), \quad . \quad . \quad (25)$$

where $\mu_c = 1/kT_c$; we have already remarked that this is equivalent to the limiting form of equation (16) in which we considered the temperature as fixed and the number of particles as our independent variable. It is now convenient to return to that view-point and to define the critical number of particles at a temperature T by the equation

$$N_c = \sum_{i\neq 0}\frac{\omega_i}{\exp[\mu(\epsilon_i-\epsilon_0)]-1}, \quad \mu = 1/kT.$$

From inequality (15) we see that $\overline{n_0}(N) > N - N_c$, and from equation (5) and inequality (21) we see that

$$\overline{n_0}(N) < \frac{\omega_0}{(Z_N/Z_{N-1})\exp(\mu\epsilon_0)-1},$$

and hence

$$\frac{\omega_0}{(Z_N/Z_{N-1})\exp(\mu\epsilon_0)-1} > N - N_c.$$

We thus obtain the inequality

$$1 < \frac{Z_N}{Z_{N-1}}\exp(\mu\epsilon_0) < 1 + \frac{\omega_0}{N-N_c} \quad \text{if} \quad N > N_c, \quad . \quad . \quad . \quad (26)$$

where the left-hand side is a restatement of (13).

Let us consider the number of particles, N, to be such that $N - N_c = rN$, where r is some positive number. Then (26) becomes

$$1 < \frac{Z_N}{Z_{N-1}}\exp(\mu\epsilon_0) < 1 + \frac{\omega_0}{rN},$$

similarly

$$1 < \frac{Z_{N-M}}{Z_{N-M-1}}\exp(\mu\epsilon_0) < 1 + \frac{\omega_0}{rN-M},$$

where $M < rN$. By forming the product of these inequalities with M running from zero to N^{β}, where β is some number less than 1 (so that $N^{\beta} \ll rN$ for large N), we obtain, after some rearrangement

$$\exp(\mu\epsilon_0 N^{\beta}) > \frac{Z_{N-N^{\beta}}}{Z_N} > \left(1+\frac{\omega_0}{rN-N^{\beta}}\right)^{-N^{\beta}} \exp(\mu\epsilon_0 N^{\beta}), \quad (N^{\beta} < rN).$$

If we now use this inequality for $Z_{N-N^{\beta}}/Z_N$ in equation (5) and proceed in a manner similar to that used in the derivation of (22), we find

$$\bar{n}_i(N) \sim \frac{\omega_i}{\exp[\mu(\epsilon_i-\epsilon_0)]-1}\{1-\theta\exp[-N^{\beta}\mu(\epsilon_i-\epsilon_0)]\},$$

where $0<\theta<1$.

If $(\epsilon_i-\epsilon_0)$ is of order $N^{-\gamma}$ where $\gamma<1$, β can be chosen so that $\gamma<\beta<1$ and the coefficient of θ is exponentially small for $i\neq 0$. For a perfect three-dimensional gas, for instance, $\gamma=2/3$, so that this condition is met. Thus

$$\left.\begin{aligned} &\bar{n}_i(N) \sim \frac{\omega_i}{\exp[\mu(\epsilon_i-\epsilon_0)]-1}, \quad i\neq 0, \\ \text{and hence} \quad &\bar{n}_0(N) \sim N - \sum_{i\neq 0} \frac{\omega_i}{\exp[\mu(\epsilon_i-\epsilon_0)]-1}. \end{aligned}\right\} \quad . \; . \; . \; . \quad (27)$$

(27) has been proved for $N-N_c=rN$, where r is any positive number, however small, so long as it remains finite as N tends to infinity.

If the particle density ρ is such that the condensation temperature, defined by (25) is T_c, then any temperature $T''<T_c$ will correspond to a critical density ρ'', where

$$\underset{V\to\infty}{\mathrm{Lt}} \left\{\frac{1}{V}\sum_{i\neq 0}\frac{\omega_i}{\exp[\mu''(\epsilon_i-\epsilon_0)]-1}\right\} = \rho'',$$

and $\mu''=1/kT''$. ρ'' will be less than ρ by some finite difference, $r\rho$ say. Therefore at the temperature T'', $N-N_c=rN$ and the argument used above is valid. Hence equation (27) is valid at all temperatures $T<T_c$.

Thus we may sum up the results of this and the preceding section as follows.

If T_c is defined by the equation

$$\underset{V\to\infty}{\mathrm{Lt}} \left\{\frac{1}{V}\sum_{i\neq 0}\frac{\omega_i}{\exp[\mu_c(\epsilon_i-\epsilon_0)]-1}\right\} = \rho = \underset{V,N\to\infty}{\mathrm{Lt}} N/V,$$

where $\mu_c=1/kT_c$, then

$$\bar{n}_i(N) \sim \frac{\omega_i}{(Z_N/Z_{N-1})\exp(\mu\epsilon_i)-1} \qquad \text{for } T>T_c,$$

and

$$\left.\begin{aligned} &\bar{n}_i(N) \sim \frac{\omega_i}{\exp[\mu(\epsilon_i-\epsilon_0)]-1}, \quad i\neq 0, \\ &\bar{n}_0(N) = N - \sum_{i\neq 0}\bar{n}_i(N), \end{aligned}\right\} \quad \text{for } T<T_c.$$

In obtaining these expressions we have assumed that the limit used in defining T_c exists and that $(\epsilon_1-\epsilon_0)$ is of order greater than $N^{-\gamma}$, $\gamma<1$.

§ 6. Fluctuations.

We have seen in equation (4) that

$$\overline{n_i n_j}=\frac{1}{\mu^2 Z_N}\frac{\partial^2 Z_N}{\partial\epsilon_i\partial\epsilon_j}.$$

By differentiating (2) twice we find

$$\begin{aligned}\overline{n_i n_j}&=\omega_i\omega_j\sum_{r=2}^{N}\frac{Z_{N-r}}{Z_N}\frac{\exp\left[-(r-1)\mu\epsilon_i\right]-\exp\left[-(r-1)\mu\epsilon_j\right]}{\exp(-\mu\epsilon_i)-\exp(-\mu\epsilon_j)}\exp\left[-\mu(\epsilon_i+\epsilon_j)\right]\\&=\frac{1}{\exp(-\mu\epsilon_i)-\exp(-\mu\epsilon_j)}\{\omega_j\exp(-\mu\epsilon_j)\overline{n_i}-\omega_i\exp(-\mu\epsilon_i)\overline{n_j}\}\ \text{ if }\ i\neq j,\end{aligned} \qquad . \quad . \quad . \quad (28)$$

and when $i=j$, we find

$$\overline{n_i^2}=\overline{n_i}+\omega_i(\omega_i+1)\sum_{r=2}^{N}\frac{Z_{N-r}}{Z_N}(r-1)\exp(-r\mu\epsilon_i), \qquad . \quad . \quad . \quad (29)$$

(28) and (29) are exact formulæ.

By arguments similar to those which lead to equations (23) and (27), we obtain from (29)

$$\overline{(\overline{n_i}-n_i)^2}\sim\frac{(\overline{n_i})^2}{\omega_i}+\overline{n_i}$$

for all i when $T>T_c$ and for $i\neq 0$ when $T<T_c$.

To find the value of $\overline{n_0^2}$ for $T<T_c$, we observe that

$$N\overline{n_0}=\overline{n_0^2}+\Sigma\overline{n_0 n_i},$$

hence $$\overline{(\overline{n_0}-n_0)^2}=\overline{n_0}\sum_{i\neq 0}\overline{n_i}-\sum_{i\neq 0}\overline{n_0 n_i}$$

and using (28) with $j=0$, we obtain

$$\overline{(\overline{n_0}-n_0)^2}=\overline{n_0}\left\{\sum_{i\neq 0}\overline{n_i}-\sum_{i\neq 0}\frac{\omega_i}{\exp\left[\mu(\epsilon_i-\epsilon_0)\right]-1}\right\}+\sum_{i\neq 0}\frac{\omega_0\exp\left[\mu(\epsilon_i-\epsilon_0)\right]\overline{n_i}}{\exp\left[\mu(\epsilon_i-\epsilon_0)\right]-1}. \qquad . \quad . \quad . \quad (30)$$

Although $\overline{n_i}$ is given asymptotically by (27) for $T<T_c$, we cannot necesarily neglect the first term in (30), since

$$\overline{n_0}\sum_{i\neq 0}\left(\overline{n_i}-\frac{\omega_i}{\exp\left[\mu(\epsilon_i-\epsilon_0)\right]-1}\right),$$

while neglible compared with $\overline{n_0}\sum\limits_{i\neq 0}\overline{n_i}$ need not be negligible in comparison with the second term in (30). Since, by (5) and (13),

$$\overline{n_i}<\frac{\omega_i}{\exp\left[\mu(\epsilon_i-\epsilon_0)\right]-1},$$

we can deduce from (30) that

$$\overline{(\overline{n}_0-n_0)^2} < \sum_{i\neq 0} \frac{\omega_0 \exp[\mu(\epsilon_i-\epsilon_0)]\overline{n}_i}{\exp[\mu(\epsilon_i-\epsilon_0)]-1} \sim \frac{\omega_0}{\exp(\mu\epsilon_0)} \sum_{i\neq 0} \frac{(\overline{n}_i)^2 \exp(\mu\epsilon_i)}{\omega_i}.$$

Thus we have shown that

$$\overline{(\overline{n}_i-n_i)^2} \sim \frac{(\overline{n}_i)^2}{\omega_i}+n_i, \qquad \text{for all } i \text{ if } T>T_c,$$

$$\left.\begin{aligned}\overline{(\overline{n}_i-n_i)^2} &\sim \frac{(\overline{n}_i)^2}{\omega_i}+n_i, && \text{for all } i\neq 0,\\ \overline{(\overline{n}_0-n_0)^2} &\leqslant \frac{\omega_0}{\exp(\mu\epsilon_0)} \sum_{i\neq 0} \frac{(\overline{n}_i)^2 \exp(\mu\epsilon_i)}{\omega_i}, &&\end{aligned}\right\} \text{if } T<T_c.$$

The expressions for these fluctuations which are obtained by the method of steepest descents differ from these only in that the " less than or equals " sign in the expression for $\overline{(\overline{n}_0-n_0)^2}$ when $T<T_c$ is replaced by an "equals" sign. The expressions for $i=0$ are sometimes quoted as holding generally, even for $i=0$ in the condensed state. That this cannot be so can easily be seen, for if

$$\overline{(\overline{n}_0-n_0)^2}=(n_0)^2+\overline{n}_0$$

(we have taken $\omega_0=1$ for simplicity), then

$$\overline{n_0^2}=2(\overline{n}_0)^2+\overline{n}_0.$$

At a sufficiently low temperature more than $1/\sqrt{2}$ of the total number of particles will be in the lowest state. Therefore $2(\overline{n}_0)^2$ will be greater than N^2 and hence $\overline{n_0^2}$ will be greater than N^2. This is impossible, since $n_0<N$. The formulæ which Fowler (1936) obtains by the method of steepest descents are not open to this criticism and reduce to the formulæ given above with the inequality replaced by an equality.

§ 7. CONCLUSIONS.

The formulæ obtained in this paper show that the expressions obtained by the method of steepest descents are correct, except possibly for a very small range of temperature near the condensation temperature which decreases to zero as the number of particles and the volume increase to infinity. The only new assumption which we have made is that the separation between the lowest pair of energy levels, $(\epsilon_1-\epsilon_0)$, is of order greater than $N^{-\gamma}$, where $\gamma<1$. If this assumption were not made, complications would arise in the condensation phenomenon even if the orthodox formulæ were valid everywhere, since condensation would take place into more than one level. If, for instance, $\epsilon_1-\epsilon_0=\epsilon/N$, then if

$$\overline{n}_i=\frac{1}{\lambda^{-1}\exp(\mu\epsilon_i)-1}$$

and $\overline{n_0}=\alpha N$, λ would have the value

$$\lambda=\frac{\exp(\mu\epsilon_0)}{1+1/\alpha N}$$

and $\overline{n_1}$ the value

$$\overline{n_1}=\frac{N}{\mu\epsilon+1/\alpha}.$$

In other words, a comparable number of particles would have condensed into the level above the lowest.

From the results obtained in §§4 and 5 we can deduce that the macroscopic behaviour of a perfect Bose–Einstein gas is identical with that found by London (1938) and Fowler and Jones (1938). This is in agreement with the conclusions reached in paper I. (Fraser 1951).

The only work which appears to be in positive disagreement with the results obtained by the method of steepest descents is that of Temperley (1949). Since this work deals essentially with a finite (although large) number of particles, it is difficult to compare with the conclusions of §§4 and 5 of this paper. Temperley's conclusion that, in his particular model, condensation only takes place at a temperature much lower than that predicted by the method of steepest descents is, however, in disagreement with the consequences of equations (15) and (16). This disagreement arises from the choice of a criterion for condensation. Temperley has required that, when the gas is condensed, all particles added to the gas should go into the lowest state. This, however, can never occur for a gas consisting of a finite number of particles. In fact equations (10) and (18) of this paper show that the addition of a single particle leads to an increase of all the occupation numbers. It is only in the limit of infinite volume that we can speak of the occupation numbers of the excited states being independent of the total number of particles when the gas is condensed. Relations deduced by Temperley for his model can be used to prove that, when the temperature is below the orthodox condensation temperature, almost all particles added to the system condense into the lowest state.

ACKNOWLEDGMENTS.

I wish to thank Mr. H. N. V. Temperley and Mr. O. Penrose for helpful discussions. I am also indebted to the Department of Scientific and Industrial Research for a maintenance grant.

REFERENCES.

ANSBACHER, F., and EHRENBERG, W., 1949, *Phil. Mag.*, **40**, 626.
DINGLE, R. B., 1949, *Proc. Cam. Phil. Soc.*, **45**, 275.
FOWLER, R. H., 1936, *Statistical Mechanics* (Cambridge : University Press).
FOWLER, R. H., and JONES, H., 1938, *Proc. Cam. Phil. Soc.*, **34**, 573.
FRASER, A. R., 1951, *Phil. Mag.*, **42**, 156.
LONDON, F., 1938, *Phys. Rev.*, **54**, 947.
SCHROEDINGER, E., 1945, *Statistical Thermodynamics* (Cambridge: University Press).
SCHUBERT, G., 1946 and 1947, *Z. Naturforsch.*, **1**, 113, and **2a**, 250.
TEMPERLEY, H. N. V., 1949, *Proc. Roy. Soc.* A, **199**, 361.

XVI. *The Unsteady Flow of Viscous Incompressible Fluid Inside an Infinite Channel.*

By L. SOWERBY,
Department of Applied Mathematics, University of Liverpool†.

[Received November 22, 1950.]

SUMMARY.

The problem considered is the motion of viscous incompressible fluid inside an infinite wedge-shaped channel of angle π/n, the channel being started suddenly from rest with uniform velocity in the direction of its length. The solution is obtained by considering a suitable Green's function for the heat conduction equation. The velocity is found to be expressible either in terms of error functions or in the form of integrals which are suitable for computation, depending on the value of n. In all cases the skin friction appears as a simple expression involving well known functions.

Particular reference is made to the right angled channel ($n=2$), the results being extended, by Rayleigh's hypothesis, to include some discussion of the steady flow inside a right angled channel having leading edges normal to the incident stream. From this, also, an approximation is derived for the frictional force on the interior of a finite rectangular channel of suitable dimensions.

1. *Statement of Problem.* Choosing cylindrical coordinates (r, θ, z), two semi-infinite plates coinciding with the planes $\theta=0$, $\theta=\pi/n$, respectively, form an infinite wedge-shaped channel of angle π/n (n is an integer$\geqslant 1$). The region inside the channel is filled with viscous incompressible fluid, and initially the channel and the fluid are at rest. At $t=0$ the channel is set in motion impulsively with uniform velocity W parallel to Oz; the problem is to determine the subsequent motion of the fluid.

2. *The Equation of Motion and Boundary Conditions.* Let (u, v, w) be the components of velocity of the fluid in the given coordinate system; in particular, w is the component parallel to the axis $r=0$. Then it is clear that there is a solution of the hydrodynamical equations, and the solution of the above problem, in which $u=v=0$, provided $w(r, \theta, t)$ can be determined to satisfy

$$\frac{\partial w}{\partial t}=\nu\left(\frac{\partial^2 w}{\partial r^2}+\frac{1}{r}\frac{\partial w}{\partial r}+\frac{1}{r^2}\frac{\partial^2 w}{\partial \theta^2}\right), \quad . \quad . \quad . \quad . \quad . \quad . \quad (2.1)$$

---

† Communicated by Dr. A. Fletcher.

and the boundary conditions

$$\begin{aligned} &w=0 \quad \text{when} \quad t=0,\\ &\left.\begin{aligned} &w=W \quad \text{if} \quad \theta=0,\ \theta=\pi/n,\\ &w\longrightarrow 0 \quad \text{as} \quad r\longrightarrow\infty\,(\theta\neq 0,\ \pi/n), \end{aligned}\right\} \text{when } t>0 \end{aligned} \quad . \quad . \quad . \quad (2.2)$$

(ν is the coefficient of kinematic viscosity.)

3. *The Solution of* (2.1) It is convenient to write

$$w^*=W-w \quad . \quad . \quad . \quad . \quad . \quad . \quad . \quad . \quad . \quad (3.1)$$

so that w^* must also satisfy the equation (2.1) and the boundary conditions

$$\begin{aligned} &w^*=W \quad \text{when} \quad t=0,\\ &\left.\begin{aligned} &w^*=0 \ \text{if} \ \theta=0,\ \theta=\pi/n\\ &w^*\longrightarrow W \ \text{as} \ r\longrightarrow\infty\,(\theta\neq 0,\ \pi/n), \end{aligned}\right\} \text{when } t>0. \end{aligned} \quad . \quad . \quad (3.2)$$

The expression for w^* can be obtained directly by considering a Green's function relating to the equation (2.1) and appropriate to the boundary considered (Carslaw and Jaeger 1947). An expression is obtained for $w^*(r, \theta, t)$ at the point (r', θ'), say, and the required Green's function, u, is of the form

$$u=F(r, \theta, r', \theta', t-\tau) \quad . \quad . \quad . \quad . \quad . \quad . \quad . \quad . \quad (\text{i.})$$

(in this, and in all that follows, we take $t>\tau$.)

We require u to satisfy the equation

$$\frac{\partial u}{\partial t}=\nu\left(\frac{\partial^2 u}{\partial r^2}+\frac{1}{r}\frac{\partial u}{\partial r}+\frac{1}{r^2}\frac{\partial^2 u}{\partial\theta^2}\right). \quad . \quad . \quad . \quad . \quad . \quad . \quad (\text{ii.})$$

and the following conditions

$$\lim_{t\to\tau+0} u=0. \quad . \quad . \quad . \quad . \quad . \quad . \quad . \quad . \quad . \quad (\text{iii.})$$

everywhere in the region $S(0\leqslant\theta\leqslant\pi/n)$, except at the point (r', θ') where

$$u\longrightarrow\frac{1}{4\pi\nu(t-\tau)}\exp\left[-\frac{1}{4\nu(t-\tau)}(r^2+r'^2-2rr'\cos(\theta-\theta'))\right], \quad . \quad . \quad (\text{iv.})$$

and also $\quad u=0 \ \text{if} \ \theta=0,\ \theta=\pi/n. \quad . \quad . \quad . \quad . \quad . \quad . \quad (\text{v.})$

In addition, we shall require u and $\partial u/\partial\theta$ to tend to zero in a suitable manner as $r\longrightarrow\infty$, to ensure the vanishing of a certain line integral. The function u which we shall choose will certainly satisfy this last condition. Finally, under these conditions, and the conditions imposed on w^*, the required expression for w^* is

$$w^*(r', \theta', t)=W\int_{\theta=0}^{\pi/n}\int_{r=0}^{\infty} u_{\tau=0}r\,dr\,d\theta. \quad . \quad . \quad . \quad . \quad . \quad (3.3)$$

It remains, therefore to select the appropriate function u.

Consider

$$u(r,\theta,r',\theta',t-\tau)=\frac{1}{4\pi\nu(t-\tau)}$$

$$\times\sum_{m=0}^{n-1}\left[\begin{array}{l}\exp-\dfrac{1}{4\nu(t-\tau)}\left\{r^2+r'^2-2rr'\cos\left(\theta'-\left\{\theta+\dfrac{2m\pi}{n}\right\}\right)\right\}\\ -\exp-\dfrac{1}{4\nu(t-\tau)}\left\{r^2+r'^2-2rr'\cos\left(\theta'-\left\{2(m+1)\dfrac{\pi}{n}-\theta\right\}\right)\right\}.\end{array}\right] \quad . \quad . \quad . \quad (3.4)$$

Then u satisfies (ii.), since each term is a solution of (ii.), and clearly all the remaining conditions (iii.)–(v.) are also satisfied. Moreover, u and $\partial u/\partial\theta \longrightarrow 0$ suitably as $r\longrightarrow\infty$, so that

$$w^*(r',\theta',r)=W\int_{\theta=0}^{\pi/n}\int_{r=0}^{\infty}u(r,\theta,r',\theta',t)r\,dr\,d\theta,$$

or, reverting to the usual notation,

$$w^*(r,\theta,t)=W\int_{\alpha=0}^{\pi/n}\int_{z=0}^{\infty}u(z,\alpha,r,\theta,t)z\,dz\,d\alpha, \quad . \quad . \quad . \quad (3.5)$$

where

$$u(z,\alpha,r,\theta,t)=\frac{1}{4\pi\nu t}$$

$$\times\sum_{m=0}^{n-1}\left[\begin{array}{l}\exp-\dfrac{1}{4\nu t}\left\{z^2+r^2-2rz\cos\left(\theta-\left\{\alpha+\dfrac{2m\pi}{n}\right\}\right)\right\}\\ -\exp-\dfrac{1}{4\nu t}\left\{z^2+r^2-2rz\cos\left(\theta-\left\{2(m+1)\dfrac{\pi}{n}-\alpha\right\}\right)\right\}.\end{array}\right] \quad . \quad . \quad . \quad (3.6)$$

It is at once evident that the expression (3.5) satisfies the boundary conditions on $\theta=0$, $\theta=\pi/n$, since the integrand u is zero for these values of θ. The expression can be reduced further by carrying out the integration with respect to z, and, indeed, except for a certain group of the integers n, the integration with respect to α can also be performed, the expression then reducing to a (finite) sum of tabulated functions.

Writing $p^2=1/4\nu t$, $c=\cos(\theta-\beta)$, $s=\sin(\theta-\beta)$, we have

$$\frac{1}{4\nu t}\int_{z=0}^{\infty}\exp\left\{-\frac{1}{4\nu t}(z^2+r^2-2rz\cos\{\theta-\beta\})\right\}z\,dz$$

$$=p^2\exp(-p^2r^2s^2)\int_{z=0}^{\infty}\exp\{-p^2(z-rc)^2\}z\,dz$$

$$=p^2\exp(-p^2r^2s^2)\int_{-rc}^{\infty}\exp(-p^2x^2)\,.\,(x+rc)\,dx$$

$$=\tfrac{1}{2}\exp(-\eta^2)+\eta c\,.\,\exp(-\eta^2s^2)\frac{\pi^{\frac{1}{2}}}{2}\{1+\operatorname{erf}(\eta c)\},$$

where $\eta=\dfrac{r}{2(\nu t)^{\frac{1}{2}}}$, and $\operatorname{erf}(y)=\dfrac{2}{\pi^{\frac{1}{2}}}\displaystyle\int_0^y\exp(-x^2)\,dx.$

Hence, placing $\gamma_m = \theta - 2m\pi/n$

$$w^* = \frac{W}{2\pi^{\frac{1}{2}}} \int_{\alpha=0}^{\pi/n} \eta \sum_{m=0}^{n=1} \left[\begin{array}{l} \cos(\gamma_m - \alpha) . \exp(-\eta^2 \sin^2\{\gamma_m - \alpha\})\{1 + \operatorname{erf}(\eta \cos\{\gamma_m - \alpha\})\} \\ -\cos(\gamma_{m+1} + \alpha) . \exp(-\eta^2 \sin^2\{\gamma_{m+1} + \alpha\})\{1 + \operatorname{erf}(\eta \cos\{\gamma_{m+1} + \alpha\})\} \end{array} \right] d\alpha \qquad . \quad . \quad . \quad (3.7)$$

or, writing $f(\eta, \phi) = \cos\phi . \exp(-\eta^2 \sin^2\phi)\{1 + \operatorname{erf}(\eta\cos\phi)\}$, . . (3.8)

$$w^* = \frac{W}{2\pi^{\frac{1}{2}}} \sum_{m=0}^{n-1} \left[\int_{2m\frac{\pi}{n}-\theta}^{(2m+1)\frac{\pi}{n}-\theta} \eta f(\eta, \phi)\, d\phi - \int_{\theta-2(m+1)\frac{\pi}{n}}^{\theta-(2m+1)\frac{\pi}{n}} \eta f(\eta, \phi)\, d\phi \right]$$

$$= \frac{W}{2\pi^{\frac{1}{2}}} \sum_{m=0}^{n-1} \left[\int_{2m\frac{\pi}{n}-\theta}^{(2m+1)\frac{\pi}{n}-\theta} \eta f(\eta, \phi)\, d\phi - \int_{(2m+1)\frac{\pi}{n}-\theta}^{2(m+1)\frac{\pi}{n}-\theta} \eta f(\eta, \phi)\, d\phi \right]$$

(since $f(\eta, \phi)$ is an even function of ϕ)

$$= \frac{W}{2\pi^{\frac{1}{2}}} \sum_{m=0}^{2n-1} (-1)^m \int_{m\frac{\pi}{n}-\theta}^{(m+1)\frac{\pi}{n}-\theta} \eta f(\eta, \phi)\, d\phi.$$

Thus

$$\frac{w^*}{W} = \frac{1}{2\pi^{\frac{1}{2}}} \sum_{m=0}^{2n-1} (-1)^m \int_{m\frac{\pi}{n}-\theta}^{(m+1)\frac{\pi}{n}-\theta} \eta f(\eta, \phi)\, d\phi \qquad . \quad . \quad . \quad (3.9)$$

$$= \frac{1}{2\pi^{\frac{1}{2}}} \sum_{m=0}^{2n-1} (-1)^m \int_0^{\pi/n} \eta f\left(\eta, \phi + \frac{m\pi}{n} - \theta\right) d\phi. \qquad . \quad (3.10)$$

From these last results it can easily be verified that w^* does, in fact, satisfy the remaining boundary conditions (3.2), the first and third of these now being included in the single condition $w^* \longrightarrow W$ as $\eta \longrightarrow \infty$ $(0 < \theta < \pi/n)$. For convenience, take $n \geqslant 2$, and consider

$$I_m = \int_{\varphi_m}^{\varphi_m + \frac{\pi}{n}} \eta f(\eta, \phi)\, d\phi,$$

where

$$\phi_m = m\pi/n - \theta.$$

Then, since $0 < \theta < \pi/n$, the range $\phi_m \leqslant \phi \leqslant \phi_m + \pi/n$ excludes the points $\phi = 0$, $\phi = \pi$ except when $m = 0$, n respectively. Thus, if $m \neq 0$, n

$$I_m = \int_{\varphi_m}^{\varphi_m + \frac{\pi}{n}} \eta \cos\phi . \exp(-\eta^2 \sin^2\phi) . \{1 + \operatorname{erf}(\eta\cos\phi)\}\, d\phi$$

$$= \exp(-\eta^2 \sin^2\xi)\eta\cos\xi \int_{\varphi_m}^{\phi_m + \frac{\pi}{n}} \{1 + \operatorname{erf}(\eta\cos\phi)\}\, d\phi,$$

where $\phi_m < \xi < \phi_m + \pi/n$.

Hence, since $\sin\xi \neq 0$, and $|\operatorname{erf} x| < 1$,

$$I_m \longrightarrow 0 \quad \text{as} \quad \eta \longrightarrow \infty.$$

In the cases $m=0$ and n, $\cos\phi$ does not change sign in the range of integration, so that

$$I_m=\{1+\operatorname{erf}(\eta\cos\xi)\}\int_{\varphi_m}^{\varphi_m+\frac{\pi}{n}}\eta\cos\phi\,.\exp(-\eta^2\sin^2\phi)\,d\phi$$

$$=\frac{\pi^{\frac{1}{2}}}{2}\{1+\operatorname{erf}(\eta\cos\xi)\}\left[\operatorname{erf}\left(\eta\sin\left(\phi_m+\frac{\pi}{n}\right)\right)-\operatorname{erf}(\eta\sin\phi_m)\right].$$

Now, if $m=n$, $\cos\xi<0$, so that $\operatorname{erf}(\eta\cos\xi)\longrightarrow-1$ as $\eta\longrightarrow\infty$, and therefore $I_n\longrightarrow0$. But if $m=0$, $\cos\xi>0$, and $\phi_0<0<\phi_0+\pi/n$, and therefore $I_0\longrightarrow2\pi^{\frac{1}{2}}$ as $\eta\longrightarrow\infty$. This establishes the required result.

Thus, finally, the expression for w is given by

$$\frac{w}{W}=1-\frac{1}{2\pi^{\frac{1}{2}}}\sum_{m=0}^{2n-1}(-1)^m\int_{m\frac{\pi}{n}-\theta}^{(m+1)\frac{\pi}{n}-\theta}\eta f(\eta,\phi)\,d\phi, \quad . \quad . \quad . \quad (3.11)$$

Henceforward we shall consider the simplification of this result when n takes certain values. Accordingly, it is convenient to introduce the siffix n, w now being replaced by w_n, and so on for other quantities we shall consider. In particular w_1 and τ_1 will refer to the velocity and skin friction respectively for the standard flat plate problem of Rayleigh (1911).

Writing $$g(\eta,\phi)=\cos\phi\,.\exp(-\eta^2\sin^2\phi) \quad . \quad . \quad . \quad . \quad . \quad (3.12)$$

and $$h(\eta,\phi)=\cos\phi\,.\exp(-\eta^2\sin^2\phi)\operatorname{erf}(\eta\cos\phi), \quad . \quad . \quad . \quad (3.13)$$

then $$f(\eta,\phi)=g(\eta,\phi)+h(\eta,\phi),$$

and $$g(\eta,\phi+\pi)=-g(\eta.\phi),$$

$$h(\eta,\phi+\pi)=h(\eta,\phi).$$

The expression (3.11) now simplifies as follows :—

(i.) $n=2p+1$ (p an integer $\geqslant0$). The terms involving h in (3.11) vanish, and hence

$$\frac{w_n}{W}=1-\frac{1}{\pi^{\frac{1}{2}}}\sum_{m=0}^{2p}(-1)^m\int_{\frac{m\pi}{n}-\theta}^{(m+1)\frac{\pi}{n}-\theta}\eta\cos\phi\,.\exp(-\eta^2\sin^2\phi)\,d\phi$$

$$=1-\tfrac{1}{2}\sum_{m=0}^{2p}(-1)^m\left[\operatorname{erf}\left(\eta\sin\left\{(m+1)\frac{\pi}{n}-\theta\right\}\right)-\operatorname{erf}\left(\eta\sin\left\{\frac{m\pi}{n}-\theta\right\}\right)\right],$$

i. e. $$\frac{w_n}{W}=1+\sum_{m-0}^{2p}(-1)^m\operatorname{erf}\left(\eta\sin\left\{\frac{m\pi}{n}-\theta\right\}\right). \quad . \quad . \quad . \quad (3.14)$$

(ii.) $n=2p$ (p an integer $\geqslant1$). In this case the terms in g in (3.11) vanish, and we have

$$\frac{w_n}{W}=1-\frac{1}{\pi^{\frac{1}{2}}}\sum_{m=0}^{2p-1}(-1)^m\int_{\frac{m\pi}{n}-\theta}^{(m+1)\frac{\pi}{n}-\theta}\eta\cos\phi\,.\exp(-\eta^2\sin^2\phi)\,.\operatorname{erf}(\eta\cos\phi)\,d\phi, \quad . \quad . \quad . \quad (3.15)$$

(ii.*a*) There is a further simplification of (3.15) if $n=4p+2$ (p an integer $\geqslant0$).

For, writing

$$I_m=(-1)^m\int_{\frac{m\pi}{n}-\theta}^{(m+1)\frac{\pi}{n}-\theta}\eta\cos\phi\,.\exp(-\eta^2\sin^2\phi)\,.\,\mathrm{erf}(\eta\cos\phi)\,d\phi,$$

then

$$I_{2p+1+m}=(-1)^{m+1}\int_{\frac{\pi}{2}+\frac{m\pi}{n}-\theta}^{\frac{\pi}{2}+(m+1)\frac{\pi}{n}-\theta}\eta\cos\phi\,.\exp(-\eta^2\sin^2\phi)\,.\,\mathrm{erf}(\eta\cos\phi)\,d\phi$$

$$=(-1)^{m+1}\int_{\frac{m\pi}{n}-\theta}^{(m+1)\frac{\pi}{n}-\theta}\eta\sin\phi\,.\exp(-\eta^2\cos^2\phi)\,.\,\mathrm{erf}(\eta\sin\phi)\,d\phi,$$

and therefore

$$I_m+I_{2p+1+m}$$

$$=(-1)^m\int_{\frac{m\pi}{n}-\theta}^{(m+1)\frac{\pi}{n}-\theta}\left[\begin{array}{l}\eta\cos\phi\,.\exp(-\eta^2\sin^2\phi)\,.\,\mathrm{erf}(\eta\cos\phi)\\-\eta\sin\phi\,.\exp(-\eta^2\cos^2\phi)\,.\,\mathrm{erf}(\eta\sin\phi)\end{array}\right]d\phi$$

$$=(-1)^m\frac{\pi^{\frac{1}{2}}}{2}\Big[\mathrm{erf}(\eta\cos\phi)\,.\,\mathrm{erf}(\eta\sin\phi)\Big]_{\frac{m\pi}{n}-\theta}^{(m+1)\frac{\pi}{n}-\theta}.$$

Thus, finally

$$\frac{w_n}{W}=1+\sum_{m=0}^{2p}(-1)^m\,\mathrm{erf}\left(\eta\cos\left\{\frac{m\pi}{n}-\theta\right\}\right).\,\mathrm{erf}\left(\eta\sin\left\{\frac{m\pi}{n}-\theta\right\}\right). \quad . \quad (3.16)$$

The results (3.14) and (3.16) give simple expressions for w_n in terms of error functions, and deal with all cases of n with the exception of the group $n=4p$ (p an integer). In this case w_n may be computed from (3.15). The first three examples of w_n are

$$\left.\begin{array}{l}w_1=W[1-\mathrm{erf}(\eta\sin\theta)] \quad \text{(Rayleigh's case)},\\ w_2=W[1-\mathrm{erf}(\eta\cos\theta)\,.\,\mathrm{erf}(\eta\sin\theta)],\\ w_3=W\left[\begin{array}{r}1-\mathrm{erf}(\eta\sin\theta)-\mathrm{erf}(\eta\sin\{\pi/3-\theta\})\\+\mathrm{erf}(\eta\sin\{2\pi/3-\theta\}).\end{array}\right]\end{array}\right\} . \quad . \quad (3.17)$$

In all cases the velocity distribution must be symmetrical about the plane $\theta=\theta_n=\pi/2n$. Fig. 1 shows $1-w_n/W$ plotted against $\theta_n-\theta$ for $\eta=1$, 2, 3 respectively in the cases $n=2$ and $n=3$.

4. *The Skin Friction.* Since the motion is symmetrical about $\theta=\theta_n$ it is clearly sufficient to consider the skin friction τ_n on one plate only. Selecting the plate $\theta=0$, then for $t>0$

$$\tau_n=-\frac{\mu}{r}\cdot\frac{\partial w_n}{\partial\theta}=-\frac{\mu}{2(\nu t)^{\frac{1}{2}}\eta}\cdot\frac{\partial w_n}{\partial\theta} \quad \text{(evaluated for } \theta=0)$$

$$=\frac{\mu W}{4(\pi\nu t)^{\frac{1}{2}}}\sum_{m=1}^{2n-1}(-1)^m\left[f\left(\eta,\frac{m\pi}{n}\right)-f\left(\eta,\{m+1\}\frac{\pi}{n}\right)\right]$$

or

$$\tau_n=\frac{\mu W}{2(\pi\nu t)^{\frac{1}{2}}}\sum_{m=0}^{2n-1}(-1)^m f\left(\eta,\frac{m\pi}{n}\right), \quad . \quad . \quad . \quad (4.1)$$

(4.1) gives an expression for τ_n for all values of n, and it follows immediately that

$$\tau_n \longrightarrow \tau_1 \text{ as } \eta \longrightarrow \infty. \qquad (4.2)$$

That is, sufficiently far from the corner, the skin friction approximates to Rayleigh's value for the flat plate problem.

For, if $m \neq 0, n,$ then $\sin m\pi/n \neq 0,$ and $f(\eta, m\pi/n) \to 0$ as $\eta \to \infty$

while if $m=n, f(n, m\pi/\eta) = -(1-\text{erf}\,(\eta)) \to 0$ as $\eta \to \infty$

and if $m=0\; f(\eta, m\pi/n) = 1+\text{erf}\,(\eta) \to 2$ as $\eta \to \infty.$

If $n>1,$ then $\tau_n=0$ when $\eta=0,$ . . . . . (4.3)

since
$$\tau_n(0) = \frac{\mu W}{2(\pi\nu t)^{\frac{1}{2}}} \sum_{m=0}^{2n-1} (-1)^m \cos\frac{m\pi}{n} = \begin{cases} \dfrac{\mu W}{(\pi\nu t)^{\frac{1}{2}}} \, (n=1) \\ 0 \quad (n>1) \end{cases}.$$

Fig. 1.

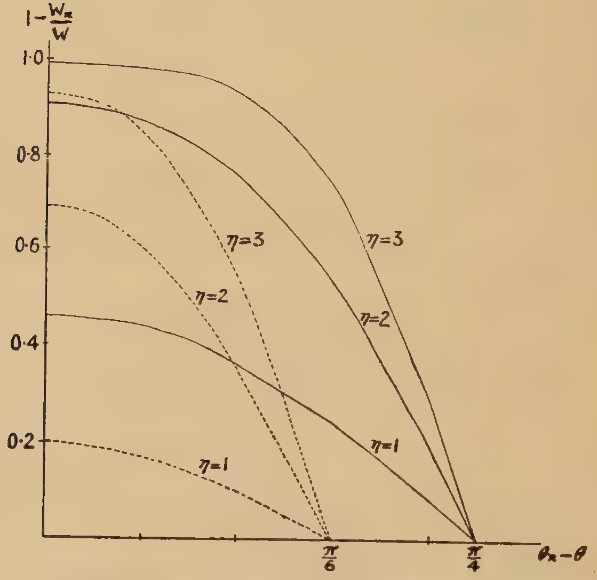

Velocity distribution for the cases $n=2, 3.$

$n=2$ ———

$n=3$ - - - - - -

Further, if $n>1$, it follows that

$$\tau_1 - \tau_n > 0. \qquad (4.4)$$

To establish this, consider the following simplified expressions for $\tau_1 - \tau_n$.

(i.) $n=2p+1$ $(p \geqslant 1)$

$$\tau_1 - \tau_n = \frac{2\mu W}{(\pi\nu t)^{\frac{1}{2}}} \sum_{m=0}^{p} (-1)^{m+1} \cos\frac{m\pi}{n} \,.\, \exp\left(-\eta^2 \sin^2\frac{m\pi}{n}\right). \qquad (4.5)$$

(ii.) $n=2p$

$$\tau_1-\tau_n=\left\{\begin{array}{ll}\dfrac{\mu W}{(\pi\nu t)^{\frac{1}{2}}}\left[1-\operatorname{erf}\eta+2\sum_{m=1}^{p-1}(-1)^{m+1}\cos\dfrac{m\pi}{n}\right. & \\ \qquad\left.\times\exp\left(-\eta^2\sin^2\dfrac{m\pi}{n}\right)\operatorname{erf}\left(\eta\cos\dfrac{m\pi}{n}\right)\right] & (p>1), \\ \dfrac{\mu W}{(\pi\nu t)^{\frac{1}{2}}}[1-\operatorname{erf}\eta] & (p=1).\end{array}\right\} \quad . \quad . \quad . \quad (4.6)$$

Now $1-\operatorname{erf}(\eta)>0$, and the terms in the series (4.5) and (4.6) are alternately positive and negative and decreasing, each series beginning with a positive term. This establishes (4.4).

Since $\tau_1-\tau_n\rightarrow 0$ as $\eta\rightarrow\infty$, it is possible to determine α_n such that τ_n is within 1 per cent (say) of τ_1 when $\eta>\alpha_n$.

Using (4.5) and (4.6) the following approximate values are easily obtained

$$\alpha_2=1{\cdot}9,$$
$$\alpha_3=2{\cdot}5,$$
$$\alpha_4=3{\cdot}2,$$
$$\alpha_5=3{\cdot}8.$$

As one would expect, α_n increases with n, that is, with the sharpness of the corner.

Thus in all the cases $n>1$, the skin friction vanishes at the corner itself, but increases away from the corner until it attains the value τ_1; this occurs (to with 1 per cent) when η exceeds α_n.

Frictional Force parallel to Oz. The frictional force F_n per unit length on the section $0\leqslant r\leqslant b$ is $\int_0^b \tau_n\,dr$, so that

$$F_1-F_n=\int_0^b(\tau_1-\tau_n)\,dr=2(\nu t)^{\frac{1}{2}}\int_0^{b'}(\tau_1-\tau_n)\,d\eta, \quad . \quad . \quad (4.7)$$

where $b'=\dfrac{b}{2(\nu t)^{\frac{1}{2}}}$.

Assuming for the moment the convergence of the infinite integrals, (4.7) may be written

$$F_1-F_n=E_n-2(\nu t)^{\frac{1}{2}}\int_{b'}^{\infty}(\tau_1-\tau_n)\,d\eta, \quad . \quad . \quad . \quad . \quad (4.8)$$

where
$$E_n=2(\nu t)^{\frac{1}{2}}\int_0^{\infty}(\tau_1-\tau_n)\,d\eta, \quad . \quad . \quad . \quad . \quad . \quad . \quad . \quad (4.9)$$

(so that $E_n>0$ if $n>1$).

The convergence of the infinite integrals follows from (4.5) and (4.6) since, in the first place,

$$\int_{x_1}^{x}(1-\operatorname{erf}\eta)\,d\eta=x(1-\operatorname{erf}x)-x_1(1-\operatorname{erf}x_1)+\frac{1}{\pi^{\frac{1}{2}}}[\exp(-x_1^2)-\exp(-x^2)],$$

and as $x\rightarrow\infty$, $x(1-\operatorname{erf}x)\rightarrow 0$, so that

$$\int_{x_1}^{\infty}(1-\operatorname{erf}\eta)\,d\eta=\frac{1}{\pi^{\frac{1}{2}}}\exp(-x_1^2)-x_1(1-\operatorname{erf}x_1), \quad . \quad . \quad (4.10)$$

while the integrals arising from the terms of the series converge, since $\sin m\pi/n\neq 0$.

Writing $E_n=\mu W\lambda_n$, F_{2n+1} and λ_{2n+1} can be found directly, and in certain special cases so can F_{2n} and λ_{2n}. From (4.1) and (4.9) it follows that λ_n is a function of n only.

The terms on the right-hand side of (4.8), and subsequent approximations to them, can be calculated by considering $Q_n(X)$, where

$$Q_n(X)=\frac{2(\nu t)^{\frac{1}{2}}}{\mu W}\int_X^{\infty}(\tau_1-\tau_n)\,d\eta,$$

i. e.

$$Q_n(X)=\frac{1}{\pi^{\frac{1}{2}}}\int_X^{\infty}\left[2+\sum_{m=0}^{2n-1}(-1)^{m+1}f\left(\eta,\frac{m\pi}{n}\right)\right]d\eta. \quad . \quad . \quad (4.11)$$

Thus

$$\lambda_n=Q_n(0). \quad . \quad . \quad . \quad . \quad . \quad . \quad . \quad . \quad . \quad (4.12)$$

$Q_n(X)$ decreases as X increases (since $\tau_1-\tau_n>0$), and it is clear from (4.5), (4.6) and (4.10) that $Q_n(X)\rightarrow 0$ as $X\rightarrow\infty$.

From (4.5), for $n=2p+1$, we have

$$Q_n(X)=2\sum_{m=1}^{p}(-1)^{m+1}\cot\left(\frac{m\pi}{n}\right)\left[1-\operatorname{erf}\left(X\sin\frac{m\pi}{n}\right)\right], \quad . \quad (4.13)$$

and therefore

$$\lambda_n=2\sum_{m=1}^{p}(-1)^{m+1}\cot\left(\frac{m\pi}{n}\right). \quad . \quad . \quad . \quad . \quad . \quad . \quad (4.14)$$

$Q_n(X)$ can also be evaluated in the special cases $n=2$ and $n=4$. Using (4.6) and (4.10)

$$Q_2(X)=\frac{2}{\pi^{\frac{1}{2}}}\left[\frac{1}{\pi^{\frac{1}{2}}}\exp(-X^2)-X(1-\operatorname{erf}X)\right] \quad . \quad . \quad . \quad (4.15)$$

and

$$\begin{aligned}Q_4(X)=&\frac{2}{\pi^{\frac{1}{2}}}\left[\frac{1}{\pi^{\frac{1}{2}}}\exp(-X^2)-X(1-\operatorname{erf}X)\right]\\&+\frac{2\sqrt{2}}{\pi^{\frac{1}{2}}}\int_X^{\infty}\exp(-\tfrac{1}{2}\eta^2)\,.\operatorname{erf}\left(\frac{1}{\sqrt{2}}\eta\right)d\eta\\=&\frac{2}{\pi^{\frac{1}{2}}}\left[\frac{1}{\pi^{\frac{1}{2}}}\exp(-X^2)-X(1-\operatorname{erf}X)\right]+1-\operatorname{erf}^2\left(\frac{1}{\sqrt{2}}X\right), \quad . \quad (4.16)\end{aligned}$$

from which $\lambda_2=2/\pi$, $\lambda_4=(2/\pi)+1$.

A first few of the values of λ_n are

$$\lambda_2=0\cdot6366,$$
$$\lambda_3=1\cdot1547,$$
$$\lambda_4=1\cdot6366,$$
$$\lambda_5=2\cdot0530,$$
$$\lambda_7=3\cdot2412.$$

An approximation to the term on the right hand side of (4.8) can always be obtained. This term will be within 1 per cent of E_n provided $b'>\beta_n$ where

$$Q_n(\beta_n)=0\cdot01\lambda_n, \quad \ldots \quad (4.17)$$

β_n can always be so chosen, since $Q_n(X)$ is positive, continuous, and $\longrightarrow 0$ as $X \longrightarrow \infty$. We obtain the following approximate values

$$\beta_2=1\cdot6,$$
$$\beta_3=2\cdot1,$$
$$\beta_4=2\cdot6,$$
$$\beta_5=3\cdot2.$$

Hence, provided $b'>\beta_n$, a convenient approximation to (4.8) is

$$F_n=F_1-\mu W\lambda_n=\mu W\left[\frac{2b'}{\pi^{\frac{1}{2}}}-\lambda_n\right]. \quad \ldots \quad (4.18)$$

5. *The Related Steady Flow Problem.* Howarth, in his discussion of the corresponding problem for a semi-infinite plate (Howarth 1950) has used a hypothesis by Rayleigh (1911) to obtain information about the steady flow past an infinite quarter plane, and the same application can be made here. That is, in the results already obtained, we replace t by z/W (so that η is replaced by $\frac{1}{2}r(W/\nu z)^{\frac{1}{2}}$) and, writing w' in place of $W-w$, we expect to derive a qualitative picture of the steady flow w' of a stream inside the corner formed by the quarter planes $\theta=0$, $\theta=\pi/n$, $z\geqslant0$, the undisturbed velocity of the incident stream being $(0, 0, W)$. Of some special interest is the case $n=2$, which will be considered now in further detail.

The Right Angled Corner ($n=2$). From (3.17) we have

$$\frac{w}{W}=1-\operatorname{erf}(X)\,.\,\operatorname{erf}(Y), \quad \ldots \quad (5.1)$$

writing $\eta\cos\theta=X$, $\eta\sin\theta=Y$.

It follows then, that if, say, $X>2$

$$\frac{w}{W}=1-\operatorname{erf}(Y), \quad \ldots \quad (5.2)$$

approximately, since $1>\operatorname{erf} X>0\cdot995$; that is, the flow is very nearly the same as that deduced by Rayleigh for the infinite flat plate. This implies that the disturbing effect of the corner is confined, for all practical purposes, to the region $0\leqslant X\leqslant2$, $0\leqslant Y\leqslant2$.

Rayleigh's hypothesis would give, for the steady flow problem, a velocity pattern of the form

$$\frac{w'}{W}=\operatorname{erf}(X')\,.\,\operatorname{erf}(Y'), \quad . \quad . \quad . \quad . \quad . \quad . \quad . \quad . \quad (5.3)$$

where $$X'=\tfrac{1}{2}x\left(\frac{W}{\nu z}\right)^{\frac{1}{2}}, \qquad Y'=\tfrac{1}{2}y\left(\frac{W}{\nu z}\right)^{\frac{1}{2}}.$$

From the point of view of boundary layer theory, therefore, we should expect some thickening of the boundary layer in the vicinity of the corner, as indicated in fig. 2, while away from the corner the divergence from the flat plate flow will be negligible. Now the exact solution of the boundary layer equations for the steady flow past a flat plate (Blasius 1908) shows that the mainstream velocity is attained when $Y'=3$, and not $Y'=2$ as indicated by Rayleigh's hypothesis. Accordingly, in this problem, it is probable that the influence of the corner on the boundary layer is effectively confined to the region $0\leqslant X'\leqslant 3$, $0\leqslant Y'\leqslant 3$. Failing an analytical solution of this problem, a numerical approach would require an assumption such as this. Carrier, in his solution (Carrier 1946) makes this assumption, though Howarth has pointed out that certain of the equations of motion have been disregarded, and the solution is therefore open to objection.

Fig. 2.

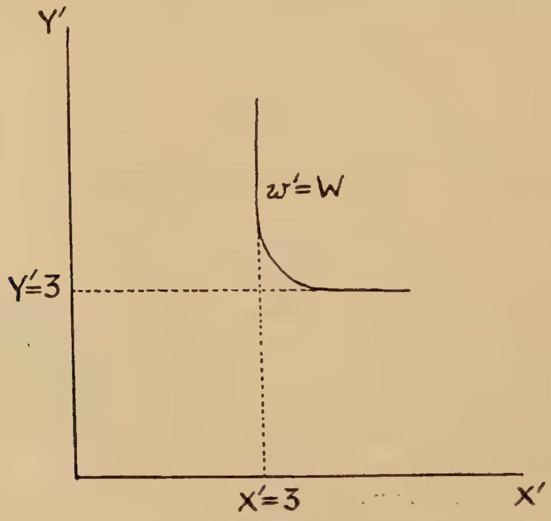

Boundary layer in right angled corner.

Referring back to the unsteady problem, we have for the frictional force F per unit length of a section of width b the approximate result (using 4.18))

$$F=\mu W\left[\frac{b}{(\pi\nu t)^{\frac{1}{2}}}-\frac{2}{\pi}\right], \quad . \quad . \quad . \quad . \quad . \quad . \quad . \quad (5.4)$$

provided $b/2(\nu t)^{\frac{1}{2}} > 1{\cdot}6$. From this we can deduce an approximation to the frictional force when a rectangular channel of sides a and b is set in motion in the same way as the original boundary. Bearing in mind the requirements of the velocity distribution (5.2) then, provided

$$a,\, b > 8(\nu t)^{\frac{1}{2}}, \qquad \text{(5.5)}$$

the frictional force per unit length on the channel would be given by

$$F = 2\mu W\left[\frac{a+b}{(\pi\nu t)^{\frac{1}{2}}} - \frac{8}{\pi}\right], \qquad \text{(5.6)}$$

taking into account all four interior faces of the channel.

If we now extend this result, by Rayleigh's hypothesis, to the problem of steady flow through the interior of a rectangular channel of finite length l, then if

$$a,\, b > 8\left(\frac{\nu l}{W}\right)^{\frac{1}{2}}, \qquad \text{(5.7)}$$

the force per unit length at distance z would be

$$2\mu W\left[(a+b)\left(\frac{W}{\pi\nu z}\right)^{\frac{1}{2}} - \frac{8}{\pi}\right], \qquad \text{(5.8)}$$

and the skin friction coefficient C_f for the interior of the channel would be given by

$$\begin{aligned} C_f &= \frac{1}{\rho W^2 l(a+b)}\int_0^l 2\mu W\left[(a+b)\left(\frac{W}{\pi\nu z}\right)^{\frac{1}{2}} - \frac{8}{\pi}\right]dz \\ &= 4\left(\frac{\nu}{\pi W l}\right)^{\frac{1}{2}}\left[1 - \frac{4l}{a+b}\left(\frac{\nu}{\pi W l}\right)^{\frac{1}{2}}\right]. \qquad \text{(5.9)} \end{aligned}$$

The result (5.9) would be of greater interest if corresponding results were available for the flow on the outside of the channel. That is, it would be useful to extend the investigation to wedge-shaped channels of any angle β. For this, a solution of (2.1) as a Fourier series in θ would be available, but it should also prove fruitful to investigate a solution of period 2β in θ given by Carslaw (1910) for use as a suitable Green's function. In this latter case it may not be possible to reduce the expression for w to single integrals, but nevertheless the method may yield an expression for τ in terms of an integral, and this would be more useful than the infinite series in any discussion of the limiting value of τ remote from the corner.

I should like to thank Professor Howarth and Mr K. Stewartson of Bristol University for their kind assistance to me in the preparation of this paper.

REFERENCES.

BLASIUS, H., 1908, *Zeitschr. fur Mathematik und Physik*, Bd. 56, p. 1—.
CARRIER, G. F., 1946, *American Quarterly of Applied Maths.* (Brown University), **4**, 367–370.
CARSLAW, H. S., 1910, *Proc. Lond. Math. Soc.*, [2] **8**, 365–374.
CARSLAW, H. S., and JAEGER, J. C., 1947, *Conduction of heat in solids* (Chap. XIII), (Oxford University Press).
HOWARTH, L., 1950, *Proc. Camb. Phil. Soc.*, **46**, pt. 1, 127–140.
RAYLEIGH, LORD., 1911, *Phil. Mag.*, [6] **21**, 697–711.

XVII. *Emission of Energetic Helium and Lithium Fragments in Nuclear Explosions.*

By S. O. C. Sörensen*.
The H.H. Wills Physical Laboratory, University of Bristol †.

[Plates VII. & VIII.]

Summary.

A phenomenological description is given of the processes which lead to the emission of energetic heavy particles from cosmic ray stars. The frequency, angular distributions and energy spectra of the particles have been determined. These, and an analysis of the associated stars, indicate that the particles cannot be generated by an evaporation process. On the other hand, direct knocking on of the heavy particle by the primary can be excluded. The fragments must therefore result from interactions which are intermediate between these two extreme possibilities. No connection has been found between the ejection of energetic heavy particles and meson showers.

Introduction.

As a result of experiments with photographic plates exposed to cosmic radiation, several reports have been given within the last few years of observations on energetic heavy nuclear "fragments" ejected during the explosive disintegration of nuclei. A striking feature of these phenomena is that the heavy particles are frequently emitted with energies much greater than that which can be accounted for in terms of the electrostatic repulsion of the residual nucleus. The problem therefore arises as to the physical mechanism through which it is possible to endow these particles with kinetic energies greatly in excess of their binding energy without disrupting them in the process. The emission of the particles is rare, and it appears likely that an extensive investigation will be necessary to explain their production in detail. It therefore appears appropriate to give a preliminary report on the material already available. As the expulsion of heavy charged particles presents similar problems to that of the ejection of α-particles, which occur much more frequently, a closer study of the latter has also been included in this investigation.

The plates used in the investigation were coated with Ilford G5 emulsion, 400 μ thick, and were exposed by means of free balloons at geomagnetic latitude 54° N. In order to have well-defined conditions for the experiment only material exposed at approximately the same altitude has been employed. This was obtained in two level flights of which details are given in Table I.

---

* Communicated by Professor C. F. Powell, F.R.S.

† On leave from the Physical Institute, University of Oslo.

TABLE I.

Plate series	Altitude	Mass of overlying air	Duration of exposure
HA. 21	68,000 feet	(52 ± 1 gm./cm.^{2})	100 minutes
HA. 30	64,000 feet	(60 ± 1 gm./cm.^{2})	5·5 hours

The present paper describes observations on (*a*) the relative numbers of ejected lithium and helium nuclei of great energy ; and (*b*) the distribution in energy of the helium particles and their directions of emission with respect to the " primary " particle producing the disintegration.

CHARGE DETERMINATION AND RELATIVE FREQUENCY OF FRAGMENTS.

It has long been recognized that some of the heavy particles which are emitted in cosmic-ray " stars " are more massive than α-particles. Apart, however, from the well-known lithium fragment (Franzinetti and Payne 1948) leading to the characteristic " hammer tracks ", it is in general difficult to obtain an accurate determination of their charge. In a recent report Perkins (1950 a) has made an extensive analysis of the emission of " low energy fragments " and has discussed the various methods of charge determination.

For the more energetic heavy fragments the most characteristic feature of the tracks is the large number of " knock on " electrons or δ-rays which the particles produce in their passage through the emulsion, and a study of the distribution of these δ-rays along the tracks provides a precise method for determining the charge of the fragments (Sörensen 1949).

The present investigation has been confined to particles which are emitted from " stars ", and which have a residual range greater than 700 μ in the emulsion. The corresponding minimum values of the energy are 45 MeV. for an α-particle and 90 MeV. for Li_3^7. If particles of shorter range are accepted, it becomes increasingly difficult to distinguish between these heavier particles and singly charged particles on the basis of δ-ray counts. On the other hand, an increase of the lower limit of the range results in a large decrease in the total number of tracks available, and thus leads to results of lower statistical weight. The results of δ-ray counts on 372 tracks is shown in fig. 1. This figure shows the relative frequency of occurrence of tracks with different numbers, N, of δ-rays of 3 or more grains, in the last 700 μ of the track. We have here included some tracks which have been found in other exposures, and a few tracks which entered and came to rest in the emulsion.

Two distinct groups of particles are immediately apparent in fig. 1, with a mean total number of δ-rays ~ 12 and ~ 30. Similar counts on protons give a mean value of ~ 3 in the last 700 μ of the track. This indicates that the most pronounced group (I.) is due to helium nuclei, and the second group (II.) mostly to lithium nuclei. In the flights referred to in Table I., 271 particles of charge $2e$ and 10 of charge $3e$ have been found so far, making the ratio.

$$\frac{\text{Lithium}}{\text{Helium}} \sim 0{\cdot}03. \qquad (1)$$

It is reasonable to assume that the given ratio represents an upper limit only, since some helium tracks of unusually low δ-ray density may have been missed in scanning the plates. This "loss" may account for the slight asymmetry in the distribution I.

That the great majority of the particles are stable or long-lived isotopes of the corresponding elements is proved by the fact that no secondary particles, such as electrons, are observed to be emitted at the point where the particles come to rest. None of the lithium fragments showed the characteristic "hammer" tracks due to Li^8.

Fig. 1.

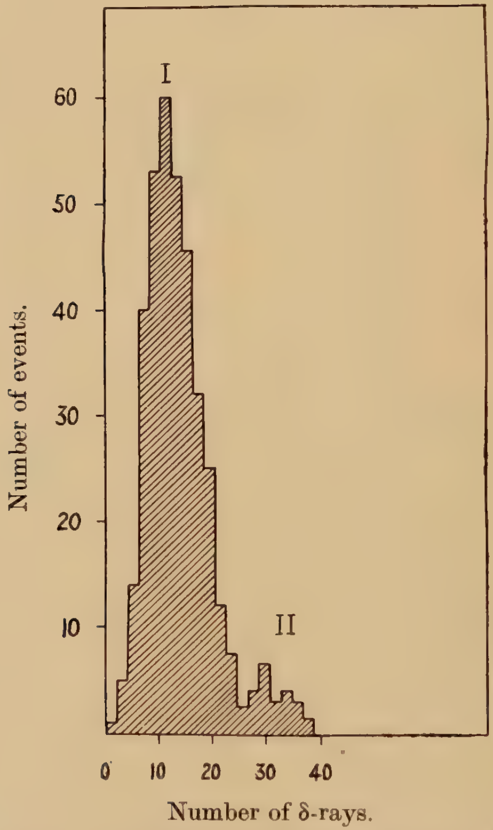

Histogram showing the distribution of the total number of δ-rays (≥ 3 grains) in the last 700 μ of the track of the fragment.

In neither of the two flights have any long tracks of heavier particles been found although a great number of heavier "low energy fragments" and "taper tracks" have been observed with a range less than 700 μ.

Angular Distributions.

In those cases in which the heavy particle has been emitted from a nuclear explosion of which the incident particle can be distinguished, the angle, γ, between its track and the line of motion of the "primary" particle has been determined. It has been assumed as a sufficient criterion that a track is that of a particle producing a particular nuclear explosion if its specific ionization is near the minimum value for charge $|e|$; and if it is the only such track in the "upper hemisphere" of the star. Camerini *et al.* (1949) have shown that the great majority of tracks so defined are due to particles which approached the nucleus and caused its disintegration.

Histograms showing the distribution of the observed values of γ, for helium particles and heavier fragments respectively, are shown in fig. 2. The curve gives the angular distribution of the particles with charge $2e$ in number per unit solid angle. In making these observations the spatial orientation of each track, taking into account the angle of dip in the emulsion has been determined. It will be seen that the difference in direction is usually less than 90°, but that much larger values are sometimes found.

Fig. 2.

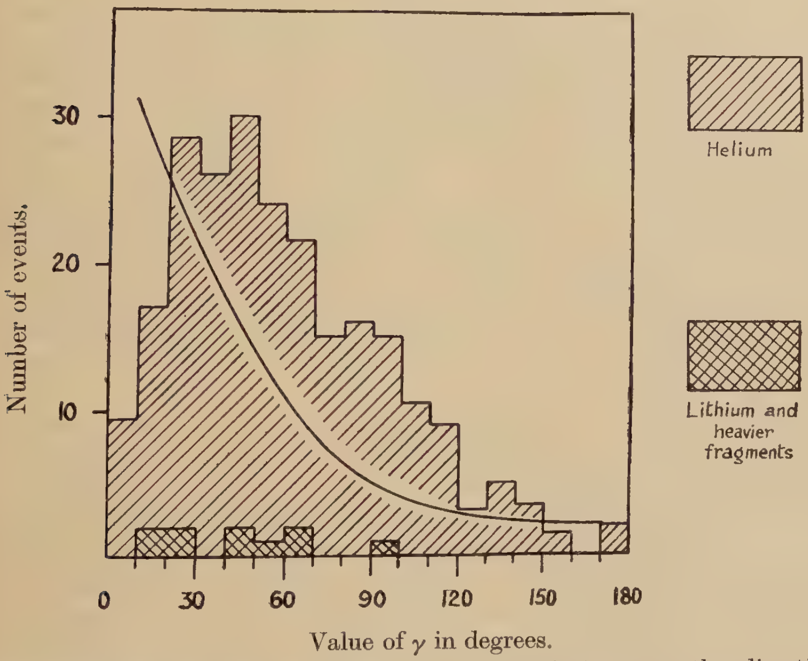

Histogram showing the distribution of the angle between the direction of motion of the primary and the heavy particle. The full curve shows the results transformed to correspond to the intensity per unit solid angle.

The number of heavier fragments is very small, but it appears that there is a collimation in the direction of the primary, a result in agreement with the observations made by Perkins on energetic heavy fragments.

With the criterion for the definition of a primary particle employed above, "stars" produced by particles with charge $2e$ are automatically eliminated. A large fraction of the "stars" from which heavy fragments are emitted ($\sim$ 20 per cent) are produced however, by fast α-particles at the altitude of the exposure and a special investigation of the angular distributions in these cases would be of interest. The difficulty in identifying the α-particle primaries except in those favourable cases in which the tracks are longer than 3 mm., has made the available material too small to allow any significant conclusions to be drawn.

THE DISTRIBUTION IN ENERGY OF THE HELIUM PARTICLES.

A number of recent papers have dealt with the energy spectrum of the various charged particles emitted in the disintegration of nuclei with very high excitation energy (Harding *et al.* 1949, Perkins 1950 b, Page 1950). The main purpose of these investigations has been to check the " evaporation theory " of highly excited nuclei (Weisskopf 1937, Bagge 1944, Le Couteur 1950) and satisfactory agreement has been obtained between theory and experiment. The particles considered in these investigations have energies up to $\sim$ 50 MeV., but all the authors report the existence of a high energy " tail " due to processes which are probably totally different from that of evaporation. The new method of combining " multiple scattering " and " grain density " (Fowler 1950) has made it possible to investigate this high energy " tail ", and energy spectra of the ejected mesons, protons, and deuterons have been determined (Camerini *et al.* 1950). It is reasonable to assume that most of the particles considered in the present investigation are the corresponding particles with charge $\geqq 2e$, and it is of interest to compare the spectra for the different groups of particles.

Owing to the high grain-density in the tracks of non-relativistic particles, with charge $\geqq 2e$ in the new electronsensitive plates, the energy cannot be measured by grain counting. One way of overcoming this difficulty is to measure the ranges of the particles and to extrapolate range–energy relations, a method which is necessarily confined to particles arrested in the emulsion. However, an ambiguity exists in the application of range–energy curves, for the particles of charge $2e$ and $3e$ because of the presence of different isotopes. It has been shown, for example, by applying scattering methods to the longest tracks in the group, that both isotopes He^3, He^4 contribute to the main group I. of fig. 1. It has not yet been possible, however, to determine the ratio of the two types.

Assuming all the particles in fig. 1 with less than 25 δ-rays in the last 700 μ of the track to be α-particles, and applying geometrical corrections for loss, we obtain the differential spectrum, fig. 3, which shows the kinetic energy, E, of the helium nuclei at their points of creation. Isotropic angular distribution with respect to the vertical was assumed.

The longest observed track of a particle with charge $2e$, ending in emulsion, has a range $\sim$ 1 cm., a value which corresponds to an α-particle with an energy of about $\sim$ 200 MeV. No helium particles with relativistic energies have been observed ejected from stars as secondaries, except in the nuclear collisions produced by heavy primaries in which they occur as fragments in the "break-up" of heavier nuclei. (Bradt and Peters 1950, Dainton and Kent 1950).

A comparison of the energy spectrum in fig. 3 with the corresponding results for protons, and deuterons and tritons as determined by the scattering method, suggests that they are rather similar in form. The spectrum may be approximately represented by a power law of the form

$$N(E)\,dE = \frac{\text{const}}{E^K}\,dE \quad . \quad . \quad . \quad . \quad . \quad . \quad . \quad (2)$$

where K is of the order of 1·6.

Fig. 3.

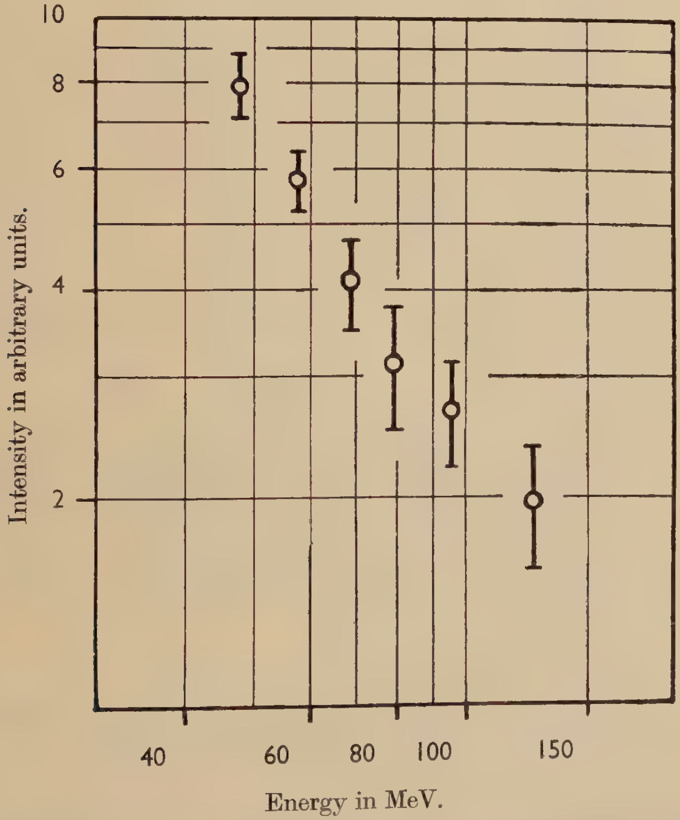

Differential distribution in the kinetic energy of α-particles ejected from stars.

The lithium fragments are too few to deduce the form of their energy spectrum, but all the fragments which have been found to end in the emulsion have a range less than 1600 μ. This value corresponds to an energy of 145 MeV. for Li^7_3.

CHARACTERISTICS OF THE "STARS" ASSOCIATED WITH THE EMISSION OF HEAVY "FRAGMENTS".

As a second mode of attack on the problem, a statistical analysis of the disintegrations from which heavy particles are emitted has been made, and a determination of their frequency of occurrence. Out of a total number of 15,000 stars in the HA. 21 plates, 189 stars of 3 or more prongs have been found from which emerge particles with charge $\geqslant 2e$, and of range $>700\,\mu$. The total number of stars giving rise to the events described in the present paper is 400. In this analysis we have included stars leading to ejection of heavy particles, which although leaving the emulsion before being brought to rest, have such a track-length and δ-ray density as to indicate that their total range in the emulsion would be greater than $700\,\mu$. Stars caused by heavy primaries have been excluded, since the mechanism of disintegration in these cases may be different. Stars of the latter type commonly show a marked asymmetry due to collimation of the secondary fragments with regard to the line of motion of the primary. Pl. VII. shows a photomicrograph of an example of this type, in which a heavy primary with charge $Z=12\pm 1e$ collides with a nucleus of silver or bromine in the emulsion and produces an energetic disintegration with 38 heavily ionizing secondary particles. Several examples of this type of event have been found in the two flights. The most striking feature of the event shown in Pl. VII. is the expulsion of a very heavy non-relativistic fragment of range $550\,\mu$. A comparison of this track with others due to particles which have been identified indicates that its charge was $Z=5\pm 1e$.

(a) *The distribution in N_h.*

Using the terminology introduced by Brown *et al.* (1949), we may divide the tracks of particles emitted from stars into three groups according to their grain density g, as compared with $g_{\min}$ the grain density of a relativistic particle of charge $|e|$:

(1) "Thin" tracks $g_{\min}\leqq g<1{\cdot}4g_{\min}$ (shower particles).
(2) "Grey" tracks $1{\cdot}4g_{\min}<g<5g_{\min}$.
(3) "Black" tracks $g>5g_{\min}$.

The sum of the "grey" and "black" tracks from a star is represented by the symbol N_h, and the number of shower particles by n_s.

Fig. 4 gives the distribution in N_h for all the stars which emit energetic helium particles: the observations have been confined to stars with $n_s\geqq 1$ or with a singly charged relativistic primary. The corresponding values of the total release of energy are indicated in the figure.

The distribution is seen to extend up to $N_h\sim 35$, with a broad maximum for $N_h\sim 11-17$.

The probability, P, that a star with a given N_h has an associated energetic helium particle is given by a comparison of the distribution shown in fig. 4 with the curve showing the frequency of occurrence of all stars of this class. This is known for the HA. 21 plates (Table I.), and fig. 5 gives the result plotted in logarithmic scale. The figure shows that there is an extremely rapid rise in the probability of emission of energetic heavy particles with increase in N_h. If, for a given N_h, the number of stars which emit energetic helium particles is represented by N_{He}, and the total number of stars by N_{total}, the results of fig. 5 may be represented approximately by the relation

$$P = \frac{N_{He}}{N_{total}} = \text{const. } e^{2N_h}. \qquad (3)$$

Fig. 4.

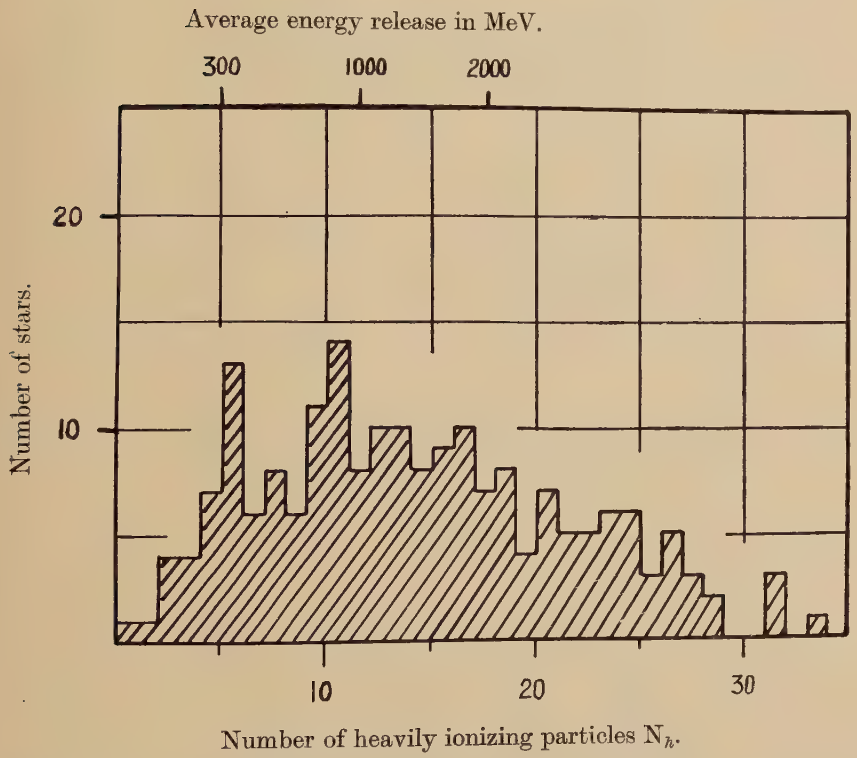

Histogram showing the distribution in N_h of stars emitting a single energetic helium particle.

The size distributions of stars emitting energetic helium particles or heavier nuclei is given in fig. 6.

Fig. 6 *b* shows the distribution in N_h of all the stars which simultaneously emit two or more fast heavy particles ($R > 700\ \mu$) *e. g.* two α-particles, or one α-particle and a lithium fragment. The displacement of the whole distribution towards higher N_h is immediately apparent. No star of this type has been observed in the lighter elements (C, N, O) in the emulsion. Pl. VIII. shows a photomicrograph of a star in which a helium particle and a lithium fragment are ejected, simultaneously with range respectively 1200 μ and 1000 μ.

In order to see if the distribution in N_h varies appreciably when particles of different energy are considered, the observations on particles with charge $2e$ were divided into two groups according to whether the range

Fig. 5.

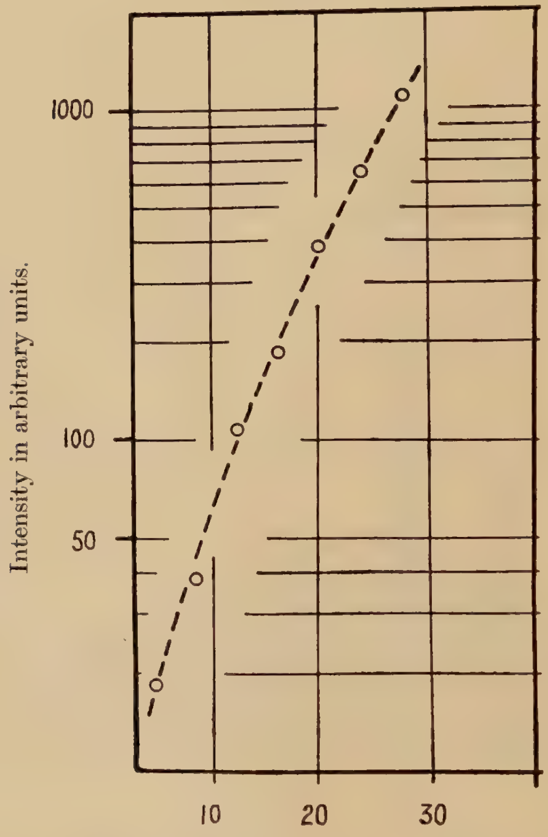

Number of heavily ionizing particles N_h.

The probability of the ejection of an energetic helium particle as a function of N_h.

of the particle was in the interval from 700 μ to 1500 μ or greater than 1500 μ. The corresponding values of the kinetic energy for α-particles are 45 MeV. $<$ E $<$ 70 MeV. and E $>$ 70 MeV. respectively. The resulting distributions in N_h for the associated stars are shown in fig. 6 *a* and *c*. It is found that, within the statistical fluctuations, the two distributions are similar in form. It appears therefore that no very strong correlation exists between the particular energy with which a helium particle is emitted and the energy release in the associated star. In this connection, it may be remarked that the longest α-particle observed (~ 1 cm.) was emitted from a star with N_h only 4. Further, a number of heavy particles have been found with energies up to ~ 140 MeV. which are not associated with any other heavily ionizing particles—a point which will be discussed later.

Fig. 6.

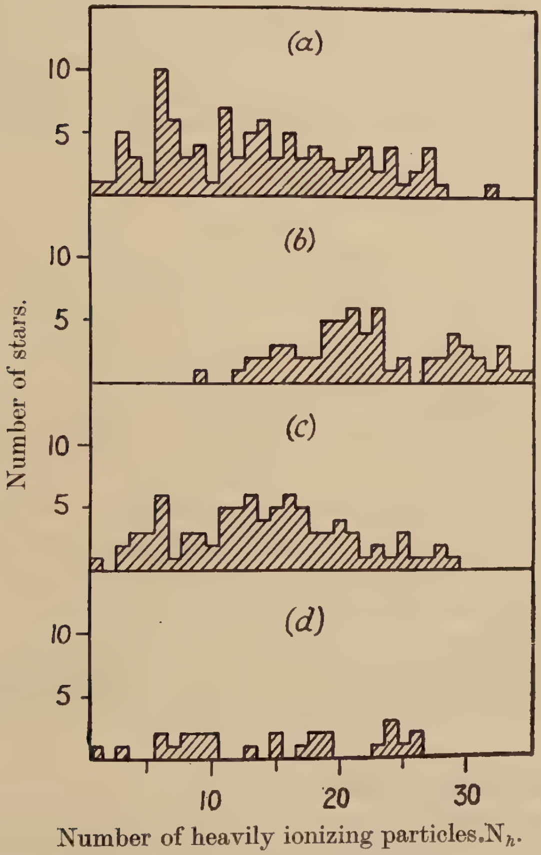

Histograms showing the distribution in N_h of stars emitting :—

(*a*) A single helium particle with range between 700 μ and 1500 μ.
(*b*) Simultaneously two heavy particles.
(*c*) A single helium particle with range greater than 1500 μ.
(*d*) Energetic fragments with charge $Z \geq 3$.

The distribution in N_h of stars which emit energetic heavy fragments with charge $>2e$ is shown in fig. 6 *d*. We have here included a few stars which emit particles heavier than lithium fragments and which are found in other exposures.

(b) *Heavy particles and shower production.*

Heisenberg (1949) suggests that a state analogous to "turbulence" exists as a result of creation of mesons during the impact of a particle on a nucleus. This would result in an increase of the "viscosity" of nuclear matter by which a higher probability should exist for dragging out "lumps" of nucleons from the parent nucleus.

In order to determine if there is any correlation between the production of energetic heavy particles and meson showers, the stars have been divided into different groups according to the values of N_h and number of shower particles n_s. For each group the ratio between the number of stars with energetic helium particles N_{He} and the total number of stars in the HA. 21 plates N_{total} has been computed. The result is shown in Table II. (The absolute values in the Table are in arbitrary units.)

TABLE II.

The ratio $\frac{N_{He}}{N_{total}}$.

n_s \ N_h	3–9	10–16	17–23	≥24
1	1·2±0·8	5·8±3·6	21±4	30±11
2–3	0·8±0·3	4·4±1·1	21±5	50±17
≥4	1·2±0·7	4·6±1·7	11±3	42±12

There is thus no significant difference in the ratios for groups of stars with the same N_h and various number of shower particles which indicates that no very strong connection exists between the ejection of energetic heavy particles and meson showers. The majority of heavy particles considered are helium nuclei, but the same conclusions appear to be valid for heavier fragments, in accordance with previous results (Perkins 1950 a).

(c) *Single energetic helium particles.*

A striking feature of the present investigation is the observation of single energetic helium particles, starting and ending in the emulsion without any associated star. One example has been found with a range of 2200 μ corresponding to an energy $\sim$ 85 MeV., and four with ranges $\sim$ 1500 μ corresponding to energies $\sim$ 70 MeV. Further single heavy tracks are observed to start in the emulsion and pass out of the surfaces.

Two-prong stars have been observed consisting of an energetic helium particle and a short track representing the recoil nucleus of range $\sim$ 5–10 μ, or with a "thin" track due to a singly charged particle with ionization near the minimum value. The latter is presumably the primary, and in most cases makes a very small angle with the direction of the heavy particle.

The single tracks may be either true one-prong stars, or stars in which the remaining particles emitted are neutrons.

Note added in proof.—Recently a two prong star has been found consisting of a " grey " track and the track of a helium particle of range 12,370 μ; this corresponds to an α-particle energy of 236 MeV. The grain density and scattering of the " grey " track is consistent with that of a relativistic α-particle, presumably the primary. The angle between the direction of motion of the two particles is 16°.

DISCUSSION.

Firstly it seems safe to exclude any explanation of the heavy fragments based on the nuclear evaporation processes. We are here observing particles of kinetic energy far in excess of that due to electrostatic repulsion. Further, the angular distributions suggest a process, quite different from that of evaporation, where the particles are emitted almost isotropically with respect to the primary.

At first sight the phenomena are very suggestive of a direct " knocking on " effect of the heavy particle by the primary or by one of the nucleons itself recoiling from the primary. Thus the fragment would leave the nucleus before energy had been statistically shared among the nucleons, that is in a time very short compared with the " cooling down " time.

We select out of the present material all the stars with one or more shower particles. In general primary particles in these stars will have energies E_p in excess of 1000 MeV. Fig. 7 shows a plot of the kinetic energy E_a of the helium nuclei against γ, the angle which they make with respect to the primary. The curves A and B represent the function

$$E_\alpha = \frac{4m_p m_\alpha}{(m_p + m_\alpha)^2} \cdot E_p \cos^2 \gamma \quad . \quad . \quad . \quad . \quad . \quad . \quad . \quad (4)$$

calculated from the conservation laws for a free non-relativistic collision between the two particles where m_α is the mass of an α-particle and m_p that of a proton. The curves A and B refer to E_p=200 MeV. and 500 MeV. respectively. It is clear that the vast majority of the α-particles cannot have been ejected as a result of a direct collision with the primary, even supposing that both the α-particles and the primary have suffered some energy loss in their passage through the nucleus. Thus we conclude that most of the helium fragments have been ejected by encounters with secondary nucleons. This conclusion is supported by the observation of α-particles at angles greater than 90° to the primary, which must necessarily result from secondary effects.

A similar analysis applied to the lithium fragments gives the same result.

The energy which an energetic secondary can transfer to the fragment would depend mainly on the relative impact parameter for the collision. This is in agreement with the absence of correlation between the energy of the heavy particle and the size of the associated star.

The close correspondence between the energy spectra for helium particles, protons and deuterons might imply a similarity in their respective ejection mechanisms. The process by which one nucleon can eject an energetic aggregate of nucleons from the parent nucleus remains to be explained. This phenomenon could perhaps be interpreted in terms of long range nuclear forces.

A point worth mentioning concerns the masses of the heavy particles in the present investigation. It may well be that a large proportion of the helium particles are of mass 3, since a surprisingly large number of energetic tritons are observed to be ejected from stars (Camerini and Fowler, private communication). Measurements are now being made to determine the He^3/He^4-ratio by the scattering method.

Fig. 7.

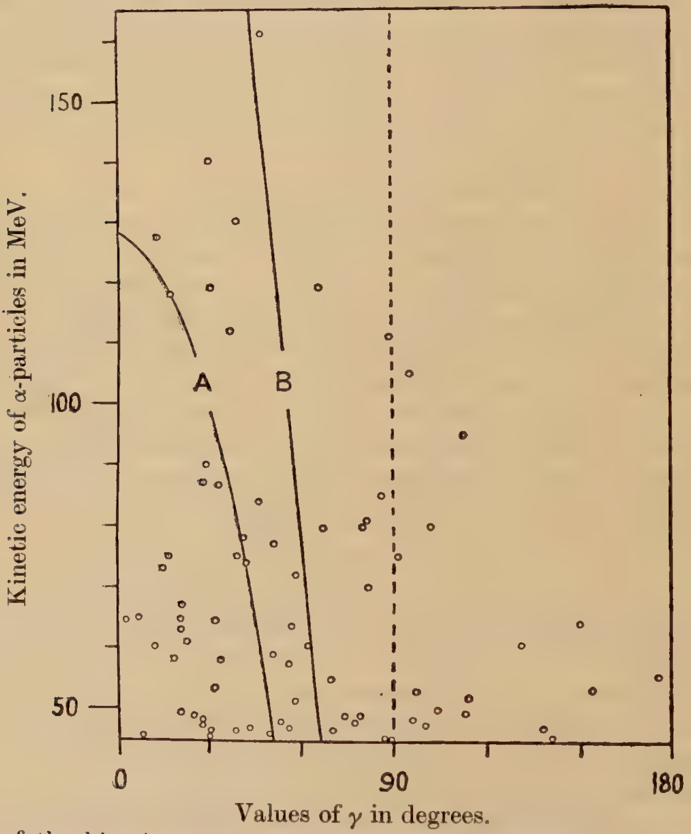

A plot of the kinetic energy against angle with primary of α-particles from stars with $n_s \geq 1$. (For explanation of curves, see text).

The present observations imply the existence of aggregates of nucleons as temporary sub-units of the nucleus. More detailed investigations may possibly throw light on the much discussed problem of the α-particle clustering in nuclei (von Weizäcker 1938, Wergeland 1941, Wheeler 1941).

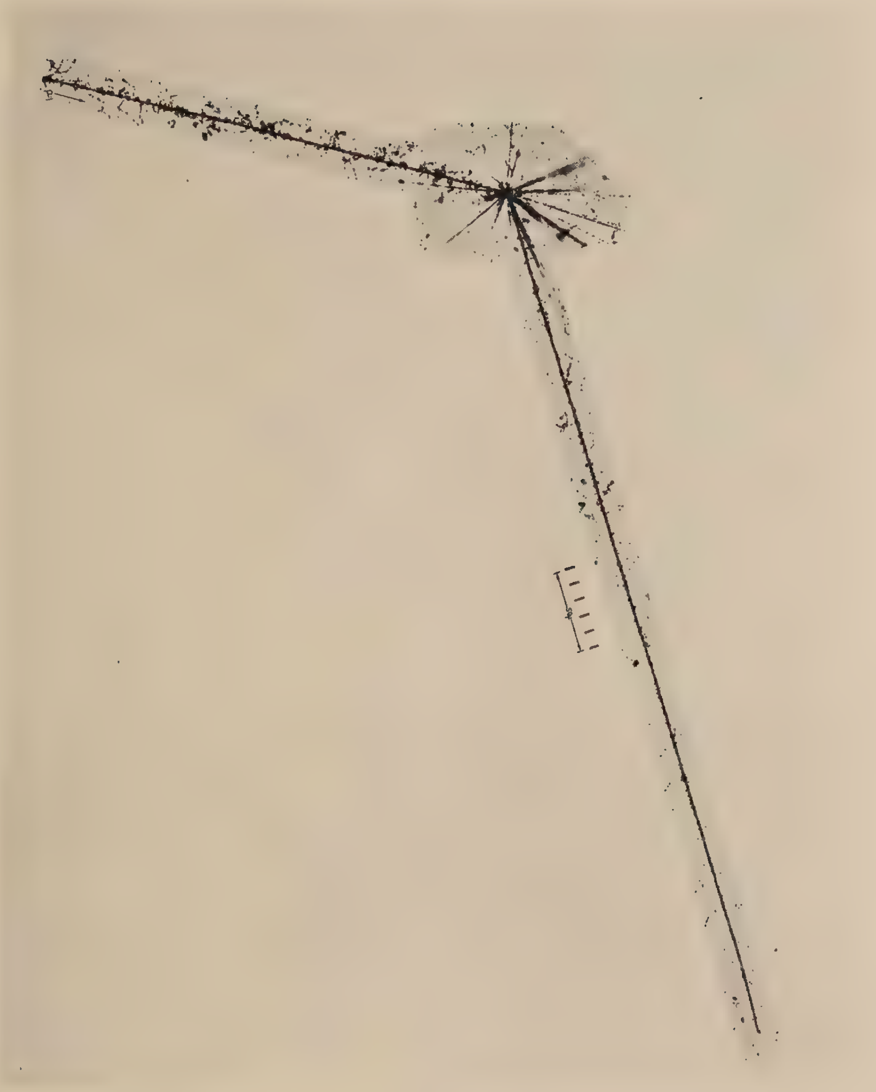

A nucleus of Magnesium (Z=12±1) strikes a silver or bromine nucleus in the emulsion. From the disintegration emerges a slow particle of charge Z=5±1.

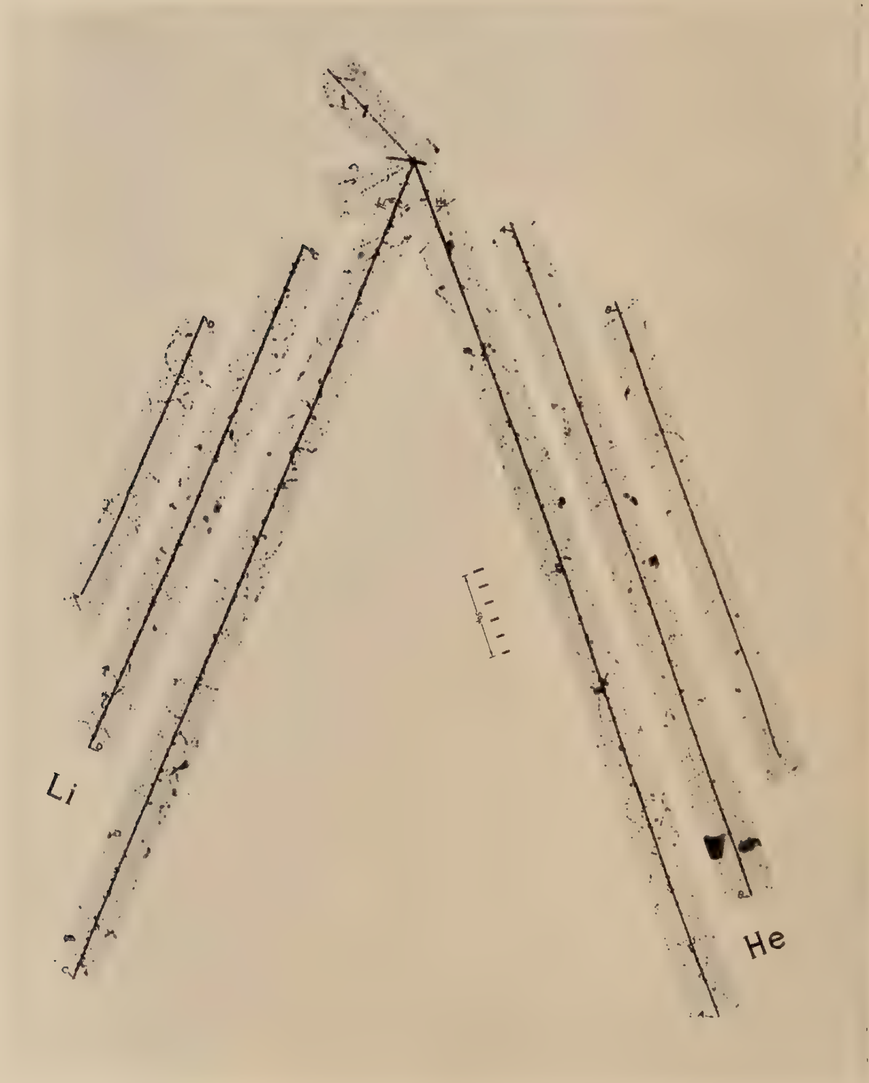

Simultaneous ejection of an energetic helium particle and a lithium fragment from a nuclear explosion.

ACKNOWLEDGMENTS.

I should like to express my gratitude to Professor C. F. Powell, F.R.S., for offering the facilities to carry out this work, and for his continued interest and help ; and I take this opportunity of thanking the research workers of this laboratory, in particular Dr. D. H. Perkins, for many discussions and suggestions. A few plates used in the present investigation were supplied by Fysisk Institutt A, University of Oslo for which I wish to thank Professor J. Holtsmark. I am indebted to the Royal Norwegian Industry Department and Norges Teknisk Naturvitenskapelige Forskningsraad for a scholarship for studying nuclear physics in England.

REFERENCES.

BAGGE, 1944, *Phys. Z.*, **39**, 461.
BRADT and PETERS, 1950, *Phys. Rev.*, **77**, 54.
BROWN, CAMERINI, FOWLER, HEITLER, KING and POWELL, 1949, *Phil. Mag.*, [7], **40**, 862.
CAMERINI, COOR, DAVIES, FOWLER, LOCK, MUIRHEAD and TOBIN, 1949, *Phil. Mag.*, [7], **40**, 1073.
CAMERINI, FOWLER, LOCK and MUIRHEAD, 1950, *Phil. Mag.*, [7], **41**, 413.
DAINTON and KENT, 1950, *Phil. Mag.*, [7], **41**, 963.
FOWLER, 1950, *Phil. Mag.*, [7], **41**, 963.
FRANZINETTI and PAYNE, 1948, *Nature, Lond.*, **161**, 735.
HARDING, LATTIMORE and PERKINS, 1949, *Proc. Roy. Soc.* A, **196**, 325.
HEISENBERG, 1949, *Z. Phys.*, **126**, 569.
LE COUTEUR, 1950, *Proc. Phys. Soc.* A, **63**, 259.
PAGE, 1950, *Proc. Phys. Soc.* A, **63**, 250.
PERKINS, 1950 a, *Proc. Roy. Soc.* A, **203**, 399 ; 1950 b, *Phil. Mag.* [7], **41**, 138.
SÖRENSEN, 1949, *Phil. Mag.* [7], **40**, 947.
VON WEIZÄCKER, 1938, *Naturwiss.*, **26**, 209, 225.
WERGELAND, 1941, *Norske Vidensk. Selsk. Skrifter*, No. 1.
WEISSKOPF, 1937, *Phys. Rev.*, **52**, 295.
WHEELER, 1941, *Phys. Rev.*, **59**, 27.

XVIII. *A Note on Hildebrand's Approximation for Thermal Pressures in Solids.*

By Kun Huang,
Department of Theoretical Physics, University of Liverpool *.

[Received November 28, 1950.]

Abstract.

The validity of a widely used approximation for thermal pressures due originally to Hildebrand is discussed. The distinction between the " vibrational " pressure and the thermal pressure is stressed ; Hildebrand's expression is shown to lie intermediate between the two for all temperatures. Since the percentage difference between the two pressures diminishes monotonically with increasing temperature, the accuracy of the approximate expression improves with increasing temperature. But at temperatures comparable with the Debye temperature, Hildebrand's expression is much closer to the vibrational (10 per cent error) than the thermal pressure (40 per cent error). It follows further from the discussion that the linearly extrapolated volume from any temperature to the absolute zero lies intermediate between the real volume at absolute zero of temperature and the volume corresponding to *static* equilibrium.

It is the purpose of the present note to discuss the validity of an approximation, which was first introduced by Hildebrand (1931) and has since been widely used in connection with the accurate calculations of cohesive energies and interatomic forces of solids (Born and Mayer 1932, Mayer and Helmholz 1932, Huggins and Mayer 1933, Fowler 1936, Huggins 1937, 1947). It is based on the assumption that the energy of a solid can be approximately considered as consisting of a purely volume-dependent and a purely temperature-dependent part. Hildebrand's procedure is the following : Let us write the internal energy of a solid as

$$E=U+E_{\text{vib}}, \qquad \qquad (1)$$

where E_{vib} and U refer respectively to the vibrational energy and the remaining, purely volume-dependent static energy. It is assumed that one can approximately write

$$\frac{dU}{dV}\cong\left(\frac{\partial E}{\partial V}\right)_T=\left(\frac{\partial F}{\partial V}\right)_T+T\left(\frac{\partial S}{\partial V}\right)_T \qquad \qquad (2)$$

F, S being respectively the Helmholtz free energy and the entropy ; or, since for normal pressures one can put $p=-(\partial F/\partial V)_T=0$,

$$\frac{dU}{dV}\cong T\left(\frac{\partial S}{\partial V}\right)_T \qquad \qquad (3)$$

$T(\partial S/\partial V)_T$ is thus used approximately as the " thermal pressure ".

---

* Communicated by Professor H. Fröhlich.

Despite the wide usage of the approximation, no pertinent discussions of its validity have, however, been offered. Hildebrand (1931) has attempted a partial justification empirically, by trying to show that alternative determinations of the interatomic forces using the above relation at different temperatures, yield the same result; the results thus obtained in fact show a distinct drift with the corresponding temperatures used. Sometimes it has been implied that (3) is valid owing to the small magnitude of the vibrational energy E_{vib}. This has led to the suggestion that (3) is a good approximation at not too high temperatures (Fowler 1936); the reverse is in fact the case (see below).

The Mie–Grüneisen equation (Grüneisen 1926):

$$p+\frac{dU}{dV}=\frac{\gamma E_{vib}}{V} \quad . \; . \; . \; . \; . \; . \; . \; . \; . \quad (4)$$

which may, for instance, be deduced by following either the Einstein or Debye treatment of vibrations, is ideally suited to a discussion of the above approximation. Differentiating (4) with respect to T, we obtain

$$\left(\frac{\partial p}{\partial T}\right)_V=\frac{\gamma C_v}{V}. \quad . \; . \; . \; . \; . \; . \; . \; . \; . \quad (5)$$

Moreover, for normal pressures, we can put $p=0$ in (4):

$$\frac{dU}{dV}=\frac{\gamma E_{vib}}{V}. \quad . \; . \; . \; . \; . \; . \; . \; . \; . \quad (6)$$

Remembering that

$$\left(\frac{\partial S}{\partial V}\right)_T=\left(\frac{\partial p}{\partial T}\right)_V$$

and comparing (3) and (5), we see that the Hildebrand approximation for the thermal pressure is given by $\gamma TC_V/V$, whereas it follows from (6) that $\gamma E_{vib}/V$ represents the true value; the ratio of the approximate to the true value is thus

$$\rho=\frac{TC_V}{E_{vib}} \quad . \; . \; . \; . \; . \; . \; . \; . \; . \quad (7)$$

which, we remark, is equal to unity only for temperatures high enough for the classical energy partition law to hold.

One notes that, owing to the fact that the energy of zero-point vibrations depends only on the volume, the "thermal pressure" can in fact be defined in two different senses:

(i.) One can include the zero-point energy as part of U. All the above formulæ remain correct as they stand, if E_{vib} refers only to the thermal vibrations. The thermal pressure defined in this way vanishes at T=0° K. (see (6)).

(ii.) Alternatively, one may, as we have already assumed above, take U as the purely static energy. Then the zero-point energy has to be included in E_{vib}. It follows that E_{vib} approaches a finite value for T=0° K. in this case, and the corresponding "thermal pressure" does not vanish; we shall thus refer to it as the *vibrational pressure.*

Hildebrand's approximation is ambiguous on this point, *i. e.* whether $T(\partial S/\partial V)_T$ should refer to the thermal or vibrational pressure; it is probably understood differently by different authors using it. To be consistent with the idea of dividing the energy into a volume-dependent and temperature-dependent part it would indeed appear the more appropriate to identify Hildebrand's expression $T(\partial S/\partial V)_T$ with the *thermal* pressure rather than the *vibrational* pressure. For one would attempt to include all the purely volume-dependent terms in U, hence also the zero-point energy; moreover, as the approximate expression $T(\partial S/\partial V)_T$ vanishes at T=0° K., it points once more to (i.) as the more fitting interpretation.

Using the Debye theory, one finds that the ratio ρ defined in (7) is only a function of T/Θ (Θ the Debye temperature), whether E_{vib} refers to the total vibrational energy or only the thermal part. The curves ρ versus T/Θ for both of these alternatives are given in the adjoining figure. Curve (i.) corresponds to the case that E_{vib} refers only to the thermal vibrations, and curve (ii.) refers to the alternative case, where E_{vib} is the total vibrational energy. If we interpret Hildebrand's expression as referring to the thermal pressure (see (i.)), curve (i.) gives the ratio of the approximate to the true value; if, on the other hand, we interpret Hildebrand's expression as referring to the vibrational pressure (see (ii.)), then curve (ii.) represents the proper ratio. Both curves are seen to approach the line of unity towards high temperatures; however, for the temperature range of practical interest, the Hildebrand's expression is much more accurate, if interpreted as the vibrational pressure (curve (ii.)) rather than the purely thermal pressure (curve (i.)). *This is exactly the reverse of the more naive anticipation explained earlier.* For all the alkali-halides except LiF and NaF, Hildebrand's expression used at room-temperatures will be within 10 per cent of the actual vibrational pressure.

An interesting conclusion can be drawn from considering the equilibrium V_0 defined by the equation

$$\left(\frac{dU}{dV}\right)_{V_0}=0 \quad . \quad . \quad . \quad . \quad . \quad . \quad . \quad . \quad . \quad (8)$$

with the approximate equation (3). By expanding dU/dV in (3) with respect to $V-V_0$ about the above equilibrium position and neglecting second and higher order terms, we find readily that

$$V_0 \simeq V-\frac{T(\partial S/\partial V)_T}{(d^2U/dV^2)_0} . \quad . \quad . \quad . \quad . \quad . \quad . \quad . \quad . \quad (9)$$

The interpretation of V_0 from the point of view of this approximation is as ambiguous as the interpretation of Hildebrand's expression itself: if the latter is taken as the thermal pressure (i.), then U should include the zero point energy and the corresponding V_0 is the volume of the solid at T=0° K; but if it is taken as the vibrational pressure (ii.), U is the static energy and V_0 is the static equilibrium volume corresponding to the hypothetical case that the atoms were at rest. The fact that the curves (i.) and (ii.) lie respectively above and below the line of unity shows that Hildebrand's expression has a value intermediate between the true thermal pressure and the true vibrational pressure, whatever the temperature. It follows, as a moment's consideration will show, that

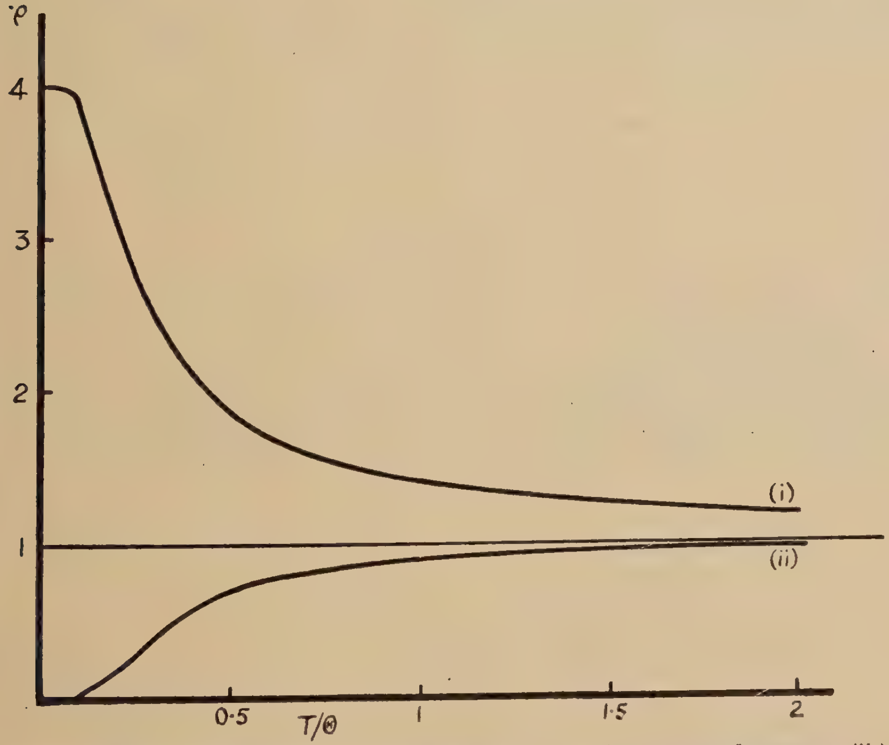

Ratio of Hildebrand's pressure to the thermal (i.) and vibrational pressure (ii.).

the value of V_0 as given by (9) lies in fact between the equilibrium volume of the static case and the actual volume at the absolute zero of temperature. Moreover, if the relation (9) is used at room temperatures, V_0 should be much nearer to the static equilibrium value than the value at T=0° K, for we have seen that the approximate expression should be much nearer to the vibrational than the thermal pressure.

Now if we write on the right-hand side of (9)

$$\left(\frac{\partial S}{\partial V}\right)_T=\left(\frac{\partial p}{\partial T}\right)_V=\frac{-(\partial V/\partial T)_p}{(\partial V/\partial p)_T}=-\left(\frac{\partial V}{\partial T}\right)_p\left(\frac{\partial p}{\partial V}\right)_T$$

and put approximately

$$\left(\frac{\partial p}{\partial V}\right)_T \cong -\left(\frac{\partial^2 U}{\partial V^2}\right)_0, \quad \text{(difference} \sim 10 \text{ per cent)}$$

(9) becomes simply

$$V_0 \cong V - T\left(\frac{\partial V}{\partial T}\right)_p \quad . \; . \; . \; . \; . \; . \; . \; . \; . \quad (10)$$

This means that the equilibrium volume V_0 deduced from Hildebrand's approximation is practically identical with that obtained by a simple linear extrapolation to the absolute zero of temperature. Hence we can express the conclusion of the last paragraph in the rather interesting form : *the linearly extrapolated value for the volume of a solid from any temperature to the absolute zero lies in between the static equilibrium volume and the actual volume at absolute zero of temperature.* Moreover, if it is extrapolated from a temperature comparable or higher than the Debye temperature of the solid, the result is expected to lie much nearer to the static equilibrium value.

REFERENCES.

BORN, M., and MAYER, J. E., 1932, *Zeit f. Phys.*, **75**, 1.
FOWLER, R. H., 1936, *Statistical Mechanics* (Cambridge : University Press), 2nd Ed., p. 324.
GRÜNEISEN, E., 1926, *Handb. d. Phys.*, **10**, 1.
HILDEBRAND, J. H., 1931, *Zeit. f. Phys.*, **67**, 127.
HUGGINS, M. L., and MAYER, J. E., 1933, *J. Chem. Phys.*, **1**, 643.
HUGGINS, M. L., 1937, *J. Chem. Phys.*, 5, 143 ; 1947, *J. Chem. Phys.*, **15**, 212.
MAYER, J. E., and HELMHOLZ, L., 1932, *Zeit. f. Phys.*, **75**, 19.

XIX. *The Emission of* Li^8 *from Cosmic Ray induced Nuclear Disintegrations.*

By P. E. Hodgson,
Imperial College of Science and Technology, London*.

[Received November 18th, 1950.]

Summary.

Lithium 8 nuclei ejected from cosmic-ray induced disintegrations have been investigated using the photographic plate method. Earlier work has been confirmed, and the frequency and energy distribution of the Li^8 nuclei determined and compared with the predictions of the evaporation theory. Some nuclear reactions involving the production of Li^8 have been identified.

§ 1. Introduction.

In 1947, Occhialini and Powell observed a T-shaped track caused by a particle emitted from a nuclear disintegration in a photographic plate exposed to cosmic rays. These events are also known as " hammer " tracks.

Franzinetti and Payne (1948) analysed thirty examples and confirmed Occhialini and Powell's conclusion that they are due to the emission of lithium 8 nuclei which decay into two alpha-particles and an electron, although the electron track was not observed in their less sensitive plates. This was later observed by Occhialini and by Pickup and Voyvodic (1949) in emulsions sensitive to particles of minimum ionization.

This work has been confirmed, and, in addition, the frequency and energy distributions of the Li^8 particles determined.

§ 2. Experimental Procedure and Summary of Results.

Several batches of Ilford Nuclear research plates, coated with C2 and G5 emulsions, and exposed to the cosmic rays on the Jungfraujoch, have been examined for hammer tracks associated with stars.

The energy distribution of the secondary alpha-particles was found from their ranges in the emulsion and it agreed with the results of Franzinetti and Payne (1948) for hammer tracks associated with cosmic ray stars and those of Baxter, Burcham and Paul (1950) and Rumbaugh, Roberts and Hafstad (1937) for Li^8 nuclei produced artificially.

Electron tracks were found associated with most of the hammer tracks in electron-sensitive emulsions.

The energy distribution of the ejected particles was measured and is discussed in § 4.

The angular distribution of the hammer tracks was found to be consistent with isotropic emission of the Li^8 nuclei.

---

* Communicated by Sir George Thomson.

The frequency of emission of particles forming hammer tracks is given in § 5 and compared with the predictions of the evaporation theory for lithium 8 nuclei of zero spin.

§ 3. NATURE OF THE PARTICLE CAUSING THE HAMMER TRACKS.

Tracks of decay electrons were found associated with most of the hammer tracks occurring in electron-sensitive emulsions. The electron is energetic enough to be at or near minimum ionization and yet slow enough to be quite considerably scattered. The electron tracks are therefore difficult to see and are in general only found if the emulsion is developed to its fullest sensitivity.

Hammer tracks associated with a decay electron may be due either to Li_3^8 or, as recently suggested by Alvarez (1950), B_5^8 :—

$$Li_3^8 \rightarrow Be_4^{8*}+e_{-1}^0, \qquad Be_4^{8*} \rightarrow 2He_2^4,$$
$$B_5^8 \rightarrow Be_4^{8*}+e_{+1}^0, \qquad Be_4^{8*} \rightarrow 2He_2^4.$$

Because of the higher charge of B_5^8 its emission probability will be less than that of Li_3^8.

The experimental results are not incompatible with some of the hammer tracks being without a decay electron, and attributable to Be_4^8. In this case the excited state of Be_4^8 must be a metastable one of long life since the life-time of the broad state at 3 MeV. is far too short to allow the nucleus to come to rest in the emulsion before disintegrating.

Since Li_3^8 and B_5^8 decay via the same excited state of Be_4^8 (Alvarez 1950) no distinction can be made between them from the energy distribution of the secondary alpha-particles.

It seems likely that the majority of the particles producing hammer tracks are Li_3^8 and in what follows it will be assumed that they are all attributable to this nucleus.

§ 4. THE ENERGY DISTRIBUTION OF THE Li^8 NUCLEI.

The energies of the lithium nuclei were determined from their ranges and a range–energy curve derived from that of Bradner, Smith, Barkas and Bishop (1950) for protons by the relation

$$E=mf\left(\frac{R\epsilon^2}{m}\right)$$

where E, R, ϵ and m are the energy, residual range, charge and mass of the particle. At very low energies the lithium nucleus picks up electrons and reduces its effective charge. The above formula cannot be used in this region with accuracy. But, since this lowering of effective charge takes place, for lithium nuclei, only over the last two or three microns, its effect is small and has been neglected.

It was found that the average energy of the lithium nuclei from large stars was appreciably greater than that of those from small stars.

This may be explained by assuming that the lithium nuclei from large stars are ejected from energetic disintegrations of silver or bromine, while the lithium nuclei from small stars are the residues after the ejection of protons and alpha-particles in the disintegration of carbon, oxygen or nitrogen. This interpretation has also been advanced recently by Courtenay Wright (1950) after examination of Li^8_3 nuclei associated with stars produced in various gases by the cyclotron beam.

In order to test this hypothesis, all stars associated with hammer tracks were separated into two classes, namely those with more than four tracks (including the hammer track), and those with less. The additional condition was applied that stars with a recoil, a short heavily ionizing track characteristic of the disintegration of a heavy nucleus, were included in the former class, irrespective of their numbers of tracks. These classes are called A and B. In addition, it is possible for a lithium nucleus to be the residue after the complete disintegration of a silver or bromine nucleus. Only one example has been found, in a star of 27 tracks, and it was included in class B.

Fig. 1.

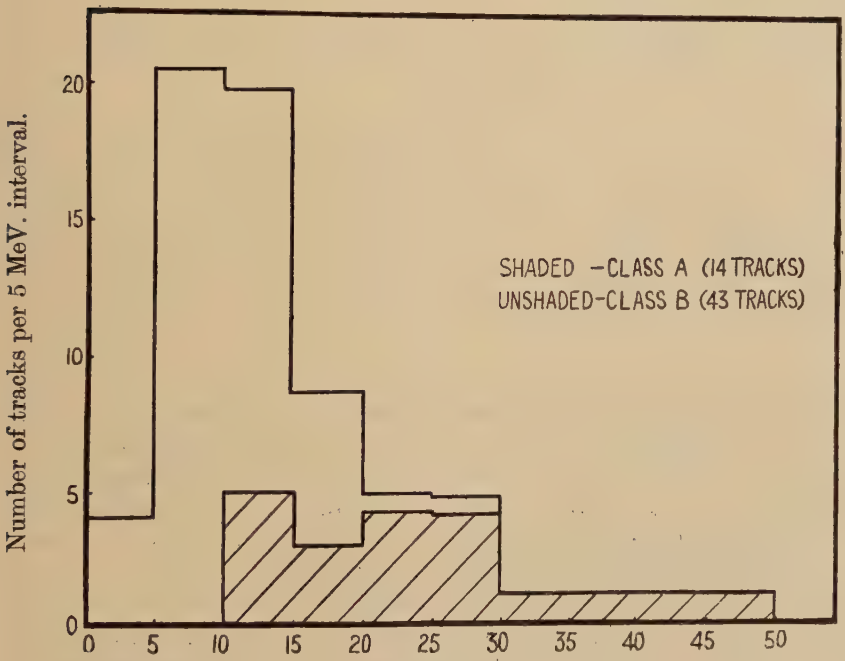

Energy of Li^8 in MeV:
Energy Distribution of Lithium nuclei.

The energy distribution of the lithium nuclei is shown in fig. 1, the two classes being distinguished by shading. The observed distribution was corrected for those long tracks which were lost because they passed out of the emulsion. The disparity between the energy distributions of lithium nuclei in the two classes is strong support for the above hypothesis on the mechanism of their production.

§ 5. FREQUENCY OF EMISSION.

In all, it was found that 74 hammer tracks were associated with stars in emulsion containing 23,700 stars of more than two tracks. Hammer tracks associated with stars caused by π^--mesons are omitted from these figures and will be considered later (§ 7). The total emission frequencies, for C2 and G5 emulsions, are showm in Table I. The value for G5 emulsion is less than that for C2 on account of the greater number of stars with more than two tracks.

The fraction of hammer tracks in class A is also given in Table I.

TABLE I.

	Observed	Corrected
Hammer tracks÷No. of stars >2 tracks in C2 emulsion	0·0032±0·0007	0·0052±0·0012
Hammer tracks÷No. of stars >2 tracks in G5 emulsion	0·0023±0·0005	0·0034±0·0006
Fraction of hammer tracks of class A	0·27 ±0·07	0·33 ±0·08

The frequency of emission of particles causing hammer tracks is plotted in fig. 2 as a function of star size and compared with the calculations on the evaporation theory by Le Couteur for the emission of lithium 8 of zero spin from nuclear disintegrations of various sizes. Comparison of the observed and calculated frequencies, which should only be made for hammer tracks of class A, shows good agreement.

Hammer tracks are lost if they pass out of the emulsion (see § 4) and also if the angle between the projected directions of the lithium and the two alpha-particles is too small to be resolved. The frequencies of emission have been corrected for tracks lost in both these ways.

From the frequencies of emission given above, and assuming an approximate value of the intensity of star-producing radiation at the Jungfraujoch, values of the cross-section for production of Li^8 from light nuclei can be deduced which are of the same order of magnitude as those given by Courtenay Wright (1950) and Titterton (1950).

§ 6. NUCLEAR REACTIONS IN THE LIGHT ELEMENTS.

On the assumption that the hammer tracks of class B come from the disintegration of light nuclei it is often possible, when the event occurs in C2 emulsion, to identify the nuclear reaction concerned. The identification is subject to some uncertainty because lightly ionizing particles are not visible in C2 emulsion, and protons, deuterons and tritons are not always separable. Analysis of events in G5 emulsion was not attempted because of the difficulty of distinguishing between protons and alpha-particles. It is possible to confirm the reactions by measurement of energy and momentum balance, providing no neutrons are emitted.

Fig. 2.

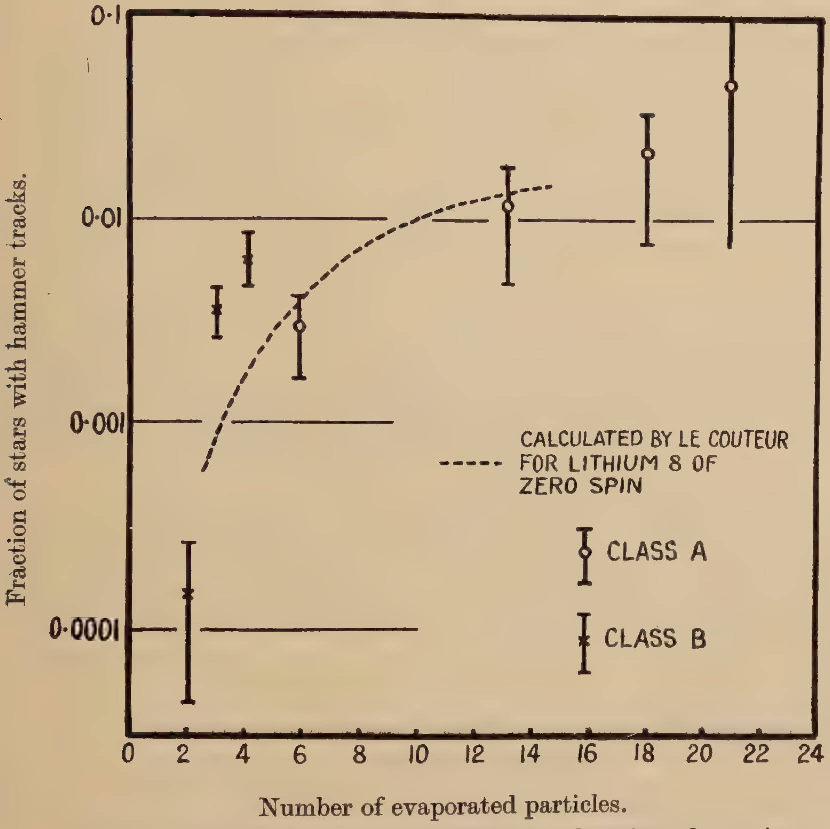

Number of evaporated particles.

Fraction of stars with hammer tracks as a function of star size.

The following reactions have been identified

$n_0^1+C_6^{12} \rightarrow Li_3^8+He_2^4+H_1^1$ (Six examples)

$n_0^1+C_6^{12} \rightarrow Li_3^8+3H_1^1+2n_0^1$
or $n_0^1+C_6^{12} \rightarrow Li_3^8+2H_1^1+H_1^2+n_0^1$
or $n_0^1+C_6^{12} \rightarrow Li_3^8+H_1^1+2H_1^2$
(Eight examples)

$n_0^1+N_7^{14} \rightarrow Li_3^8+He_2^4+2H_1^1+n_0^1$
or $n_0^1+N_7^{14} \rightarrow Li_3^8+He_2^4+H_1^2+H_1^1$
(Two examples)

$n_0^1+O_8^{16} \rightarrow Li_3^8+2He_2^4+H_1^1$ (One example)

§ 7. Lithium Nuclei emitted from Stars initiated by π^--Mesons.

In addition to the hammer tracks analysed above, six have been observed associated with stars produced by π^--mesons. The total number of such mesons in the emulsion examined was 1160. The fraction of meson-produced stars with hammer tracks is therefor $0{\cdot}005\pm0{\cdot}003$, a value which agrees with the 0·003 given by Bradner (1950) and the 11/3000 or $0{\cdot}004\pm0{\cdot}001$ found by Adelman and Jones (1949).

The following nuclear reactions have been identified :—

$$\left.\begin{aligned} &\mathrm{O}^{16}_{8}+\pi^{0}_{-1}\rightarrow \mathrm{Li}^{8}_{3}+\mathrm{He}^{4}_{2}+2\mathrm{H}^{1}_{1}+2n^{1}_{0}\\ \text{or } &\mathrm{O}^{16}_{8}+\pi^{0}_{-1}\rightarrow \mathrm{Li}^{8}_{3}+\mathrm{He}^{4}_{2}+\mathrm{H}^{1}_{1}+\mathrm{H}^{2}_{1}+n^{1}_{0}\end{aligned}\right\}\quad\text{(Two examples)}$$

$$\left.\begin{aligned} &\mathrm{C}^{12}_{6}+\pi^{0}_{-1}\rightarrow \mathrm{Li}^{8}_{3}+2\mathrm{H}^{1}_{1}+2n^{1}_{0}\\ \text{or } &\mathrm{C}^{12}_{6}+\pi^{0}_{-1}\rightarrow \mathrm{Li}^{8}_{3}+\mathrm{H}^{1}_{1}+\mathrm{H}^{2}_{1}+n^{1}_{0}\end{aligned}\right\}\quad\text{(One example)}$$

Acknowledgments.

I should like to express my thanks to Professor Sir George Thomson and Mr. N. C. Barford for many valuable discussions, to Dr. K. J. Le Couteur for communicating the results of his calculations on the emission probability of Li^8, and to Dr. E. P. George and Mr. J. Evans for permitting me to examine a number of hammer tracks in their plates.

References.

Adelman, F., and Jones, S. B., 1949, *Phys. Rev.*, **75,** 1468.

Alverez, L. W., 1950, Harwell Conference on Nuclear Physics, *Phys. Rev.*, **80,** 519.

Baxter, A. S., Burcham, W. E., and Paul, E. B., 1950, *Phil. Mag.*, **41,** 937.

Bradner, H., 1949, *U. C. R. L.*, 486, 38.

Bradner, H , Smith, F. M., Barkas, W. H., and Bishop, A. S., 1950, *Phys. Rev.*, **77,** 462.

Franzinetti, C., and Payne, R. M., 1948, *Nature, Lond.*, **161,** 735.

Le Couteur, K. J. (Private Communication.)

Occhialini, G. P. S., and Powell, C. F., 1947, *Nature, Lond.*, **159,** 93.

Pickup, E., and Voyvodic, L., 1949, *Phys. Rev.*, **76,** 1534.

Rumbaugh, L. H., Roberts, R. B., and Hafstad, L. R., 1938, *Phys. Rev.*, **54,** 1103.

Titterton, E. W., 1950, Harwell Conference on Nuclear Physics; 1951, *Phil. Mag.*, **42,** 109, 113.

Wright, S. Courtenay, 1950, *Phys. Rev.*, **79,** 838.

XX. *The Law of Constant Resolved Shear Stress in Crystal Plasticity.*

By F. R. N. Nabarro.
Department of Metallurgy, The University of Birmingham*,

[Received December 27, 1950.]

Abstract.

The formula of Peach and Koehler for the total force acting on a dislocation in a stressed crystal is derived by the use of a theorem due to Colonnetti. The same method distinguishes conservative motions of the dislocation, which do not alter the volume, from other motions. The component of the total force which produces conservative motions acts in the glide plane, and is proportional to the same component of the total stress as appears in the law of resolved shear stress discovered experimentally by Schmid.

The forces acting on dislocations are most conveniently derived by the use of a theorem due to Colonnetti (1915). Consider a body containing a closed loop of dislocation with Burgers vector **b**, and cover this loop with a cap. Let an element of this cap have area $d\boldsymbol{\Sigma}$, and let the body be subject to external stresses as a result of which the force acting across this element $d\boldsymbol{\Sigma}$ of the cap is $\mathbf{X}\,d\Sigma$. The signs of the vectors **b**, $d\boldsymbol{\Sigma}$ and $d\boldsymbol{\sigma}$ must be determined conventionally. The convention used here is that of Peach and Koehler (1950). Colonnetti's theorem then states that the work W_e done by the external forces when the dislocation is formed is given by

$$W_e=-\iint\mathbf{b}\mathbf{X}\,d\Sigma. \qquad (1)$$

If the stress produced by the external forces is $\mathfrak{P}$, **X** is given by

$$\mathbf{X}\,d\Sigma=-\mathfrak{P}\,d\boldsymbol{\Sigma}, \qquad (2)$$

and

$$W_e=\iint\mathbf{b}\mathfrak{P}\,d\boldsymbol{\Sigma}. \qquad (3)$$

Suppose now that an element $d\boldsymbol{\sigma}$ of the dislocation moves a distance $d\mathbf{x}$. The area of the dislocation loop is increased by

$$\delta\boldsymbol{\Sigma}=d\mathbf{x}\wedge d\boldsymbol{\sigma}, \qquad (4)$$

and the external forces do work

$$\begin{aligned}\delta W_e&=\mathbf{b}\mathfrak{P}\,.\,(d\mathbf{x}\wedge d\boldsymbol{\sigma})\\&=[(\mathbf{b}\mathfrak{P})\wedge d\boldsymbol{\sigma}]\,.\,d\mathbf{x}.\end{aligned} \qquad (5)$$

The force $d\mathbf{F}$ on the element $d\boldsymbol{\sigma}$ is thus given by

$$d\mathbf{F}=(\mathbf{b}\mathfrak{P})\wedge d\boldsymbol{\sigma}. \qquad (6)$$

This is the result of Peach and Koehler.

---

* Communicated by the Author.

It is now necessary to distinguish between those motions of the dislocation which conserve the volume of the crystal (conservative motions) and those motions which produce interstitial ions or vacancies (non-conservative motions). Only conservative motions can lead to steady slip, though non-conservative motions may be important in work hardening and especially in thermal recovery. The necessary and sufficient condition that a motion should be conservative is that a uniform hydrostatic pressure p should do no work when the motion occurs. For such a pressure, $\mathbf{b}\boldsymbol{\mathfrak{P}}$ is given by $\mathbf{b}\boldsymbol{\mathfrak{P}}=\mathbf{b}p$, and it follows from (5) that the motion is conservative if

$$(\mathbf{b}\wedge d\boldsymbol{\sigma})\,.\,d\mathbf{x}=0. \tag{7}$$

Thus the motion is always conservative if $\mathbf{b}\wedge d\boldsymbol{\sigma}=0$, that is to say, if the element of dislocation is of pure screw type. If $\mathbf{b}$ and $d\boldsymbol{\sigma}$ are not parallel, they define a plane, the *glide plane*, and the motion is conservative only if $d\mathbf{x}$ lies in this plane. The normal to the glide plane is the unit vector $\mathbf{n}$ defined by

$$\mathbf{n}=(\mathbf{b}\wedge d\boldsymbol{\sigma})/|\mathbf{b}\wedge d\boldsymbol{\sigma}|. \tag{8}$$

The component $d\mathbf{f}$ of the force $d\mathbf{F}$ which is effective in producing slip is the component lying in the glide plane, given by

$$\begin{aligned} d\mathbf{f}&=d\mathbf{F}-\mathbf{n}(\mathbf{n}\,d\mathbf{F})\\ &=-\mathbf{n}\wedge(\mathbf{n}\wedge d\mathbf{F}). \end{aligned} \tag{9}$$

Now

$$\begin{aligned} \mathbf{n}\wedge d\mathbf{F}&=\mathbf{n}\wedge[(\mathbf{b}\boldsymbol{\mathfrak{P}})\wedge d\boldsymbol{\sigma}]\\ &=(\mathbf{b}\boldsymbol{\mathfrak{P}})(\mathbf{n}\,d\boldsymbol{\sigma})-d\boldsymbol{\sigma}[\mathbf{n}(\mathbf{b}\boldsymbol{\mathfrak{P}})]\\ &=-d\boldsymbol{\sigma}(\mathbf{b}\boldsymbol{\mathfrak{P}}\mathbf{n}), \end{aligned}$$

and so

$$d\mathbf{f}=(\mathbf{n}\wedge d\boldsymbol{\sigma})(\mathbf{b}\boldsymbol{\mathfrak{P}}\mathbf{n}). \tag{10}$$

Since $\boldsymbol{\mathfrak{P}}\mathbf{n}$ is the force acting across unit area of the glide plane, the force per unit length tending to produce glide is b times the component in the glide direction of the force acting across unit area of the glide plane, and acts in the glide plane normal to the line of the dislocation. If a loop of dislocation lies entirely in the glide plane, its conservative motions are confined to this plane (except for those elements which are of pure screw type), and its whole length is subjected to the same normal force tending to increase the area of the loop. This is in accordance with the experimental result (Schmid 1924) that slip begins when the " resolved shear stress " $\mathbf{b}\boldsymbol{\mathfrak{P}}\mathbf{n}/b$ reaches a value which is characteristic of the crystal, but independent of the other components of the applied stress.

REFERENCES.

COLONNETTI, G., 1915, *R.C. Accad. Lincei* [5], **24**, 404.
PEACH, M., and KOEHLER, J. S., 1950, *Phys. Rev.* [2], **80**, 436.
SCHMID, E., 1924, *Proc. Internat. Cong. Appl. Mech., Delft*, p. 342.

XXI. CORRESPONDENCE

The Production of Neutrons by High Energy Protons.

By J. M. Cassels, T. C. Randle, T. G. Pickavance and A. E. Taylor*,
Atomic Energy Research Establishment, Harwell.

[Received December 8, 1950.]

The production of neutrons by high energy protons has been investigated with the help of a differential detector. The third counter in the triple coincidence telescope used previously for total cross-section work (Taylor, Pickavance, Cassels and Randle 1950) was replaced by a gridded ionization chamber sensitive only to comparatively slow protons. It followed that protons ejected from the polythene radiator were counted only if they possessed energies lying between certain limits set by a carbon absorber placed immediately in front of the chamber. The counts resulting from n, p collisions in the hydrogen content of the polythene were separated out by background runs with a carbon radiator. After correcting for protons lost while slowing down in the absorber, absolute neutron fluxes in the range 50–200 MeV. could be found with the help of the Berkeley experiments on the n, p interaction (Hadley, Kelly, Leith, Segrè, Wiegand and York 1949, Brueckner, Hartsough, Hayward and Powell 1949, Kelly, Leith, Segrè, and Wiegand 1950).

The correct operation of the telescope was checked by using it to determine the total cross sections of carbon and hydrogen at 156 and 110 MeV. The results were consistent with those of other work at Berkeley and at Harwell, showing that neutrons of the intended energy were being detected.

The energy spectra of the neutrons produced by bombarding beryllium, carbon, aluminium and uranium targets were then investigated (figs. 1–4). These targets had thicknesses of 1·67, 1·09, 1·19 and 1·82 grms.-cm.$^{-2}$ respectively. The resolution diagrams in fig. 1 show the "smearing" effect of the neutron detector only. There is additional lack of resolution caused by the slowing down in the target of the primary protons, whose energy was initially 171 MeV. The magnitude of this can be gauged from the mean proton energies set out in the Table, column 2. No corrections for "smearing" have been applied to the results given. The fluxes shown in the diagrams refer to a point 15·3 metres from the target at an angle of $2\frac{1}{2}°$ from the forward direction. They are normalized to an actual current of 1 microampere being accelerated by the cyclotron, but the effective current was greater than this because protons could traverse the target several times before being lost. It was found to be 3·4 microamperes in the carbon target by measurement of the rate of production of ^{11}C, a process

---

* Communicated by the Authors.

Fig. 1.

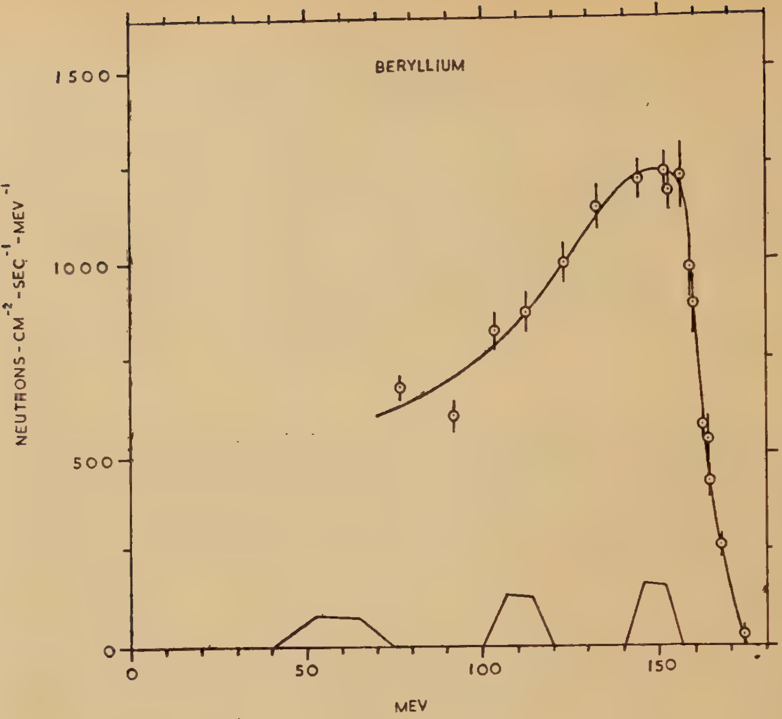

Fig. 2.

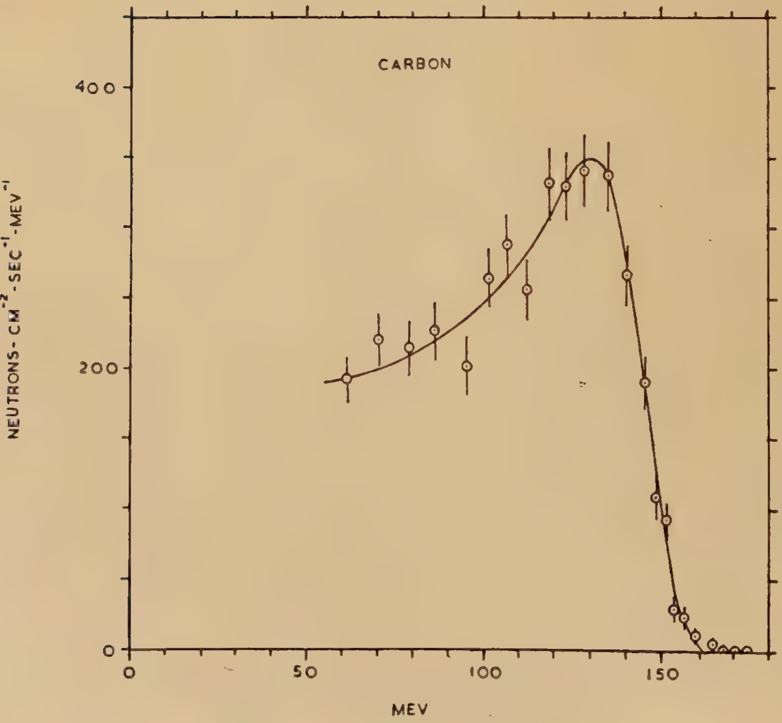

Figs. 1–2. Neutron spectra obtained from beryllium, carbon, aluminium and uranium by bombardment with 171 MeV. protons.

Fig. 3.

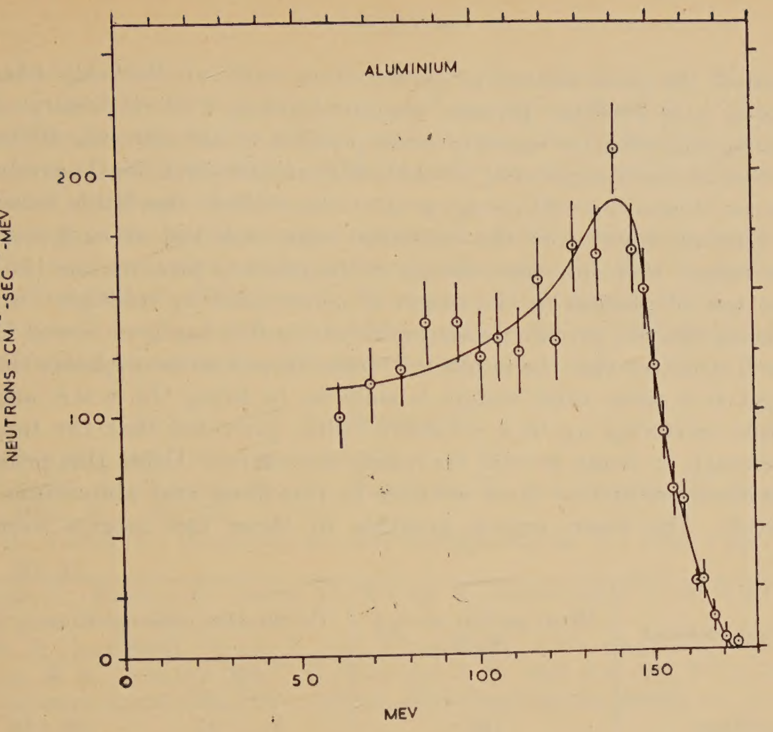

Fig. 4.

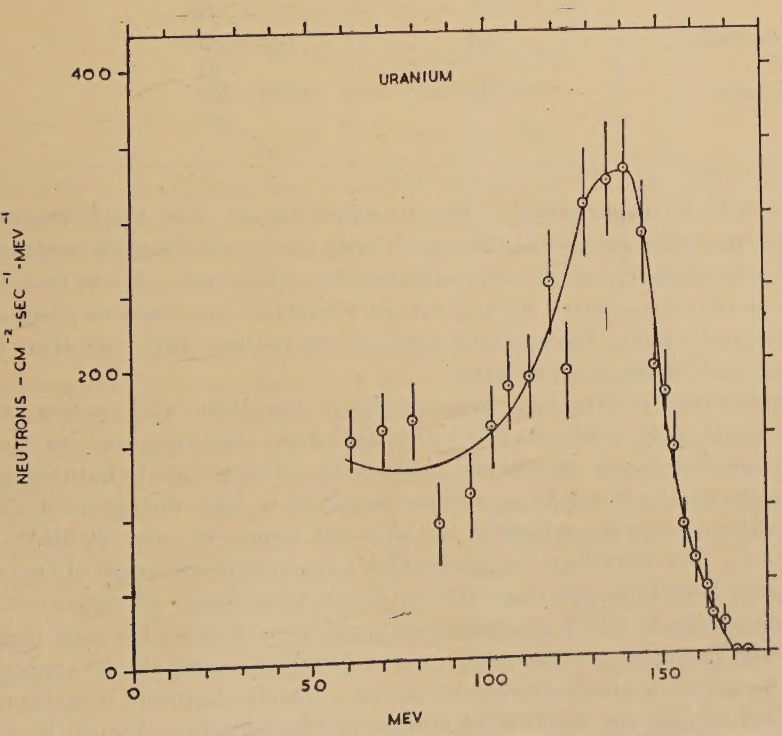

Fig. 3–4. Neutron spectra obtained from beryllium, carbon, aluminium and uranium by bombardment with 171 MeV. protons.

for which the cross-section is known from work at Berkeley (Aamodt, Peterson and Phillips, private communication, 27th February, 1950). Knowing this effective current, it was possible to calculate the differential cross-section, at an angle of 2½° from the forward direction, for the production in carbon of neutrons with energy greater than 60 MeV. (see Table, column 3). If a constant fraction of the cyclotron beam was lost at each traversal of the target, then the mean energy of the primary protons was 155 MeV.

The loss of protons in the target is determined by multiple Coulomb scattering (Moyer, private communication), and it has been found for the Harwell cyclotron that the number of times the proton beam passes through a target at a given orbit radius is such as to bring the R.M.S. angle of multiple scattering up to a constant value, provided that the target is thin enough to make several traversals necessary. Using this principle, the neutron production cross-sections in beryllium and aluminium were obtained. The mean proton energies in these two targets were 156 and 166 MeV respectively. The uranium target was thick enough to suggest that the beam went through it only once, and the cross-section and mean proton energy given were calculated on this basis. These four cross-sections may be in error by a factor of 1·5 either way because systematic errors could have been introduced in estimating the cyclotron beam current during the various runs.

Target element	Mean proton energy (MeV.)	Production cross-sections $\times 10^{27}$ (cm^2)	
		2½°	5°
Beryllium	156	91^{+45}_{-30}	99 ± 19
Carbon	155	47^{+23}_{-16}	72 ± 15
Aluminium	166	122^{+61}_{-41}	—
Uranium	166	1520^{+760}_{-507}	—

The neutron production cross-sections in beryllium and carbon targets at an angle of 5° to the forward direction were also measured, in another and more direct way (see Table, column 4). The gridded chamber in the telescope was replaced by a counter sensitive to high energy protons and the carbon absorber adjusted so that all neutrons over 60 MeV. were counted. The beryllium target for this experiment consisted of two thick sheets of beryllium interleaved with three thin sheets of carbon. After two short runs in which neutrons produced were counted for each target in turn, the targets were removed from the cyclotron and the ^{11}C content of each measured with a calibrated counter. The background measurements required to find the fraction of counts in the telescope due to hydrogen recoils had been done on the previous day, so that effectively no ^{11}C counts remained from those runs at the time of the calibration run. With the help of the known ^{12}C(p, pn)^{11}C cross-section, the neutron production cross-sections could be found. The stated standard error is intended to include all systematic errors.

The shape of the beryllium spectrum reported here seems quite consistent with the results of other experiments using protons of 110 MeV. (Bodansky 1950) and 340 MeV. (Fox, Leith, Wouters and MacKenzie 1950).

We hope to improve and extend these results and publish them, with a more detailed account, at some future time.

REFERENCES.

BODANSKY, D., 1950, *Phys. Rev.*, **80**, 481.
BRUECKNER, K., HARTSOUGH, W., HAYWARD, E., and POWELL, W. M., 1949, *Phys. Rev.*, **75**, 555.
FOX, R., LEITH, C., WOUTERS, L., and MACKENZIE, K. R., 1950, *Phys. Rev.*, **80**, 23.
HADLEY, J., KELLY, E., LEITH, C., SEGRÈ, E., WIEGAND, C., and YORK, H., 1949, *Phys. Rev.*, **75**, 351.
KELLY, E., LEITH, C., SEGRÈ, E., and WIEGAND, C., 1950, *Phys. Rev.*, **79**, 96.
TAYLOR, A. E., PICKAVANCE, T. G., CASSELS, J. M., and RANDLE, T. C., 1950 a, *Nature, Lond.*, **165**, 967 ; 1950 b, *Phil. Mag.* (in the press).

The Velocity Brownian Movement.

By D. K. C. MACDONALD *,
Clarendon Laboratory, Oxford.

[Received December 14, 1950.]

DR. FÜRTH's amplifying and detailed discussion (Fürth 1950) of the example I appended to illustrate the main argument of my paper (MacDonald 1950) is welcome, but does not, of course, alter any of the fundamental conclusions. Nevertheless, may I make the following brief comments :—

(1) The purpose of my example, which it appears Dr. Fürth may have misunderstood, was to show that the available statistical data on the observed *velocity* of a Brownian particle *would* indeed be already sufficient to determine D (and hence $k=6\pi\eta a\mathrm{D}/\mathrm{T}$), at least in order of magnitude, if a reasonable value for the discrimination-period of human vision were assumed. Since I was in fact only concerned with demonstrating the underlying principle I deliberately chose for simplicity the familiar one-dimensional Brownian movement equation.

(2) The use of the standard deviation to approximate the mean absolute velocity is clearly a good approximation for a "stationary" system in thermal equilibrium as for the Brownian particle (or in the general

---

* Communicated by the Author.

kinetic theory of gases) but, of course, for a system with an externally superposed mean velocity (as in a current-carrying medium) the two need have no connection with one another.

(3) The thesis underlying Dr. Fürth's first two sections is not entirely clear to me. However, no physical variable can have a frequency-spectrum extending without limit and consequently, of course, can never be *perfectly* random (and therefore non-differentiable). It is nevertheless quite customary to refer to a quantity as varying stochastically if within the frequency-range of observation the " power " spectrum is effectively flat as, for example, in the case of thermal noise from a resistor at all accessible radio frequencies and normal temperatures.

References.

Fürth, R., 1950, *Phil. Mag.*, **41,** 1255.
MacDonald, D. K. C., 1950, *Phil. Mag.*, **41,** 814.

XXII. *Notices of New Books and Periodicals received.*

Structural Chemistry of Inorganic Compounds, Vol. I. By W. Hückel. (Elsevier Publishing Co. Inc.) Price $9. (£3 10*s.* 0*d.*)

This is essentially a book for use in the latter stages of a University degree course. About one-eighth of the book is taken up by an excellent historical survey. The remainder is about equally divided between a presentation of the coordination theory which is the basis of the author's systematization, and a discussion of atomic structure and physical methods for investigating molecular structure. This order is a little unusual, and emphasizes the importance attached to stereo-chemistry and the coordination approach.

The author can be congratulated on the large amount of recent information which he has included, though no mention is made of the optical resolution of the dodecammine–hexol–tetracobaltic salts, the first resolution of a purely inorganic compound. An incorrect structure is assigned to this group of salts. The correct structure has in fact been determined by X-ray analysis, contrary to the statement on p. 166.

[*The Editors do not hold themselves responsible for the views expressed by their correspondents.*]